Transactions of the **13th International Conference on Structural Mechanics in Reactor Technology** (SMiRT 13), Escola de Engenharia - Universidade Federal do Rio Grande do Sul, Porto Alegre, Brazil, August 13-18, 1995

A conceptual study on vertical seismic isolation for fast reactor components

Morishita, M.
Power Reactor and Nuclear Fuel Development Corporation, Ibaraki, Japan

ABSTRACT: In a base isolated plant, the vertical component of an earthquake ground motion is directly transmitted to the upper structure, while the horizontal components sufficiently reduced. Hence, if one can combine a vertical seismic isolation at equipment level with base isolation, the plant may be three dimensionally freed from seismic load, which will substantially enhance plant safety and economy. From this point of view, a structural concept of vertical isolation system has been pursued.

1. VERTICAL ISOLATION SYSTEM -A CONCEPTUAL DESIGN-

The success of horizontal base isolation can chiefly be attributed to the use of laminated rubber bearings which have flexibility in shear deformation and high rigidity in vertical load supporting direction. In the vertical isolation system, on the other hand, the direction of isolation is the same as that of gravitation. This is the most distinctive feature of the vertical isolation system and one has to use vertically flexible isolation device while supporting the static weight of its object, which is the main cause of engineering difficulty in developing a realistic vertical isolation system. It is essential to avoid excessive static deflection (settlement) during installation and undesired rocking response to the horizontal excitation. The isolation device is therefore required to have a carefully tuned flexibility in the vertical direction while keeping a sufficient rigidity in the other degrees of freedom. The device is, from safety aspect, also required to maintain supporting capability even its failure is postulated. In addition, it should be avoided that excessive relative displacement be imposed to primary piping systems that connect the major components.

As a promising solution to the above requirements inherent to the vertical isolation system, a concept that the author calls "common deck isolation system" is proposed, see Fig. 1. Here, the idea is that the reactor vessel and the major primary components are suspended from a flat circular slab structure (common deck) inside the reactor containment vessel. This common deck is then supported by a couple of vertical isolation devices installed around each component. The isolation device adopted in the present study, as is shown in Fig. 2, basically consists of a set of large bore dish springs that surround the body of each component. These dish springs are, in connection with the movable inner cylinder and the upper ring, compressed downward when the upper structure moves downward, and compressed upward when the upper structure moves upward. In this way, the dish springs always remain in a stable compressed state. The dish springs are sized and combined in parallel and/or series so that the desired fundamental frequency and necessary stroke are achieved.

Since in this system the isolated structure is basically a flat plate and the offset between its center of gravity and supported location is small, only marginal rocking response is intrinsically expected. This unnecessitates any additional support against rocking. It also contributes to suppressing the rocking motion that a few number of large bore dish springs are utilized. One of the other advantages of this system is that no relative displacement is subjected to the primary piping systems since there occurs no relative motion among the components suspended from the common deck. It should also be noted that the dish springs can maintain their capability for the static weight support of the isolated structure even in an ultimate state of deformation and no catastrophic failure is expected.

2. ANALYSIS

2.1 Vertical response of base isolated reactor building

In order to provide with a set of input conditions for the survey of vertical isolation characteristics, a series of dynamic soil-structure interaction analyses on a base isolated reactor building was first made. The vertical ground motion used, which is shown in Fig. 3, was generated from a target spectrum which was made by modifying the horizontal design spectra of an existing plant (Watabe, 1990). A lumped mass analysis model was constructed based on a design of a loop type FBR plant, see Fig. 4. The soil condition considered ranges from a soft rock site with the shear wave velocity (Vs) of 700 m/sec to a hard rock with Vs = 2000 m/sec. The axial rigidity of the isolation layer (rubber bearing) assumed, in terms of natural frequency, fv, ranges from 10 to 20 Hz.

Some typical results of the analyses are shown in Fig. 5 in the form of floor response spectra (FRS) at the reactor support level. There are basically three peaks in these FRS's, the first of which is rather a wide peak ranging from about 0.1 sec to 0.3 sec. The other peaks correspond to the higher order modes and lie in shorter period ranges. The FRS is more dependent on the rubber bearing stiffness in the hard rock case than in the soft rock case. Especially in the hard rock case, the first peak of the FRS becomes very large when the rubber bearings are not stiff enough.

2.2 Survey for optimal isolation characteristics

Using the structure response obtained from the above analyses, a series of parametric survey was made with a single d.o.f. model to identify an appropriate range of isolation frequency and damping values.

Some typical results are shown in Fig. 6. Here, the normalized acceleration is the ratio of maximum response to input. Naturally, the response acceleration decreases as the isolation frequency is lowered, while the response displacement increases. It is noted from the figure the response acceleration is dependent more on the soil condition than on the rubber bearing stiffness, and that the isolation is more effective in the hard rock case. Higher damping is effective for the reduction of both acceleration and displacement. If one can expect at least 10% damping or more, (this value seems to be realistic for the friction damping of dish springs) it may be allowed to set the isolation frequency up to around 3 Hz, except for the very soft rock cases. From the displacement point of view, the lowest frequency applicable seems to lie around 2 Hz, since a significant increase of displacement is seen below 2 Hz. Based on these observations, it is judged the frequency range of 2 to 3 Hz is appropriate and that at least 10% damping is required for vertical isolation.

2.3 Design of dish springs as isolation device

A trial design was made on large bore dish springs as isolation devices to see if the above identified isolation frequency is achievable in an actual scale. The assumed size and weight of the isolated structure/components are;

- Common deck: 40 m in diameter, 2 m in thickness, 6000 ton in weight
- Reactor-block: 8 m in diameter, 4700 ton in weight
- IHX's and Pumps: 1400 ton (sum of 4 loops)

The isolation frequency was chosen to be 2.5 Hz, and the load supporting capacity and the stroke were set to be 2 G's (1 G of static weight plus 1 G of dynamic response including safety margin) and 80 mm, respectively.

Using Almen/Laszlo formula (Almen, 1936) for the load-deflection relation, the dimension of the dish springs were determined, as listed in Table 1.

2.4 Dynamic characteristics of vertically isolated common deck

A preliminary analysis was made on the whole common deck system to see its fundamental dynamic characteristics and the effect of isolation. Here, the common deck was modeled by shell elements, reactor-block and components by lumped mass rod elements, and the isolation devices by linear spring elements. In Fig. 7 shown are the vibration modes, where only the common deck is depicted for simplicity. While the fundamental mode (2.4 Hz) is the rigid body motion of the common deck, in the second mode (3.8 HZ) some deformation of common deck into a conical shape is seen. However, the modal mass contributing to this mode is negligibly small. Fig. 8 compares the response acceleration of the core support plate in the reactor-block. The effect of isolation, i.e., the reduction in acceleration response, is clearly seen.

3. CONCLUSION

A concept of vertical isolation system which uses common deck structure and large-bore dish springs as isolation device was proposed. Appropriate and realistic ranges of isolation frequency and damping were identified to be 2 to 3 Hz and about 10%, respectively. A trial structural design was made of the actual scale dish spring and common deck to show possibility of realization of the system. From the preliminary analysis, it was shown that the present isolation system is effective in reducing the vertical response acceleration of the components.

ACKNOWLEDGMENT

The author wishes to thank Mr. H. Machida, ARTECH Inc., and Mr. M. O-oka, PNC/OEC, who contributed to the major part of the response analysis and structural design presented in this paper.

REFERENCES

Almen, J.O. and Laszlo, A. 1936 The uniform-section disk spring. Trans. ASME, Vol. 58, pp. 305-314

Watabe, M., et. al. 1990. Peak accelerations and response Spectra of vertical strong-ground motions from near-field record in USA. Proc. 8th. Symp. Earthquake Eng.

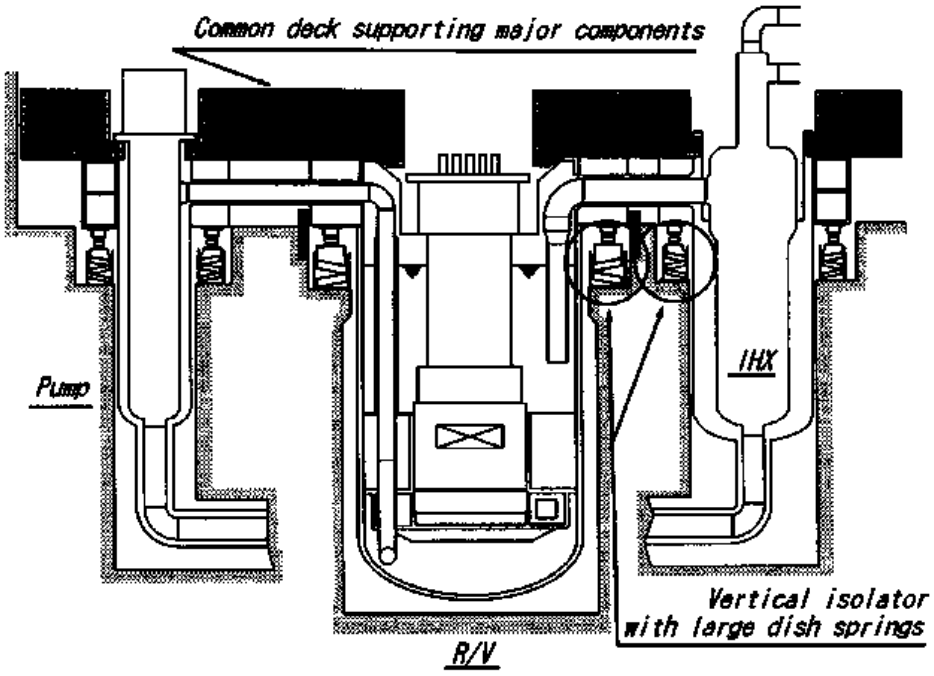

Fig. 1 Schematic drawing of common deck isolation system

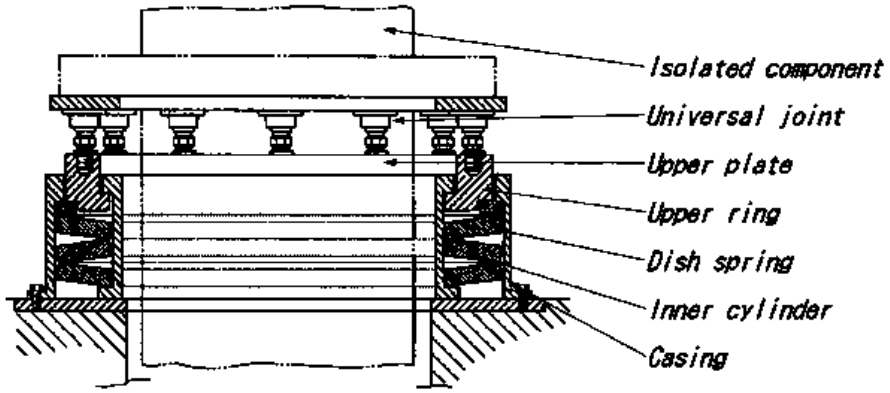

Fig. 2 Vertical isolation device with large dish springs

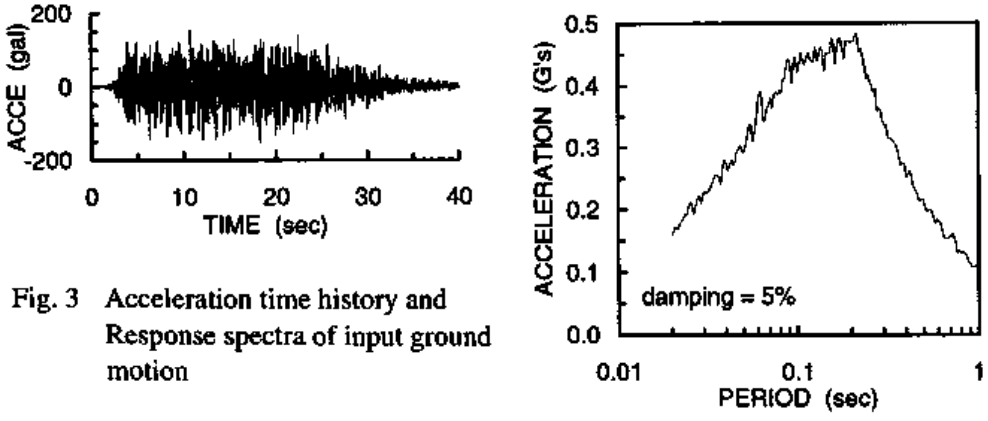

Fig. 3 Acceleration time history and Response spectra of input ground motion

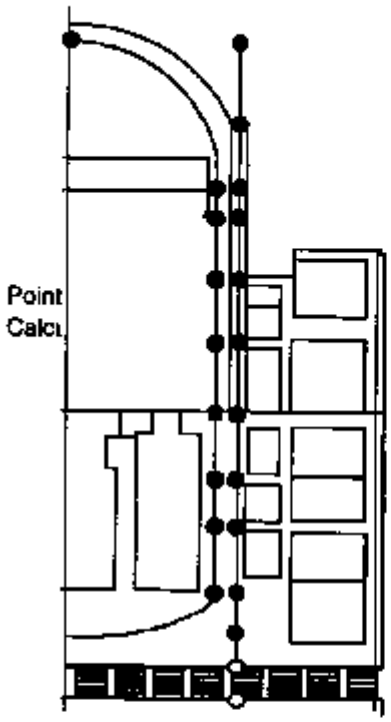

Fig. 4 Analysis model of base isolated reactor building

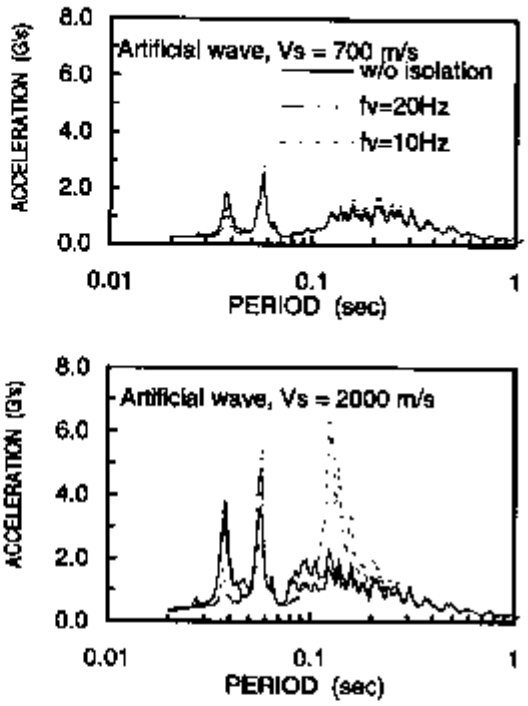

Fig. 5 Floor response spectra at reactor support level

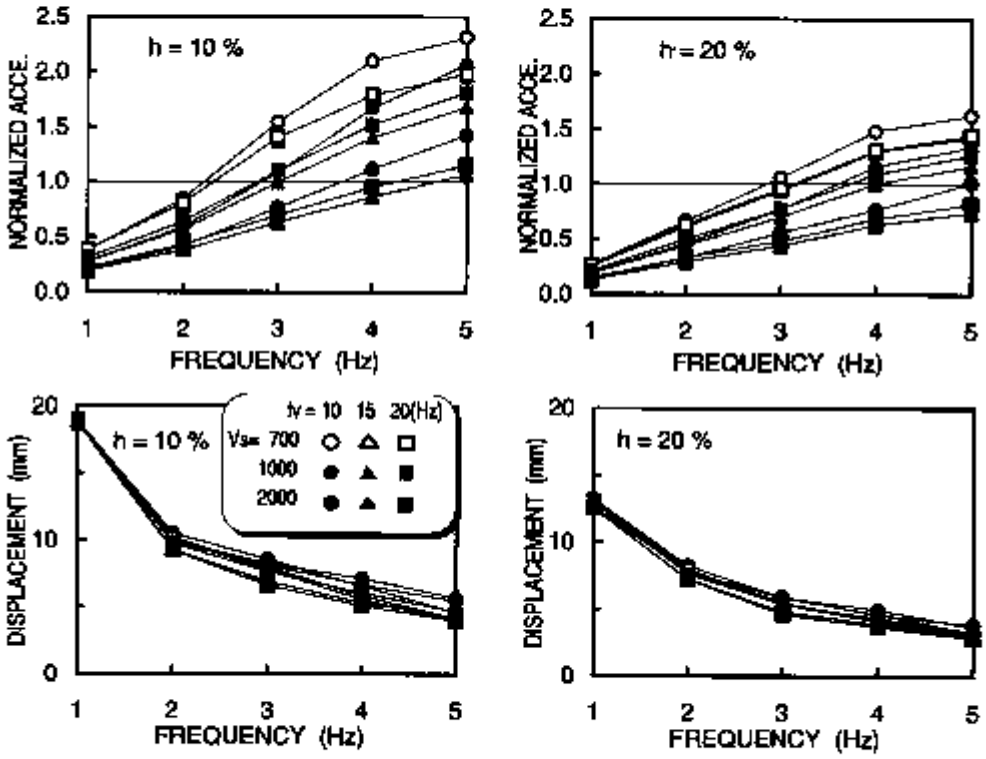

Fig. 6 Response of 1 d.o.f. system

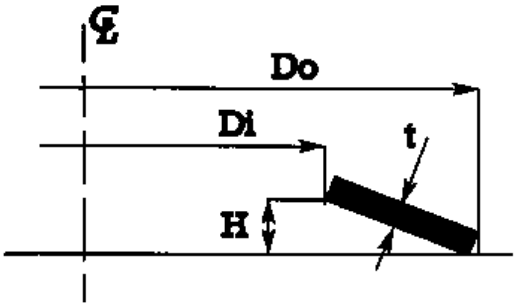

Table 1 Dimension of dish springs

	R/V	IHX	Pump
Do (m)	14.0	8.2	6.0
Di (m)	10.8	6.2	4.0
H (mm)	330	120	150
t (mm)	440	160	200
N	1	1	3 (series)

N: Number of springs

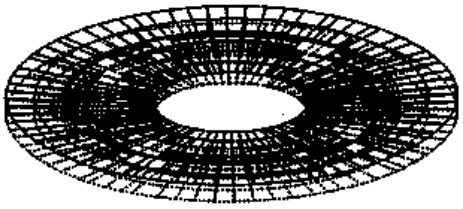

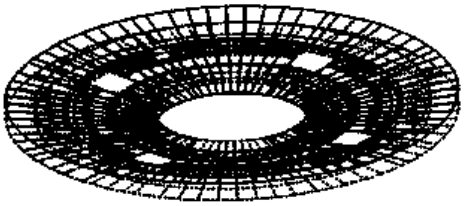

Mode 1 2.41 Hz

Mode 2 3.77 Hz

Fig. 7 Vibration modes of isolated common deck

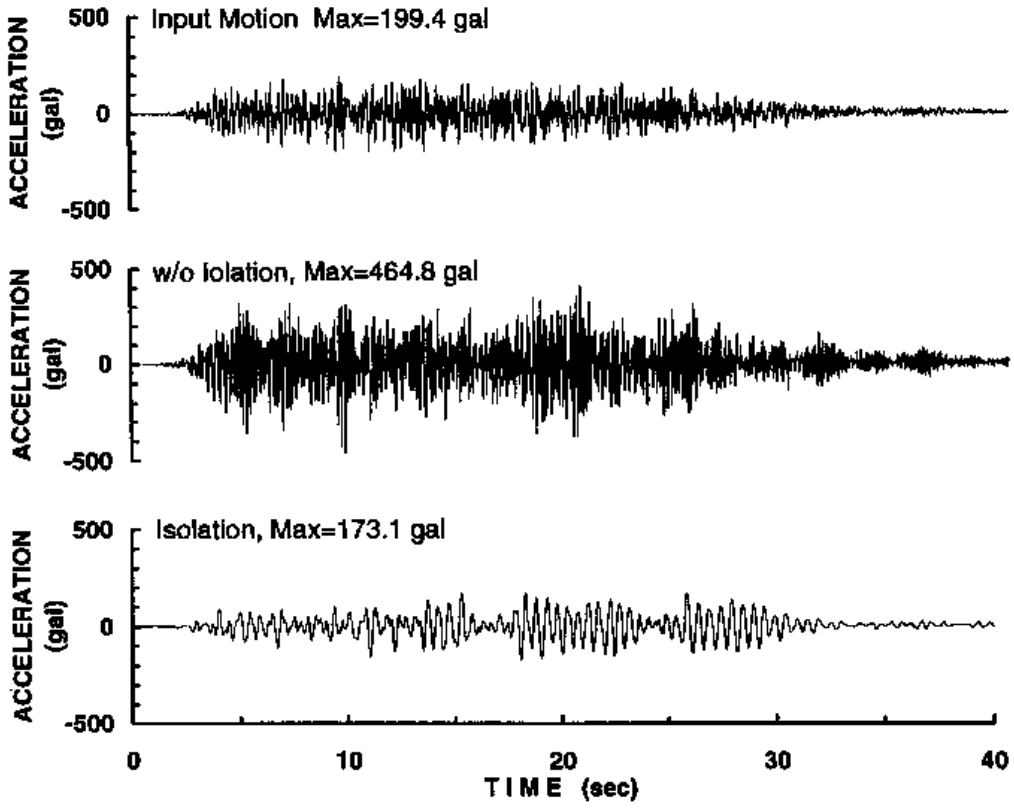

Fig. 8 Comparison of response acceleration at core support plate

Transactions of the 13th International Conference on Structural Mechanics in Reactor Technology (SMiRT 13), Escola de Engenharia - Universidade Federal do Rio Grande do Sul, Porto Alegre, Brazil, August 13-18, 1995

A European collaboration research programme to study and test large scale base isolated structures

Renda, V., Verzeletti, G., Papa, L.
European Comission, Joint Research Centre, Ispra (VA), Italy

ABSTRACT: The improvement of the technology of innovative anti-seismic mechanisms, as those for base isolation and energy dissipation, needs of testing capability for large scale models of structures integrated with these mechanisms. These kind experimental tests are of primary importance for the validation of design rules and the setting up of an advanced earthquake engineering for civil constructions of relevant interest.

The Joint Research Centre (JRC) of the European Commission (EC) offers the European Laboratory for Structural Assessment (ELSA) located at Ispra (VA) - Italy, as a focal point for an international european collaboration research programme to test large scale models of structure making use of innovative anti-seismic mechanisms. A collaboration contract, opened to other future contributions, has been signed with the national italian working group on seismic isolation (Gruppo di Lavoro sull' Isolamento Sismico GLIS) which includes the national research centre ENEA, the national electricity board ENEL, the industrial research centre ISMES and the producer of isolators ALGA.

1 INTRODUCTION

The European Commission (EC) is currently engaged in research activities about the seismic behaviour of structures, the technologies to lower the effects of an earthquake and the verification of the rules in the design standards of the field.

The effects of an earthquake on large size structures are investigated in the ELSA Laboratory of the Joint Research Centre (JRC) by means of a Reaction Wall (RW), sited at Ispra (VA), and the Pseudo-Dynamic (PsD) method. Presently the main objectives of the activities of the laboratory are related to the calibration of the rules of the EUROCODE - 8 for the design of steel and reinforced concrete structures.

During the last years the earthquake engineering technology has developed innovative anti seismic techniques, like seismic isolation, to protect the structures of relevant interest. The EC is interested in the follow-up of these techniques, not to develop an independent concept of isolation but to verify the effectiveness of the technology and the reliability of the mechanisms and of the related design standards.

EC/JRC contacted ENEA/ERG/FISS in Italy as chairing organization of the National Working Group on Seismic Isolation (GLIS) with the aim of setting up a collaborative research programme on Seismic Isolation Technology making available the ELSA Lab. for large size base isolated structures assuming that the partners will contribute designing and providing the isolators, performing shaking table tests, analysing the results and verifying/improving Design Standards.

These contacts led to the proposal of collaboration in a Seismic Isolation Programme (SIP). Other members of GLIS (ENEL, ALGA, ISMES) will participate, in the framework of GLIS cooperative activities, to the collaboration research programme through ENEA/ERG/FISS; it also noted that JRC-Ispra and ENEL-CRIS had signed an agreement to exchange experience and knowledge developed by both organizations on structural research, to which the present collaboration on seismic isolation technology is strictly correlated.

The collaboration is open to the contributions of other Organizations from other countries of the Community. The enlargement of the collaboration will be discussed by the partners and the contributions of the Organizations participant to the programme should be, at least partially, balanced.

The experimental results and the acquired engineering conclusions (but not the isolators technology that is property of the manufacturers) will be shared among the actual and future Organizations contributing to the programme.

2 OBJECTIVES OF THE COLLABORATION

The EC/JRC allows the use of the RW and the PsD method to test large size base isolated structures for the effects of a real earthquake. The structures existing in the laboratory (built and tested for other purposes) will be made available for the tests, after repair, to lower the costs of the research. The use of the RW is the only systematic way to test regularly large-size isolated structures.

The main technical objectives expected from the collaborative programme are:

Tests of large-size isolators;

Tests performed with large displacements (of the order of 30 to 40 cm.);

Tests of structures with both small-scale and large-scale isolators for large displacements to verify the validity of the models to account for the scale and experimental technique effects;

Comparison between different systems of isolation (at present the behaviour of some system is not well known);

Experimental verification of Design Standards for the isolators and the structures designed to be isolated.

JRC is particularly interested in this last item in view of a possible support to DG III and CEN. The state of the art in this field is not very advanced and, in particular, there does not exist at present a set of design rules agreed by the Member States of the Community

3 CONTENT OF THE COLLABORATION

3.1 *PsD test method validation and numerical analyses*

In principle there is no doubt about the applicability and the potentiality of the PsD method; the problem is the influence of the velocity of the test on the characteristics of the material of the isolators; some literature exists on the subject and probably the influence of strain rate is not such to invalidate the results of a PsD test; moreover this problem is probably dependent on the isolator materials.

To better clarify this aspect a comparison will be set up of the results obtained at ISMES on a shaking table with those obtained by means of the RW using the PsD method. This can be done only for scaled structures.

Adaptable isolated structures, foreseen for a Brite-Euram II project and another ENEL project, will be designed and constructed by ENEL-CRIS in collaboration with ISMES, ENEA who will cooperate in isolators design, and ALGA who will supply the isolators, to be tested on a shaking table at ISMES in the framework of the aforesaid projects. The same structures under the same condition of isolation will be tested also at the ELSA Laboratory.

In parallel with this experimental validation of the PsD method, a numerical activity will be set up to clarify how the ductility of a structure is related with the effectiveness of the isolation. A certain number of meaningful cases will be selected, nimerically analysed, compared and discussed in order to provide data about the level of interest in isolation for structures of various ductility classes.

3.2 *Tests using existing structures not designed to be isolated.*

Some test structures exist at the ELSA_Lab (Figure 1); JRC proposes, for evident economic reasons, to reuse these structures to test different concepts of isolation. This proposal is attractive both for the comparison between the isolators and because the results could be a first step to define how the same structure could have been designed to resist the effects of the earthquake taking into account the isolation.

Because the structures existing at the ELSA_Lab will be tested in the framework of the planned activity of the laboratory, these structures must thus be repaired before being tested in the framework of a Seismic Isolation Programme. Some additional investigations (as the comparison with the original eigen-frequencies, stiffness matrix, structural diagnostic,.) will be performed to verify the integrity of the structure before the reuse to test it with base isolation devices.

Figure 1. Structures existing at ELSA_Lab

3.3 *Tests of structures designed to be isolated.*

When the applicability and the potentiality of the PsD method will be clarified, some tests using structures designed and built to be isolated could be done to contribute to the verification of the Design Standards for the isolators and the isolated structures.

The realization of these tests will be decided taking into account the costs and the eventual interest of DG III for these tests aimed to verify design rules.

4 CONTRIBUTION OF THE PARTICIPANTS

The JRC ELSA Lab. will be a service laboratory in the framework of a common European Seismic Isolation Programme. The following contribution have been agreed:

4.1 *EC/JRC contribution*

The EC/JRC, contributes with large size structures existing in the laboratory (built and tested for other reasons) after repair and verification of their structural integrity, with all the laboratory work (instrumentation, tests, data acquisition...) and with a pre-elaboration of the experimental data to be supplied in the desired format.

4.2 *GLIS contribution*

The GLIS organization, contributes with the design and the supply of the isolators, the follow-up of the tests, the relevant results of dynamic tests with shaking tables, the analysis of the results, the improvement of the technology and the verification and the improvement of Design Standards.

4.3 *Details of the contribution to the planned actions*

In detail, at present the following specific contributions have been agreed:

JRC and ENEA/ERG/FISS, with the cooperation of ENEL/CRIS, will contribute to the preliminary analyses on the effect of isolation on structures; the cases to study will be agreed by the partners and the computational work will be shared between the participating laboratories.

JRC and ENEA/ERG/FISS, with the cooperation of ENEL/CRIS and ISMES, will contribute to tests to verify the applicability and limits of the PsD method by testing at the Reaction Wall a structure provided by ENEL/CRIS, isolated by means of high damping rubber bearings (HDRBs), which will be also tested on a shaking table.

JRC will perform first tests on an existing large scale structure, using HDRBs as isolators, with the cooperation of ENEA, ENEL-CRIS and ISMES as GLIS members.

ENEA/ERG/FISS, through the GLIS member ALGA, will supply all the base isolators of interest for Italy.

The detailed first part of the programme, related to existing structures only, and the planning of the activities is shown as GANTT (Figure 2) and PERT (Figure 3) charts.

It has been agreed also that JRC will be provided with results of previous relevant tests performed by the partners when this is compatible with the protection of the industrial know-how.

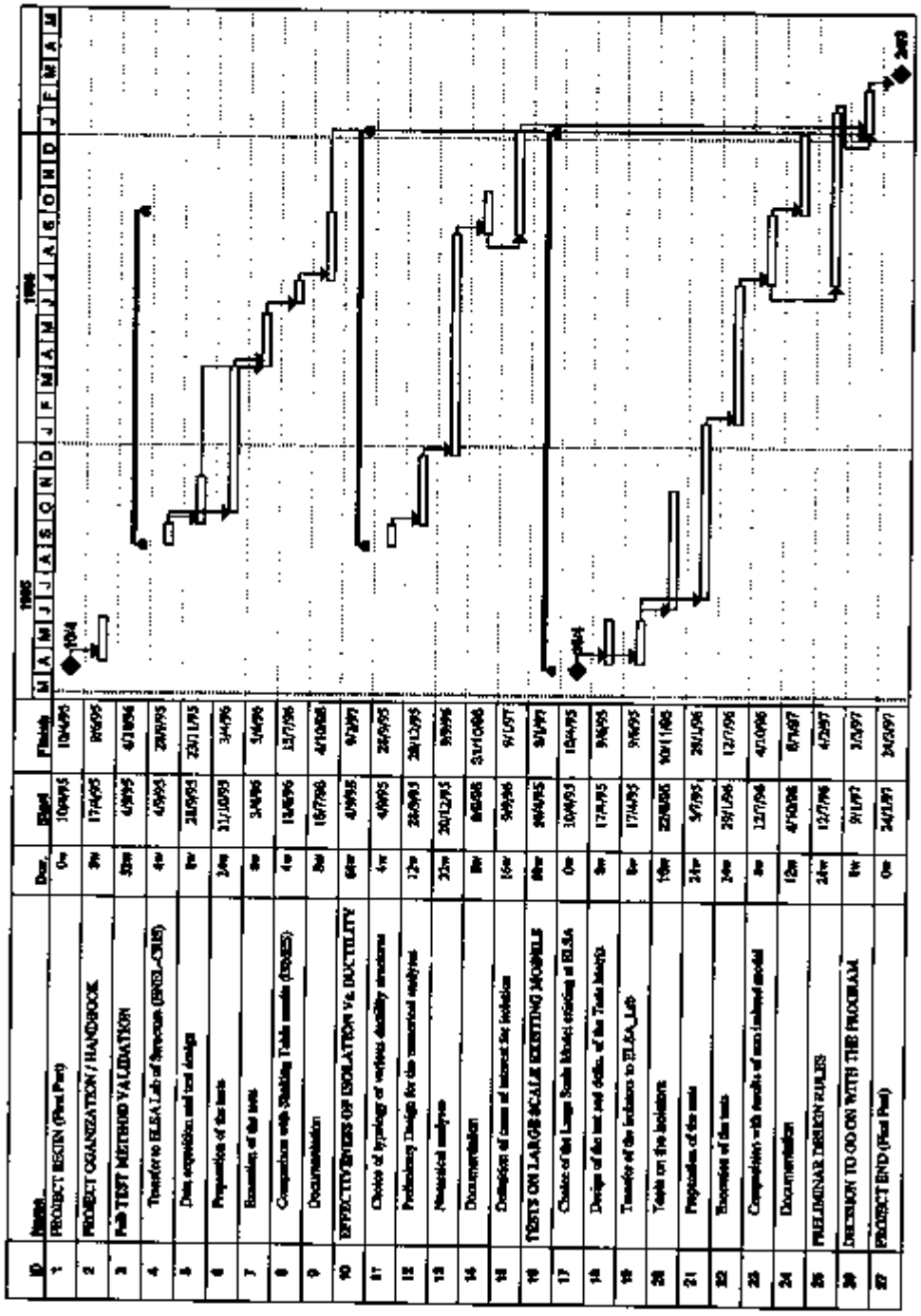

Figure 2. Seismic Isolation Programme - GANTT chart

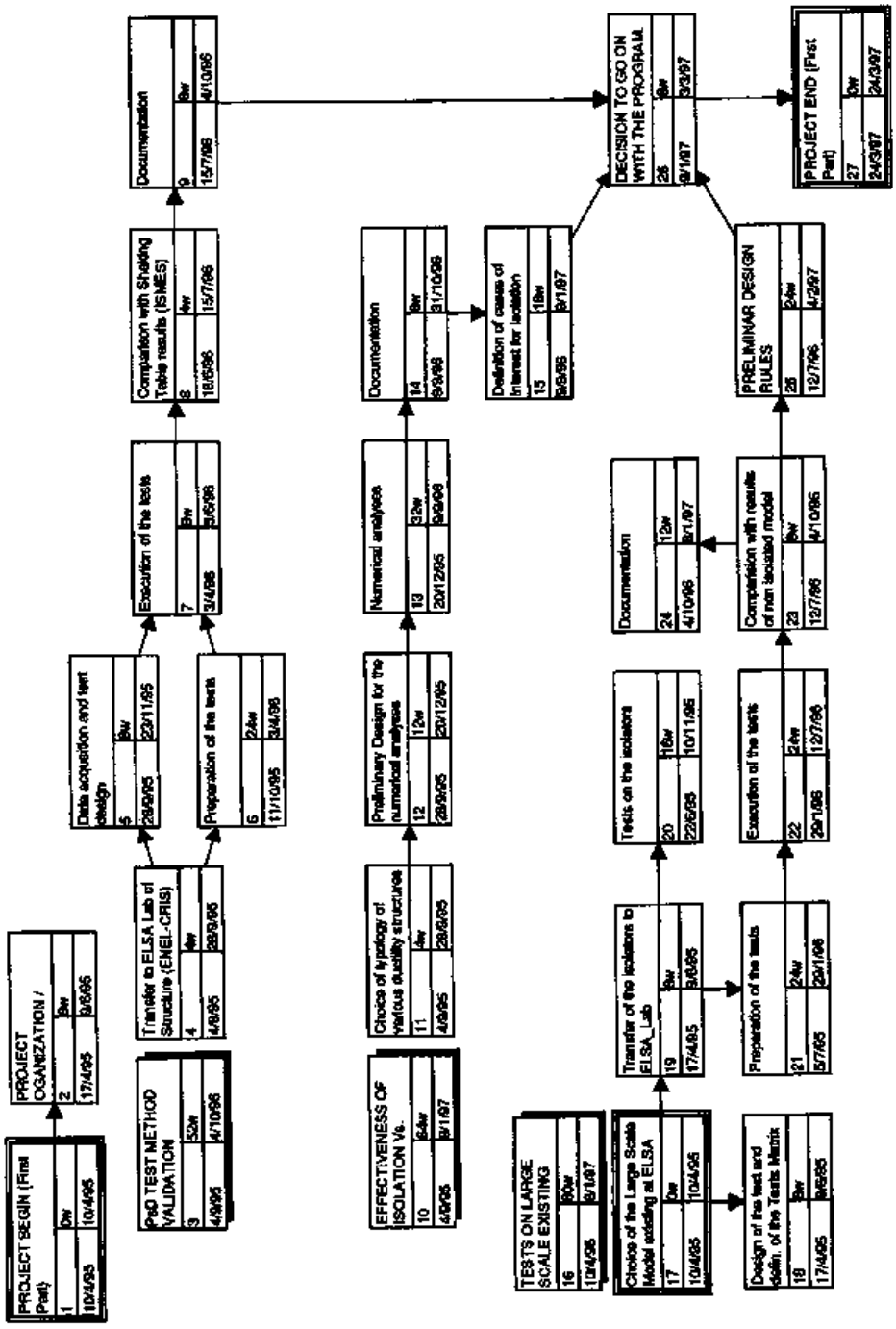

Figure 3. Seismic Isolation Programme - PERT chart

Transactions of the 13th International Conference on Structural Mechanics in Reactor Technology (SMiRT 13), Escola de Engenharia - Universidade Federal do Rio Grande do Sul, Porto Alegre, Brazil, August 13-18, 1995

Analysis of base isolation and energy dissipation systems for NPP structures using fragility models

Vulpe, A.
Technical University of Iasi, Dept. of Structural Mechanics, Romania
Căruşu, A.
Technical University of Iasi, Dept. of Mathematics, Romania

ABSTRACT: Some extensions of analytical models for base isolation and energy dissipation systems, involving fragility models, are presented. The equation of motion is extended with a term corresponding to ED effect, and the fragility of IEDS is evaluated using a bilinear regression line.

1 INTRODUCTION

Among various types of techniques and devices developed (during the last decade) for reducing the effect of strong earthquake excitations on NPP facilities, the base isolation systems have been rather widely accepted or even preferred (Kato, Watanabe & Kato 1991), (Tajirian & Abrahamson 1991), (Ishida et al. 1991). They are better suited for isolating heavy structures constrained to high safety level requirements (like the reactor vessel, for example). However, restrictions have to be observed on the relative displacements between the upper structure and foundation / ground (Kouizumi et al. 1991). Therefore, it has appeared as useful to combine base isolation devices with hysteretic energy dissipators / absorbers (Zhou 1991), (Sone & Yamamoto 1991). As regards the analytical models behind the aforementioned techniques and devices, it has to be remarked that the probabilistic and stochastic concepts and methods have been involved up to a rather limited extent.

In this paper we present extensions of some energy-based models for base isolation and energy dissipation systems (IEDS) of NPP structures / facilities, thus developing our research reported at the SMiRT 12 Conf. (Căruşu & Vulpe 1993). Starting from a model of F.Zhou (1991), we derive simpler analytical expressions for the acceleration attenuation ratio AR and for the maximum relative displacement between structure and ground (base mat) $D_{\max}$. Other parameters as equivalent damping ratio and the restoring force are also reformulated. Next, A.Hadjian's (1993) BMER (balance mitigation of earthquake responses) model is extended in two ways. The expression of the restoring function also includes the damping effect on the vertical displacement of the supports by the hysteretic energy dissipation, what leads to an alternative equation of motion. Finally, fragility curves are derived for the proposed IEDS, using an equivalent linearization on the hysteretic multilinear curve. The fragility of IEDS is then evaluated using a multilinear regression line. Formulas for the estimation of regression parameters are also given by adapting our previuosly derived expression presented in (Carauşu & Vulpe 1993). They can be employed in connection with efficient simulation techniques like the LHS (Latin hypercube sampling).

2 BASE ISOLATION AND ENERGY DISSIPATION SYSTEMS

Let us consider a structure of mass M subjected to a ground displacement X_g with the structural response X_a. The basic differential equation of motion is (Zhou 1991):

$$(1) \qquad M\ddot{X}_a + C_e \dot{X}_a + K X_a = C_e \dot{X}_g + K X_g ,$$

where C_e = the equivalent viscous damping, and K = the elastic stiffness of the IEDS, respectively. An analytical expression is given in (Zhou 1991) for the acceleration attenuation ratio $AR = \ddot{X}_a / \ddot{X}_g$. We propose a simpler expression for this parameter using the ratio $\eta = \omega / \omega_n$ where ω is the circular and ω_n is the natural circular frequency of the IEDS :

$$(2) \qquad AR = \frac{1}{\sqrt{\dfrac{1}{\eta} + \dfrac{\eta^3 - 2\eta}{1 + 4B^2}}} ,$$

in which B = the energy dissipation ratio. As regards the maximum relative displacement, its expression (Eq.(4) in (Zhou 1991)) in terms of AR, $\ddot{X}_g$, ω and ω_n can be replaced by the simpler one

$$(3) \qquad D_u = \frac{\operatorname{sgn} \ddot{X}_g}{\omega} \cdot \frac{\| (\ddot{X}_a, \ddot{X}_g) \|}{\sqrt{\omega^2 - 2\omega_n^2}} .$$

In Eq.(3), sgn is the well-known signum function and $\| \cdot \|$ is the Euclidean norm in the 2-space : $\| (u, v) \| = \sqrt{u^2 + v^2}$. The equivalent damping ratio $E_e = C_e / 2M\omega_n$ can be expressed in terms of AR and η by

$$(4) \qquad E_e = \frac{1}{2\eta} \sqrt{\frac{1 - AR^2 (1 - \eta^2)^2}{AR^2 - 1}} .$$

Finally, the energy dissipation ratio B can be written as

$$(5) \qquad B = \frac{2 (D_u - D_y) D_y}{D_u^2 \pi} ,$$

where D_y is the relative displacement at the yield point.
These parameters may be introduced in the equation of motion for a base isolated structure with a nonlinear damper, given by (Sone & Yamamoto 1991) for a SDOF model as $m\ddot{x} + kx + f(x, \dot{x}) = -m\ddot{y}$, where m, k are the mass of the isolated structure and the spring constant of the rubber bearing (respectively), while $f(x, \dot{x})$ is the damping force, x is the relative displacement response and y is the seismic input

ground motion. Taking into account Eq.(1) and replacing M by m, K by k (and so on), we get

(6) $f(x, \dot{x}) = C_e \dot{x}$ and $m\ddot{y} + C_e \dot{y} + ky = 0$.

Another model we have taken into account is BMER (balance mitigation of earthquake response) due to A. Hadjian (1993), of which we recall the expression of the restoring force only :

(7) $$g_r(x, \dot{x}) = \frac{x^{b-1}[a^2 b^2 (b-1) x^{b-2} \dot{x}^2 + a b g]\, \dot{x}}{1 + a^2 b^2 x^{2b-2}},$$

where x is the relative horizontal displacement (as above) while a, b are parameters in the equation of the cross section of the bowls which the cylindric supports roll in :

(8) $z = a x^b$.

The BMER is completed as to damp the vertical displacement of the supports by hysteretic energy dissipation due to a set of rubber bearings, as represented in Fig.1. The resulting equation of motion will be

(9) $m\ddot{x} + kx + f(y, \dot{y}) + g_r(x, \dot{x}) = -m\ddot{y}$,

and it can be integrated using a Runge-Kutta numerical integration method.

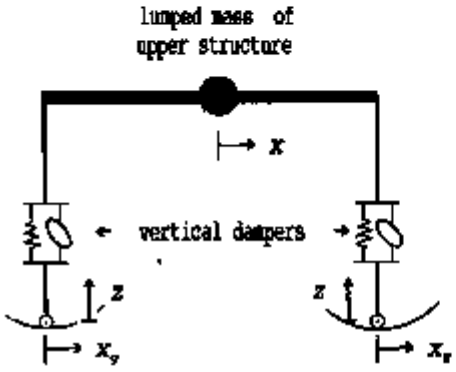

Fig.1 Base IEDS with vertical dampers and rollers-in-bowls ED supports

The restoring function $g_r(x, \dot{x})$ in Eq.(9) can also be expressed as a function of z, $\dot{z}$ using Eq.(8); thus, $\dot{z} = a b x^{b-1} \dot{x}$. Parameters a, b giving the shape of the cross-sectional curve of Eq.(8), that is, the generatrix of the cylindrical surface of the support bowls, have to be found so as to achieve a maximum ED effect. They will depend on mechanical and geometric properties of the upper structure and base isolation system. For instance, the vertical restoring force to be taken into account for one of the n supports of the base plate will be equal to

(10) $$-\frac{M\ddot{z}}{n} = a b x^{b-2} [(b-1)\dot{x}^2 + b\ddot{x}].$$

Before deriving the horizontal restoring force in the case of (generalized) parabolic contact surfaces for the bowls, let us remark that expression (7) of the restoring function $g_r(x, \dot{x})$ is obtained not from Eq.(8) of (Hadjian 1993) but from

(11) $(1 + a^2 b^2 x^{2b-2})\ddot{x} + a b g x^{b-1} \dot{x} + (b-1) a^2 b^2 x^{2b-3} \dot{x}^3 = 0$.

Let us now consider an upper structure of mass M equally distributed on the n

supports, giving (on each support) a mass $m = M/n$, and a vertical force $= mg\vec{k}$. If it is decomposed along the horizontal direction $\vec{i}$ and the normal direction $\vec{v}$ to the surface of Eq.(8) at a contact point P on it we get

$$(12) \qquad mg\vec{k} = \frac{mg}{\cos\theta}\vec{v} + (mg)_x \vec{i}$$

where $\vec{v} = \dfrac{-a x^b \vec{i} + \dfrac{x}{b}\vec{k}}{\sqrt{a^2 x^{2b} + x^2/b^2}}$. After some computations we find

$$(13) \qquad (mg)_x = -\operatorname{sgn}\theta\,(mg\tan\theta) = (-\operatorname{sgn}\theta)\, a b x^{b-1}\dot{x}.$$

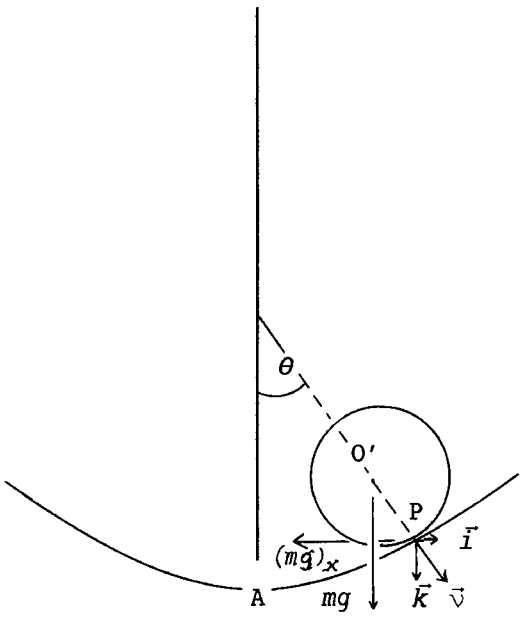

Fig.2 Forces at a contact point P on the rolling surface (Eq.(8))

The parameters and forces involved in the above equations are (in part) represented in Fig.2.

Let us denote by W_x the energy corresponding to the horizontal component of the restoring force $(mg)_x$. Then the energy equilibrium equation (extending Eq.(1) of Sone & Yamamoto (1991)) should also include the term W_x :

$$(14) \qquad W_e + W_h + W_p + W_x = E,$$

where the forst three terms denote the elastic vibrating energy, the energy dissipated by the linear damping mechanism and the cumulative inelastic strain energy. E is the total energy input by a seismic ground motion. According to the assumptions included in our model (see Fig.1), W_h should also include the energy dissipating effect of the rubber bearings for damping the vertical motions implied by the oscillations of the roller supports on the bowl surfaces. Alternatively, Eq.(1) should be extended by an additional term corresponding to the horizontal restoring force of Eq.(13). In both alternatives, the resulting equation of motion is similar to Eq. (11) in (Hadjian 1993), with the additional term that appears corresponding to the vertical energy damper / to the horizontal restoring force.

The numerical integration method there applied (of Runge-Kutta type) could also be used for solving the resulting equations.

3 EVALUATING FRAGILITY OF IEDS SYSTEMS

The above models do not include any probabilistic approach. However, they offer a more realistic basis for evaluating the fragility, that is, the conditional probability of failure for the base isolation and energy dissipating systems.

The previously presented model can be further extended to nonlinear damping systems (similar but more general than the ones considered in (Koizumi et al. 1991)) that is of types $x^{\lambda}\dot{x}^{\lambda}$ with λ not necessarily $= 1,2$).

The fragility curves are derived for the structure with an isolation and energy dissipation system (IEDS), using the well-known equivalent linearization technique on the hysteretic multilinear curve and the multilinear regression method, as presented in an extended version of our paper (Cărăuşu & Vulpe 1993).

The failure probability of the IEDS is evaluated using HCLPF (high confidence low probability of failure) values, corresponding to the adopted fragility model under the "double lognormal format" :

$$(15)\qquad \begin{cases} F_A(a) = \Phi\left[\dfrac{\ln\,(a/A_m)}{\sigma_R}\right], \\ f_C(c) = \dfrac{1}{\sqrt{2\pi}\sigma_U c}\exp\left[-\dfrac{1}{2}\left[\dfrac{\ln\,(c/C_m)}{\sigma_U}\right]^2\right], \end{cases}$$

where the fragility parameters in Eq.(15) are well known (see (Hirata et al. 1991), (Hirata et al. (1993)).

The evaluation of the fragility parameters is performed in terms of a bilinear regression model, with the regression coefficients estimated on the basis of statistical evidence and what we have called 'tolerance intervals'. This regression line is derived on the basis of an equivalent linearization technique. The effective estimation of the regression coefficients and fragility parameters is performed by means of the LHS method (Latin hypercube sampling), known as an efficient simulation method.

5 CONCLUDING REMARKS

We have discussed some existing models and techniques for base isolation and energy dissipation devices in NPP structures and equipment, giving some extensions and stating proposals for a combination of well-known elastic (rubber) dampers and BMER system due to Hadjian (1993). Our study is rather theoretical, so far. It follows to introduce some numerical data and check the efficiency of our models. The fragility of isolation systems has received a rather limited attention [(Hirata 1989, 1991, 1993)]. It seems that out methods for evaluating fragility parameters for isolating and energy dissipating systems (extending the ones due to Hirata et al.) would be applicable.

REFERENCES

Cărăuşu, A. & A. Vulpe 1993. Fragility estimation for seismically isolated nuclear structures by HCLPF values and bi-linear regression. *Trans. SMiRT-12*, Vol. **M**, 237-242.

Hadjian, A.H. 1993. BMER - balance mitigation of earthquake responses - theory. *Trans. SMiRT-12*, Vol. **K2**, 327-332.

Hirata, K., Y. Kobayashi, H. Kameda, & H. Shiojiri 1989. Reliability analysis for seismically isolated FBR system. *Trans. SMiRT-10*, Vol. **M**, 115-120.

Hirata, K., S. Yabana, K. Ishida, H. Shiojiri & S. Yoshida 1991. Fragility estimation of isolated FBR structure. *Trans. SMiRT-11*, Vol. **M**, 235-240.

Hirata, K., A. Yamamoto & K. Ishida 1993. Evaluation of component fragility in isolated structure. *Trans. SMiRT-12*, Vol. **M**, 255-260.

Ishida, K., S. Yabana, G. Yoneda, J. Suhara & K. Yoshikawa 1993. Analytical Study on Ultimate Response Characteristics of Base Isolated Structures. *Trans. SMiRT-11*, Vol. **K2**, 309-314.

Kato, M., Watanabe, A. & A. Kato 1991. Study on the seismic base-isolated reactor building for demonstration FBR plant in Japan. *Trans. SMiRT-11*, Vol. **K2**, 97-102.

Koizumi, T., N. Tsujiuchi, F. Kishimoto, H. Iida & T. Fujita 1991. Base isolation technique for Tokamak type tusion teactor using adaptive control. *Trans. SMiRT-11*, Vol. **K2**, 49-54.

Sone, A. & S. Yamamoto 1991. Response analysis of base isolated structure with nonlinear damper. *Trans. SMiRT-11*, Vol. **K2**, 259-264.

Tajirian, F.F. & N.A. Abrahamson 1991. Response of seismic isolated structures during extreme events. *Trans. SMiRT 11*, Vol. **K2**, 247-252.

Zhou, F.L. 1991. Optimal design of base isolation and energy dissipation system for nuclear power plant structures. *Trans. SMiRT-11*, Vol. **K2**, 91-96.

Transactions of the 13th International Conference on Structural Mechanics in Reactor Technology (SMiRT 13), Escola de Engenharia - Universidade Federal do Rio Grande do Sul, Porto Alegre, Brazil, August 13-18, 1995

Three-dimensional base isolation system for assumed FBR reactor building

Tokuda, N.[1], Kashiwazaki, A.[1], Omata, I.[1], Ohnaka, T.[2]
1) Ishikawajima-Harima Heavy Industries Co., Ltd., Yokohama, Japan
2) Yokohama Rubber Co., Ltd.., Hiratsuka, Japan

ABSTRACT : A three-dimensional base isolation system for an assumed FBR reactor building is proposed, where a horizontally isolated building by laminated rubber bearings is supported by an intermediate slab which is vertically isolated by using air springs of high pressure. From some fundamental investigations on the above system, it is concluded that the system can be sufficiently practical by using the current industrially available techniques.

1. INTRODUCTION

Many works on seismic isolation of nuclear reactor facilities have been reported, where the majority deals with the use of horizontal isolation system only. In case of FBR, the use of vertical isolation is expected to result in significant benefits in the seismic design of thin walled structures due to severe thermal conditions. Because of the magnificent weight of reactor building, however, sufficiently flexible vertical isolator for reactor building has been considered to be unpractical.

The published works on the application of vertical isolation techniques to FBR seem to be confined to local isolation of the primary systems in reactor building. The most critical problem to be solved in the above local isolation method lies in the allowance of relative displacement between the isolated primary systems and the other non-isolated secondary ones. From this point of view, vertical as well as horizontal isolation of reactor building is the ideal one.

In the present paper, a three-dimensional base isolation system for an assumed FBR reactor building is proposed as shown in Fig.1. Here the horizontally isolated building using laminated rubber bearings is supported by an intermediate slab. Then, the above system is vertically isolated by using air springs of high pressure arranged under the intermediate slab.

A work of spring support system of buildings was reported (Huffmann,1988), where an example of 16,000 tons building is supported by metal coil springs. However, this application is for vibration isolation from environmental disturbances such as traffic ones in areas of low frequent earthquake attack.

The use of air springs as vertical isolator is promising from the view point of its potentially large loading capacity. The present authors developed a three-dimensional seismic isolation floor system using air springs and laminated rubber bearings (Uriu et al,1993).

The weight of FBR reactor building is supposed to be about 200,000 tons with base support area of 64m x 64m. Fundamental studies were carried out to investigate the

feasibility of high pressure air spring with such loading capacity under the current industrially available techniques. It is found that such an air spring is feasible by suppressing its horizontal deformation. This can be realized by using vertically flexible horizontal stopper for the intermediate slab. The existing technique of laminated rubber bearing suffices to the above objective.

Furthermore, seismic response of the above system was also evaluated by using an equivalent mass-spring model taking rocking motion into account. It is found that the rocking response under here used seismic input (Ishida et al,1989) is sufficiently small and vertical response can be reduced significantly.

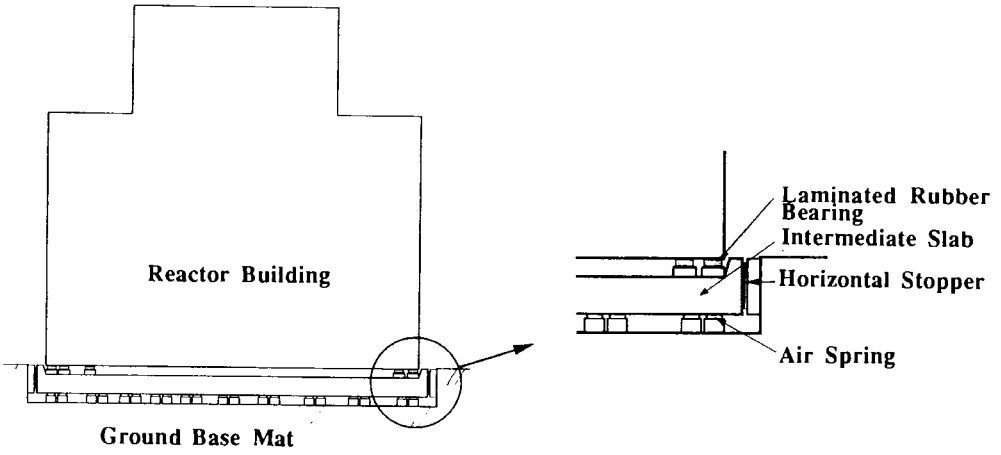

Fig.1 Three-Dimensional Base Isolation System for FBR Building

2 DESCRIPTION OF THE ISOLATION SYSTEM

2.1 General arrangement

As was mentioned, the fundamental structure of here proposed three-dimensional seismic isolation system for FBR reactor building is shown in Fig.1.

1.FBR reactor building is horizontally isolated by using laminated rubber bearing which are arranged under the base slab of the building and assumed to be very stiff in the vertical direction. This horizontal isolation system has been technically well established.

2.The above laminated rubber bearings in turn are supported on the upper surface of intermediate slab.

3.The weight of FBR reactor building is supposed to be 200,000 tons including the weight of intermediate slab. This weight is supported by using air springs arranged under the intermediate slab. The support area is assumed to be 64m x 64m.

4.The arrangement of air springs is shown in Fig.2. The support area of 64m x 64m is divided into 1024 small block areas of 2m x 2m. Keeping the maintenance path with 2m width and the spaces for support columns necessary during construction period or periodical inspection, 484 to 505 small block areas are available for the arrangement of air springs. In the following, 484 block areas for air springs is assumed.

5.From the view point of construction and maintenance works, the effective diameter of air springs to be stored in the small block area 2m x 2m is supposed to be 1.6m. In order to support 200,000 tons weight by 484 such air springs, the required loading capacity is about 410 tons per an air spring with its air pressure of 2.0 MPa.

6. In order to design the required air spring of the above high pressure, it is desirable to

suppress the horizontal deformation of air spring as small as possible. From this point of view, 84 horizontal stoppers are arranged along the side surface of intermediate slab. The stoppers are supported at the wall of ground base mat as shown in Fig.2. This stopper is required to be very stiff in the horizontal direction and deformable in the vertical direction. The existing technique of laminated rubber bearing suffices to the above objective.

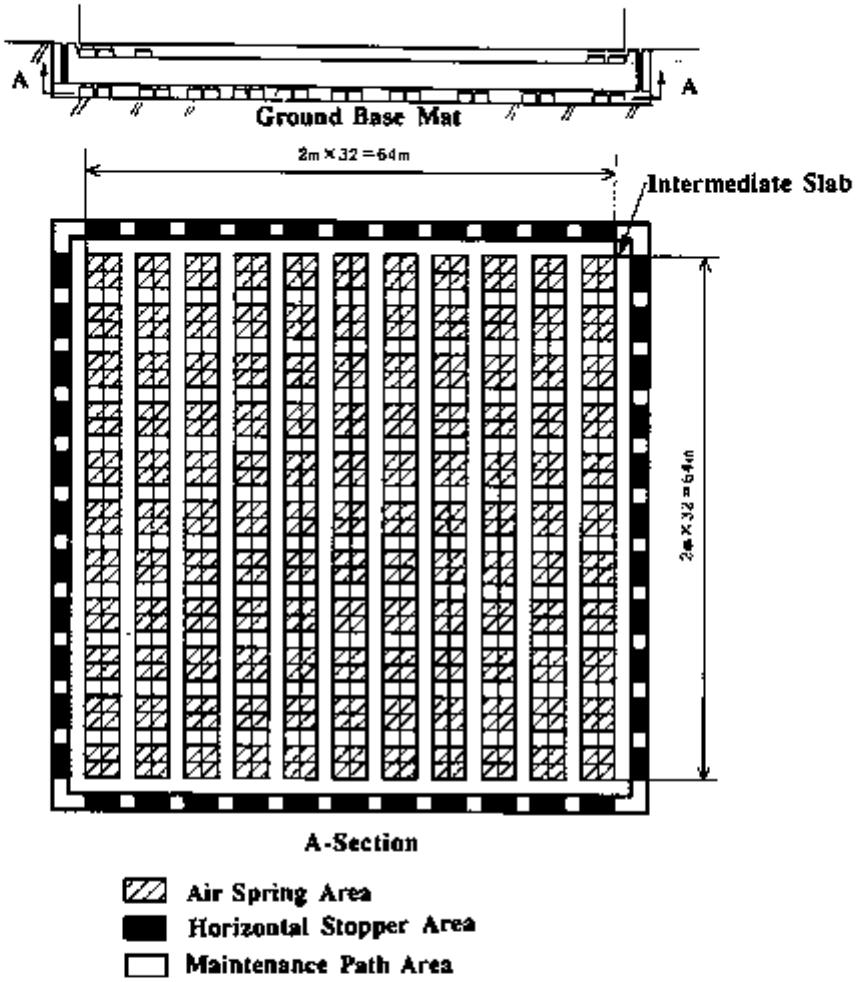

Fig.2 Arrangement of Air Springs and Horizontal Stoppers

2.2 Air spring

The air spring is schematically shown in Fig.3. The air spring is composed of outer and inner cylindrical shells, upper and lower circular plates and fiber reinforced rubber membrane. The components except for rubber membrane are made of steel.

The outer diameter of slackened part of rubber membrane is designed to be 40mm from the view point of its strength for required air pressure of 2MPa at its nominal condition. The allowable vertical stroke of air spring is designed to be 100mm considering the vertical deformation due to vertical and rocking motions under earthquake loading.

The air damping is utilized as a vertical damper with the auxiliary use of air tank, where the damping force is inducted from the air resistance generated at an orifice. By the parallel use of lead rubber bearing or high damping rubber bearing as horizontal stopper, the vertical damping ratio of 20% is easily ensured.

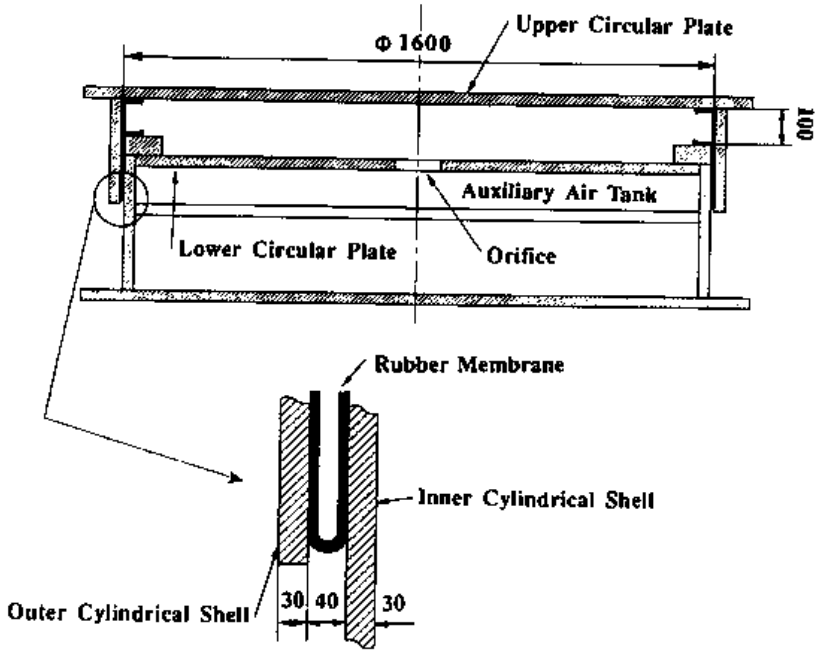

Fig.3 Air Spring

2.3 Horizontal stopper

Fig.4 schematically shows the horizontal stoppers. The laminated rubber bearings arranged lengthwise are used as horizontal stoppers, which are installed between the side surface of intermediate slab and the wall of ground base mat.

Their compressive (horizontal) stiffness can be very large so as to suppress horizontal deformation of air springs. The vertical stiffness of the above air springs is not sufficient for suppressing rocking motion. From this point of view, the vertical (shear) stiffness of the horizontal stopper is designed to keep sufficiently large. The allowable vertical displacement is designed to be 100mm, same as that of air springs.

The earthquake horizontal force should be supported by the compressive sides of horizontal stoppers alone, considering their low tensile strength. Therefore, for the installation of horizontal stopper between the intermediate slab and the ground base mat, the Dowel Pin method is adopted.

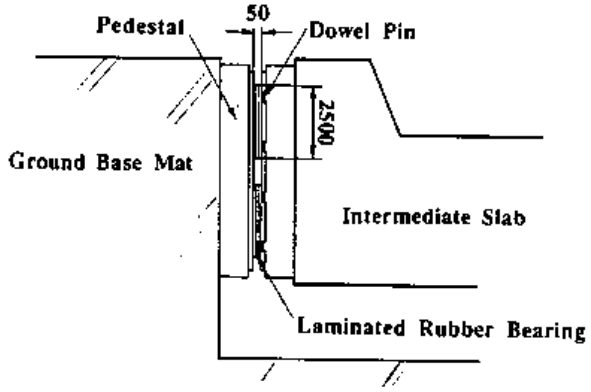

Fig.4 Horizontal Stopper

2.4 Intermediate slab

The intermediate slab is required to be keep sufficient bending stiffness by being made of steel or prestressed concrete.

3 EARTHQUAKE RESPONSE EVALUATION

3.1 Analysis Model

To evaluate earthquake response of the present three-dimensional isolated FBR reactor building, the response spectrum method was used. Fig.5 exhibits analytical model representing horizontal, vertical and rotational motions. The building was assumed to be rigid body and simple mass distribution. And the height of the center of gravity from the horizontal spring was supposed to be 20m.

Horizontal and vertical natural periods of isolation system were determined to be 2sec and 0.5sec, respectively, and every modal damping ratio were set to be 20%. To simplify the calculation, the weight of intermediate slab was added to that of building.

As the horizontal earthquake force, the response spectrum proposed by the Ishida et al (Fig.6) was used. And vertical input force was supposed to be a half of horizontal one without changing period characteristics.

To calculate the response of the FBR building (damping ratio of 20%) from the response spectrum by Ishida et al (damping ratio of 5%), the correction coefficient of 0.56 (MITI,1981) was used.

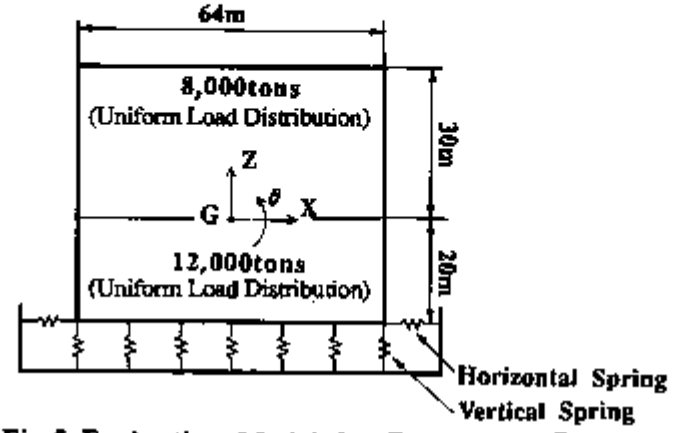

Fig.5 Evaluation Model for Earthquake Response

3.2 Evaluation

The earthquake response of building is represented by three vibration modes. One is the vertical translatory motion excited by vertical earthquake motion. And the other two are the so called rocking motions under horizontal excitation.

Table 1 shows the calculated responses of three vibration modes. According to the rocking motion, the maximum vertical response displacement occurs at the side edges of building. The absolute summation of maximum vertical displacements of air springs in Table 1 amounts to 30mm, which is less than a half of allowable vertical displacements of air spring (100mm). And horizontal and vertical response acceleration at the center of gravity are 0.2G and 0.18G, respectively.

From these results, excellent three dimensional isolation performance are found.

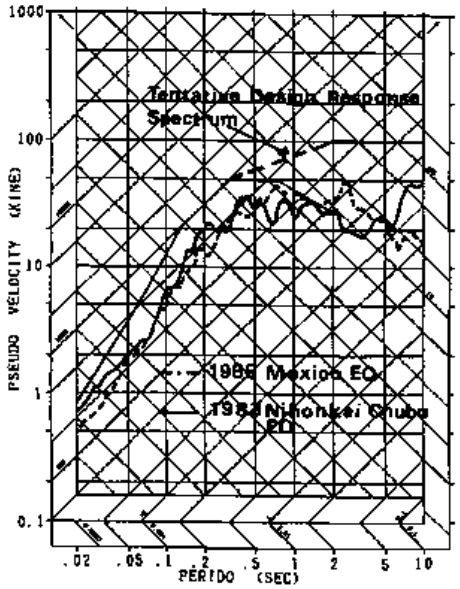

Fig.6 Response Spectrum (Ishida,1989)

Table 1 Calculated Responses by Response Spectrum Method

Vertical Translatory Mode	Natural Period Vertical Displacement Vertical Acceleration	0.5sec 14mm 0.18m/sec
Rocking Mode Dominated by Horizontal Motion	Natural Period Horizontal Displacement Horizontal Acceleration Vertical Displacement at Side Edge	2.1sec 181mm 0.20m/sec 14mm
Rocking Mode Dominated by Rotational Motion	Natural Period Vertical Displacement at Side Edge	0.5sec 2mm
	Absolute Summation of Vertical Displacement	30mm

4 CONCLUDING REMARKS

A three-dimensional base isolation system for an assumed FBR reactor building is proposed, where high pressure air springs are used as vertical isolator. Through the fundamental investigations on the above system, it is concluded that the present system can be sufficiently practical by using the current industrially available techniques.

Another merit of air spring is that it can play a role of a jack, which is very attractive from the view point of construction and maintenance works.

REFERENCES

Ishida,K. et al 1989. Tentative design response spectrum for seismically Isolated FBR, Trans. of 10th SMiRT K:685-690

Huffmann, G.K. 1988. Spring support of buildings : A Gerb system for full base isolation and protection against subsidences, ASME PVP Conf. Vol.147:101-107

The Ministry of International Trade and Industry 1989. Seismic design standard for high pressure gas facilities, MITI Notification 501 Sec.6, in Japanese

Uriu,K. et al 1993. Three-dimensional seismic isolation floor system using air spring and its installation into a nuclear facility, Trans. of 12th SMiRT K:363-368

Transactions of the 13th International Conference on Structural Mechanics in Reactor Technology (SMiRT 13), Escola de Engenharia - Universidade Federal do Rio Grande do Sul, Porto Alegre, Brazil, August 13-18, 1995

Influence of various parameters on effectiveness of seismic base isolation of nuclear equipments

Ebisawa, K.[1], Kameoka, H.[2], Takenouchi, I.[3], Kajiki, S.[3]
1) Japan Atomic Energy Research Institute, Ibaraki-ken, Japan
2) CRC Research Institute, Chiba-chi, Japan
3) Oiles Corporation, Japan

ABSTRACT: Authors developed a methodology and EBISA code for evaluating the applicability and the effectiveness of seismic base isolation of nuclear equipments.In order to investigate the influence of various parameters on the effectiveness of seismic base isolation, a sensitivity analysis was carried out for an emergency transformer with the base isolation devices. It was proved that seismic base isolation of equipment is very effective.This effectiveness can be influenced by the differences of the base isolation devices and the direction of the input seismic wave.

1 INTRODUCTION

Authors proposed a methodology for evaluating the applicability and the effectiveness of seismic base isolation for nuclear equipments [1].This methodology is based on the theory of Reliability Engineering and the method used in seismic Probabilistic Safety Assessment (PSA).Based on the above procedure, an Equipment Base Isolation System Analysis (EBISA) code was developed for evaluating the applicability and the effectiveness of seismic base isolation of equipments.

An emergency transformer which was identified to be important by previous seismic PSA [2] and usually used in Japanese commercial nuclear power plants was selected for the analysis.The transformer was seismically isolated by the base isolation devices of various types.In order to investigate the influence of various parameters on the effectiveness of seismic base isolation, a sensitivity study was carried out using the EBISA code.

This paper describes the results of sensitivity study on the differences of the isolation structure, the seismic base isolation device, its viscosity, and the frequency characteristic and the direction of input seismic wave.

2 METHODOLOGY FOR EVALUATING THE EFFECTIVENESS OF SEISMIC BASE ISOLATION OF NUCLEAR EQUIPMENTS

The procedure to evaluate the applicability and effectiveness of seismic base isolation of equipments consists of two steps; (1) quantitative evaluation and (2) comparative evaluation, as shown in Fig. 1.

In the first step, to decide the applicability of base isolated structures, the functional failure probability, F(t), during the life time, t (year), of equipment without base isolation devices is quantified. In the case that F(t) is significant in the context of safety and replacement cost considerations, the comparative evaluation is carried out.

In the second step, the ratio of the functional failure frequency, λ(1/year), without base isolation devices to that with them is quantified.The effectiveness can then be judged based on the ratio as shown in Fig. 1.

These F(t) and λ are estimated based on the methodology used in Reliability Engineering and the seismic PSA. F(t) can be calculated according to the formula:

$$F(t) = 1 - \exp(-\lambda \cdot t). \tag{1}$$

Parameter λ can be calculated using the density function of seismic hazard [3], H(α), which represents the annual exceedance occurrence frequency of ground motion level above α, and the functional failure probability, p(α), of equipment under α as follows:

$$\lambda = \int_0^\infty \left[\left(-dH(\alpha)/d\alpha \right) \cdot p(\alpha) \right] d\alpha. \tag{2}$$

If the seismic response, $f_R(\alpha, x)$, that affects the equipment failure is independent of the seismic capacity, $f_C(x)$, of the equipment, p(α) can be expressed as follows:

$$p(\alpha) = \int_0^\infty f_R(\alpha, x) \left\{ \int_0^x f_C(x)\, dx \right\} dx, \tag{3}$$

where $f_R(\alpha, x)$ and $f_C(x)$ are the probability density function of the logarithmic normal distribution. x represents parameters of acceleration and stress etc.

After both failure mode and vulnerable part of equipment are identified, the realistic response of equipment at the vulnerable part is estimated based on the response factor method [4]. In this method, the realistic response, $f_R(\alpha^D, x)$, against the design ground motion level α^D is estimated by dividing the design response, q^D, to α^D by the response factor F_R.

Assuming that $f_R(\alpha^D, x)$ is proportional to an acceleration level α, the realistic response, $f_R(\alpha, x)$, is estimated according to the formula Eq. (4).

Where F_R is introduced as a measure of conservatism in seismic design analysis.

It is defined as a ratio of conservative design response to realistic response and has a probability density function represented by the logarithmic normal distribution of the median $\overline{F_R}$ and the logarithmic standard deviation β_R.

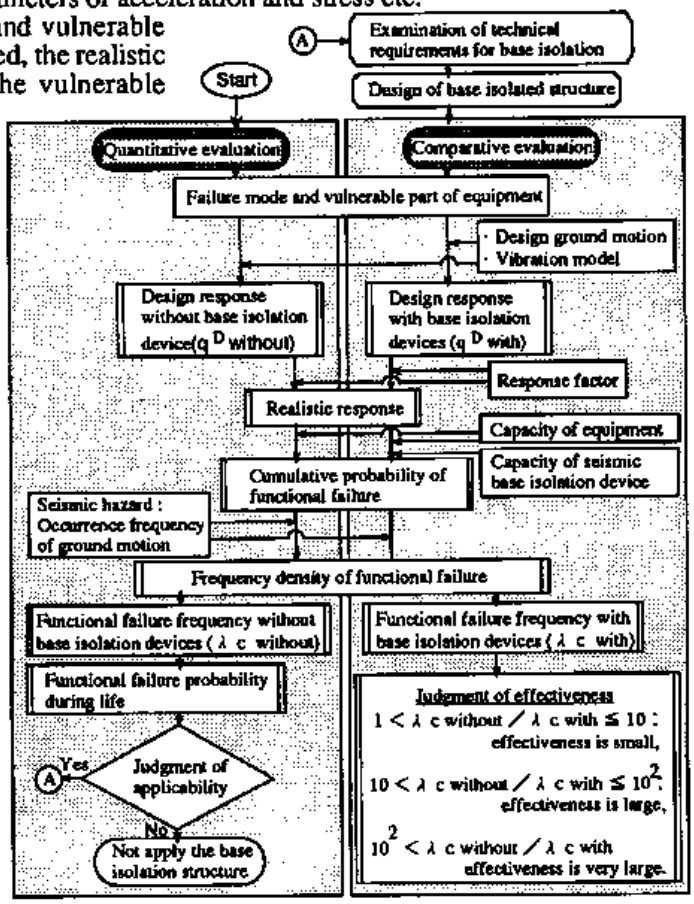

Fig.1 Evaluation methodology for applicability and effectiveness of seismic base isolated structure

$f_C(x)$ is also represented by the logarithmic normal distribution of the median M_C and the logarithmic standard deviation β_C to the formula Eq. (5).

$$f_R(\alpha, x) = \frac{1}{\sqrt{2\pi}\beta_R x} \exp\left[-\left(\ln x - \ln \frac{q^D \alpha}{\overline{F_R} \alpha^D} \right)^2 / 2\beta_R^2 \right]. \tag{4}$$

$$f_C(x) = \frac{1}{\sqrt{2\pi}\beta_C x} \exp\left[-\left(\ln x - \ln M_C \right)^2 / 2\beta_C^2 \right]. \tag{5}$$

3 CONDITUIONS OF SENSITIVITY ANALYSIS

3.1 SEISMIC BASE ISOLATION STRUCTURE

(1) Transformer with Ceramic Tubes
A high voltage type emergency transformer of 275 kV with ceramic tubes was selected for the analysis. This transformer was identified to be an important equipment by previous seismic PSA and usually used in Japanese commercial nuclear power plants.
The transformer consists of three ceramic tubes charged with the isolation oil, the body and the foundation etc. as shown in Fig. 2. A weight of the ceramic tube and the body is about 1.9 and 78 tf, respectively.

The transformers are presumed to be in use for 40 years as a design life and to locate at Tokai site of the Japan Atomic Energy Research Institute (JAERI).

(2) Seismic Base Isolation Devices
The transformer was seismically isolated by the base isolation devices of three types; a high damping rubber bearings (HRB), a lead rubber bearing (LRB) and a ball bearing with coil springs and viscous dampers (BCV), which have a beneficial effect on base isolated structure of heavy equipment such as the transformer.They were installed on each pedestal of square corners between the body and the foundation as shown in Fig. 2.

Rated weight, horizontal stiffness corresponds to natural frequency and mean damping value for the above isolation devices are shown in Table 1.

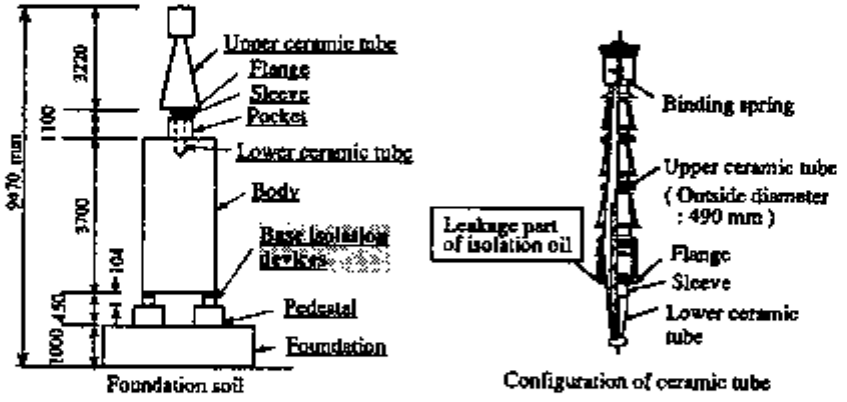

Fig.2 Geometry of transformer structure with ceramic tube and situation of base isolation devices

Table 1 Main specification of seismic base isolation devices

	Rated weight (tf)	Horizontal stiffness (Hz)	Mean damping value (%)
High damping rubber bearing (HRB)	20	1.0	14
Lead rubber bearing (LRB)		0.5	20
Ball bearing with coil springs and viscous dampers (BCV)		0.3	30

! SEISMIC HAZARD, RESPONSE AND CAPACITY OF BASE ISOLATION STRUCTURE

Seismic Hazard
: seismic hazard at JAERI Tokai site which was estimated by one of the authors [3] (Fig. 3) was used in the analysis.

(2) Seismic Response
The realistic response of the transformer is estimated using its response factor F_R and design response q^D. The F_R estimated by one of the authors was used ($\overline{F_R}$ =1.21,β_R = 0.58) [5].The q^D was calculated by the direct integration method using the time history of design ground motion and the multi-lumped mass vibration model. In this model, the spring constants of sway and rocking represented the soil-transformer interaction have values of 1.6×10^4 ton/cm and 4.0×10^9 ton·cm/rad, respectively. The rocking spring constant between the sleeve and the upper ceramic tube has a value of 1.0×10^5 ton·cm/rad.

In the vibration model, the response of tube is considered to be dominated by the rocking spring between the sleeve and the upper ceramic tube.

(3) Seismic Capacity
The functional failure of the base isolation structure which consists of the transformer and isolation devices is supposed to be caused by at least one failure of the transformer and isolation devices.The smaller value between the functional failure value of the transformer and isolation devices was presumed to be the capacity of the isolation structure.

The vulnerable part of the transformer in section 3.1 was considered to be the area at the flange between the upper tube and the sleeve, and the functional failure mode was identified to be the leakage of isolation oil from at least one tube based on the records of disaster earthquake.The capacity of transformer were estimated by one of authors using the vibration test data for the functional failure of the transformer [1].

The functional failure mode of LRB or HRB was considered to be the shear rupture of rubber. One of BCV was presumed to be the leap of the ball bearings caused by the uplift of the ball bearing part. From comparing the capacity of the transformer with that of LRB or HRB, the capacity of the transformer with LRB or HRB was presumed to be derived from the transformer failure [6],[7]. In the same way, the capacity of the transformer with BCV was presumed to be derived from BCV failure [6],[7].

Each capacity of the transformer with LRB, HRB and BCV is shown in Table 2.

Table 2 Capacities of transformer with seismic base isolation devices

	Mean value (Gal)	Logarithmic standard deviation	Failure mode/ Vulnerable part
Transformer with high damping rubber bearing (HRB)	650	0.1	Leakage of isolation oil at flange between upper ceramic tube and sleeve
Transformer with lead rubber bearing (LRB)			
Transformer with ball bearing with coil springs and viscous dampers (BCV)	1440	0.2	Leap of ball bearings caused by uplift of BCV part

4 RESULTS OF SENSITIVITY ANALYSIS

4.1 PARAMETERS OF SENSITIVITY ANALYSIS

Parameters of the sensitivity analysis are as follows.

Case 1: the difference of structure; structure without and with base isolation devices,

Case 2: the difference of base isolation devices; LRB , HRB and BCV,

Case 3: the difference of BCV's viscosity by temperature; -3, 13.5 and 30 °C.,

Case 4: the difference of frequency characteristic of input seismic wave; S_1F^H (maximum acceleration: 287 Gal) of the predominant frequency of about 2.9 Hz by far earthquake, and S_1N^H (maximum acceleration: 267 Gal) of about 6.3 Hz by near earthquake, and

Case 5: the difference of direction of input seismic wave; S_1F^H of horizontal wave, and $S_1F_V^H$ that consists of both S_1F^H and S_1F_V (maximum acceleration: 137 Gal) of vertical wave.

4.2 RESULTS OF SENSITIVITY ANALYSIS

The results of the design response q^D and the functional failure frequency λ of transformer without isolation devices or with them for each case are shown in Table 3.

(1) Case 1: the difference of structure
The vulnerable part of transformer without isolation devices is the upper ceramic tube and $q^D_{without}$ at its part to S_1F^H was calculated to be about 755 Gal. An amplification to $q^D_{without}$ of maximum acceleration of S_1F^H is about 2.6.

By substituting $q^D_{without}$ and the estimated others values for Eq. from (2) to (5), the functional failure frequency, $\lambda_{without}$, of the transformer without isolation devices was calculated to be about 1.0×10^{-3}(1/year). From $\lambda_{without}$ and Eq. (1), F(40) during the life time of 40 years was about 4 %.

Assuming that this value is significant, the comparative evaluation was carried out.

(2) Case 2: the difference of base isolation devices
Each design response at the upper ceramic tube of transformer with LRB, HRB and BCV (temperature:13.5°C.) to S_1F^H was about 77, 185 and 49 Gal, respectively. Each amplification to q^D_{with} of maximum acceleration of S_1F^H ranges from about 1/2 to 1/6 for all the isolation devices. Thus, the effect of isolation system is very large.

Each vulnerable part of transformer with LRB and HRB is the upper ceramic tube and design response q^D_{with} at its part is about 77 and 185, respectively. The vulnerable part of transformer with BCV is the ball bearing part and q^D_{with} at its part is about 296 Gal.

Each functional failure frequency, λ_{with}, at the vulnerable part of the transformer with LRB, HRB and BCV was calculated to be about 2.0×10^{-8} (Case2-1), 4.7×10^{-6} (Case2-2) and 1.6×10^{-6} (1/year) (Case2-3), respectively. The ratio of $\lambda_{without}$ to λ_{with} for each devices is larger than about 10^3 for all the isolation devices. Fig. 3 shows cumulative probabilities and frequencies densities of functional failure of transformer with base isolation devices or without them as a function of the acceleration level at bedrock.
From these results, it is proved that seismic base isolation of equipment is very effective.

Table 3 Results of design responses and functional failure frequencies for each case on sensitivity analysis

Case	Base isolation devices	Seismic wave	Temperature	Design response at upper ceramic tube qD (Gal)	Design response at vulnerable part qD (Gal)	Functional failure frequency l (1/year)
Case 1	without base isolation devices	S_1F^H	–	755	755	1.0×10^{-3}
Case2-1	with LRB	S_1F^H	–	77	77	2.0×10^{-8}
Case2-2	with HRB	S_1F^H	–	185	185	4.7×10^{-6}
Case2-3	with BCV	S_1F^H	13.5°C	49	296	1.6×10^{-6}
Case3-1	with BCV	S_1F^H	30°C	40	296	1.6×10^{-6}
Case3-2	with BCV	S_1F^H	-3°C	78	296	1.6×10^{-6}
Case 4	with LRB	S_1N^H	–	52	52	5.2×10^{-9}
Case 5	with LRB	$S_1F^{H}_{V}$	–	191	191	1.3×10^{-5}

LRB : Lead rubber bearing HRB : High damping rubber bearing BCV : Ball bearing with coil springs and viscous dampers
S_1F^H, S_1N^H : Only horizontal direction of input seismic wave S_1F or S_1N
$S_1F^{H}_{V}$: Both horizontal and vertical direction of input seismic wave S_1F

(3) Case 3: the difference of BCV's viscosity by temperature
Each design response at the upper ceramic tube of transformer with BCV of temperature of -3 and 30°C. to S_1F^H was about 78 and 40 Gal, respectively. Each amplification to these design response of maximum acceleration of S_1F^H ranges from about 1/4 to 1/7, respectively. Then the effect of BCV system is larger than that of LRB or HRB.

Each λ_{with} for the above temperature are the same 1.6×10^{-6} (1/year) as case2-3. Because the design response at the vulnerable part is the same value 296 Gal as case2-3. In this case, the effectiveness of seismic base isolation is independent of the temperature.

(4) Case4: the difference of frequency characteristic of input seismic wave

The q^D_{with} at the upper ceramic tube of transformer with LRB to ${}_{S_1}N^H$ was about 52 Gal. λ_{with} estimated was smaller than that to ${}_{S_1}F^H$ (Case 2-1).

From this result, it is proved that the effectiveness of the seismic base isolation of equipment to the wave of high predominant frequency is lager than that to low frequency.

(5) Case 5: the difference of direction of input seismic wave

The q^D_{with} at the upper ceramic tube of transformer with LRB to ${}_{S_1}F^H_V$ was about 191 Gal.The λ_{with} in this case was over three order larger than that to ${}_{S_1}F^H$ (Case 2-1).

From this result, it is proved that the effectiveness of seismic base isolation of equipment is influenced by the differences of direction of the input seismic wave.

5 SUMMARY

In order to investigate the influence of various parameters on the effectiveness of seismic base isolation of nuclear equipments, a sensitivity analysis was carried out using EBISA code. From the results of sensitivity analysis,it is proved that seismic base isolation of equipment is very effective. Therefore it can be applied to improve the plant safety.

The effectiveness of seismic base isolation can be influenced by the differences of the base isolation devices and the component of the input seismic wave.

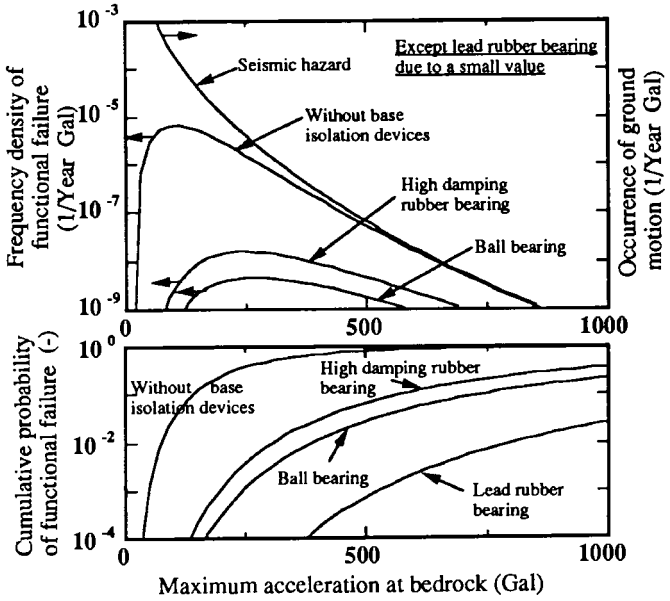

Fig.3 Calculated results of cumulative probabilities and frequency densities of functional failure of transformer with ceramic tube and with base isolation devices or without them

References

[1] K.Ebisawa and T.Uga: Evaluation methodology for seismic base isolation of nuclear equipments, Nucl. Engrg. and Des. 142, (1993).
[2] NRC,NUREG-1150, (1989).
[3] K.Ebisawa, et al.: A methodology of probabilistic seismic hazard evaluation and sensitivity study, Proc. of Japan Society of Civil Engineers, Vol.437/I-17, (1991).*
[4] R.P.Kennedy, et al.: Seismic fragilities for nuclear power plant risk studies, Nucl. Engrg. and Des.79, (1984).
[5] K.Ebisawa, et al.: Evaluation of response factors for seismic probabilistic safety assessment of nuclear power plants, Nucl. Engrg. and Des.147, (1994).
[6] K.Ebisawa, et al.: Selection criteria of seismic base isolation devices to nuclear equipment, Proc. of 9th Japan Earthquake Engineering Symp., No. 296, (1994).*
[7] Y.Kameoka, et al.: Response performance on seismic base isolation of emergency transformer with ceramic tubes, Proc. of the 22th Japan Society of Civil Engineers Earthquake Engineering Symp., No. 213, (1993).*
*: In Japanese

Transactions of the 13th International Conference on Structural Mechanics in Reactor Technology (SMiRT 13), Escola de Engenharia - Universidade Federal do Rio Grande do Sul, Porto Alegre, Brazil, August 13-18, 1995

F.E. models of steel-laminated rubber bearings for seismic isolation of nuclear facilities

Forni, M.[1], Martelli, A.[1], Dusi, A.[2], Castellano, G.[3]
1) ENEA-ERG-FISS, Bologna, Italy
2) ENEL-CRIS, Milano, Italy
3) University of Ancona, Italy

ABSTRACT: Non-linear finite-element models of high damping rubber bearings have been developed and implemented in the ABAQUS code in the framework of Italian co-operative studies for seismic isolation development. The hyperelastic models used have been based on the results of tests on rubber specimens. The isolators models are being validated through comparisons of numerical results with complete bearing test data. The main features of the analysis are reported, together with an example of validation.

1 INTRODUCTION AND SCOPE

Aim of this study is the implementation, in the ABAQUS code, and validation of non-linear (both axisymmetric and three-dimensional) finite-element models (FEMs) of High Damping steel-laminated Rubber Bearings (HDRBs) used for the seismic isolation of civil structures and industrial plants. The work has been performed in the framework of the Italian activities on seismic isolation development and application (see Marioni et al. 1995 and Forni et al. 1995a). Validation of the models is based on the results of a wide ranging experimental campaign which is in progress at ISMES on single HDRBs (Martelli et al. 1995a).

2 ISOLATORS CONSIDERED

The HDRBs are formed by alternate vulcanized rubber layers and steel plates, bonded together by use of chemical compounds. They are usually placed between the structure and its foundations. Their features provide high stiffness in the vertical direction (to support the dead load) and low stiffness in the transverse direction (which minimizes amplification of ground acceleration, by leading, however, to large horizontal displacements during strong earthquakes). Figure 1 shows the sketch of an optimized full-scale isolator, manufactured by ALGA, which is being analysed in the above-mentioned experimental campaign. Three different *scales* (1:1, 1:2 and 1:4) and two *shape factors* (S = 12 and S = 24) are being considered in the tests for this bearing. This study refers to the half scale isolators with S=12 shape factor, because only for these measured data are already available.

In addition, five *attachment systems* between the isolator and the structure are being considered in the experiments: 'recess', 'bolts', 'bolts & central dowel', 'central dowel' and

'bonding'. 'Recess' and 'central dowel' attachments are very similar and the most difficult to model because they involve monolateral contact between rigid surface and deformable body. 'Bolts', 'bolts & central dowel' and 'bonding' attachment systems are practically equivalent from the kinematic point of view and correspond to a perfect encastre of the two bases of the isolator to the structure. In this work, only the 'recess' and 'bolts' attachments have already been considered (see Figure 2-a, b).

As regards *materials*, because the HDLRBs are characterized by a highly non-linear behaviour in terms of stiffness, a hyperelastic model is necessary for the rubber and an elastic-plastic for steel (at large displacements) to correctly describe the actual behaviour. HDRB damping is pratically independent of velocity and non-linearly dependent on displacement (hysteretic damping). Its effects on the isolator stress distribution and stiffness have been neglected in the present step of the analysis. In a near future, an appropriate model (UMAT subroutine in ABAQUS) will be prepared to take into account the damping behaviour. Although two different rubber compounds (soft, G = 0.4 MPa, and hard, G = 0.8 MPa), developed by MRPRA, have been considered in the tests, the hard rubber only has been analysed to date. This rubber is the most difficult to model, due to the high design loads which involve some creep and plastic effects, impossible to be calculated by the hyperelastic theory.

Finally, as regards *loads*, it is noted that the full-scale isolator of Figure 1 supports a design vertical load of 1600 kN (800 kN in the case of soft rubber). In order to have the actual stress in the rubber (which is required by a correct application of similitude laws), the values for the 1:2 and 1:4 scales have been 400 kN and 100 kN respectively (the half in the case of soft rubber). The design shear strain (that is the shear strain corresponding to design earthquake) has been assumed to be 100% of the total rubber thickness (150 mm for the full scale in the tests of Martelli et al. 1995a). Qualification tests are generally carried out up to twice the design displacement (i.e. generally to at least 200% shear strain) under the design vertical load; during failure tests, 400% shear strain is often exceeded (Martelli et al. 1995a). Figures 3-a and 3-b show a compression and a shear test under vertical compression load on a half-scale isolator performed using SISTEM.

3 FINITE ELEMENT MODELS

Axisymmetric models of the above-mentioned isolators have been developed and implemented in ABAQUS (see ABAQUS User's Manual). Due to the geometry considered and the loads applied (see Figures 2, 3), axisymmetric elements with non-axisymmetric deformation have been used to model the seismic isolator. Some detailed meshes have been analysed in order to reach stability and convergence. A minimum of three layers of CAXA4Hn elements for each rubber layer have been necessary to model the rubber parts (n=1 is generally sufficient). SAXA11 shell elements have been used for the steel plates. Seven subdivisions along the radius have been sufficient for the 'bolts' attachment systems, thus the isolator FEM consists of 630 CAXA4H1 elements and 224 SAXA11 shell elements in the case of the lower shape factor and 1260 CAXA4H1 elements and 434 SAXA4H1 shell elements in that of the higher shape factor.

In addition to axisymmetric models, a *three-dimensional model* has been implemented to verify the CAXA elements' behaviour, to model the monolateral 'recess' attachment system and to reach large non-axisymmetric shear strains. 3D models are also usefull to correctly describe the tensile stress on bolts (if present), combined compression - shear - torsion stress-strain distribution (if eccentricity is relevant), presence of defects, and effects of the construction tolerances and others asymmetries. Some 3D meshes have

been implemented using PREABC, a computer program developed by ENEA which writes the ABAQUS input files for 3D cylindrical models based on a few geometric input data. In this case also, 7 subdivision along the radius and three layers of solid (C3D8H) elements for each rubber layer have been necessary to model the rubber. Steel plates have been modelled by using S4R5 shell elements. Taking into account 32 subdivision along the external circumference, the 3D model for the lower shape factor isolator includes 9680 nodes and 4868 elements and requires a minimum of four hours of CPU time on a RISC6000 work station (against ten minutes of the axisymmetric model) for the execution of two static steps (compression and shear).

4 HYPERELASTIC MODEL

The hyperelastic model of ABAQUS is based on the definition of the stress components as function of the strain energy potential U, a very complex function of λ_i (principal stretch ratio, which is the current specimen length over the original length in the principal i-direction), $C_{i,j}$ (material constants describing the hyperelastic behaviour) and D_i (material constants describing compressibility, equal to zero for incompressible materials). The function U is written in polynomial form of the first order (used for small strains) or second order (recommended for large strains). The calibration of the hyperelastic model consists of the definition of the $C_{i,j}$ and (if compressibility is relevant) D_i material constants. This can be done in particular test configurations where, due to the specimen shape and the loading conditions, one or two λ_i components can be neglected or correlated between themselves and some σ_{ij} (stress) components can be put equal to zero, thus considerably simplifying the expression of U.

According to Rebelo (1991) and ABAQUS User's Manual, uniaxial, biaxial and shear experiments on specimens were designed and performed (Martelli et al. 1995a). Each test was performed on 3 specimens drawn from the centre of each rubber batch used for the manufacturing of isolators, both in the unscragged and scragged conditions. It is noted that no compressibility tests were executed, due to the relatively low shape factor of the analysed isolators.

Uniaxial tensile and compression tests must satisfy the following conditions:

$$\sigma_{22} = \sigma_{33} = \sigma_{12} = \sigma_{13} = \sigma_{23} = 0 \qquad (1)$$

$$\lambda_2 = \lambda_3 = 1/\sqrt{\lambda_1} \qquad (2)$$

The correlation (2) is strictly valid for incompressible materials only, which is the case of rubber specimens that have the possibility to strain in two principal directions at least.

The tensile tests were carried out according to ASTM D 412 on dog-bone specimens (30mm x 6mm x 2mm). No significative scattering of test results was detected. Some simple calculations were executed on a single C3D8H element to evaluate the differences of the two hyperelastic models proposed by the ABAQUS User's Manual (Ogden and the above mentioned polynomial). Figure 4 shows the good agreement between both the models and with the measured curve.

The compression tests were carried out according to ASTM D 395 on 3 cylindrical specimens (diameter = 29 mm, height =13 mm) with lubricated bases. In this case also, no significant scattering of test results was present and perfect agreement between the calculated and measured results was found (Figure 5).

As an alternative option to the uniaxial compression tests, *equibiaxial (no shear) tests* may be performed. We executed such tests on thin square specimens (300mm x 300mm x 5mm), strained in the principal directions 1 and 2 (using a constant velocity of 100 mm/min), thus to satisfy the following conditions:

$$\sigma_{11} = \sigma_{22};\ \sigma_{33} = \sigma_{12} = \sigma_{13} = \sigma_{23} = 0 \tag{3}$$

$$\lambda_1 = \lambda_2 = 1/\sqrt{\lambda_3} \tag{4}$$

These tests are quite expensive and rather difficult to be executed, but allow larger deformations to be achieved with respect to the compression tests, where friction between the specimen and the test device does not permit to reach strains higher than 35% in real uniaxial conditions (see equations 1 and 2). Figure 6 shows the equipment that we used for the equibiaxial tests and the optical instrumentation that we adopted to measure the strain in the central part of the specimen, far away from boundary perturbations. The calculated and measured stress-strain curves don't agree perfectly in this case (Figure 7); however, for the second order polynomial model, the agreement can be considered sufficient.

Finally, *planar (pure shear) tests* were carried out on rectangular specimens (300mm x 120mm x 5mm) strained along their longer edge (principal direction=1), using a constant velocity of 100 mm/min, in order to satisfy the following condions:

$$\sigma_{33} = 0 \tag{5}$$

$$\lambda_2 = 1;\ \lambda_1 = 1/\lambda_3 \tag{6}$$

The test equipment shown in Figure 8 allowed for large displacements; in fact, the optical instrumentations measured a strain larger than 300% in the central part of the specimens. In this case also, the second order polynomial model provided the best agreement with the experimental results (Figure 9).

5 VERIFICATION OF THE ISOLATOR FEMs

Based on the results of the previous section, the polynomial hyperelastic model with N=2 has been adopted for the analysis of the experimental tests on the complete isolators. The curves shown in Figures 4, 7 and 9 were used for input data.

An axisymmetric model with five elements for each rubber layer was used for calculating the *vertical stiffness*. Both scragged and unscragged rubber hyperelastic models with input data at 150% for uniaxial test, 120% for biaxial test and 300% for planar test, were used. Figure 10 shows that the agreement between the calculated and measure values for the unscragged rubber is good up to the design load (400 kN), then the model becames too stiff. This is probably due to rubber plasticity and creep phenomena occurred during the isolator tests at high loads. For the scragged rubber, the agreement is good to 1.5 times the design vertical load.

Both axisymmetric (for low shear strains) and 3D models (for high shear strains) were used for calculating the *horizontal stiffness* at 50%, 100% and 200% shear strain, under the design vertical compression load (Martelli et al. 1995a). Due to the quite large range of deformation, it is not possible to use a unique hyperelastic model, but an appropriate

model must be calibrated for each deformations of interest. For the evaluation of the horizontal stiffness at 50% shear strain, an axisymmetric FEM (with three layers of elements for each rubber layer) using the unscragged rubber input data not exceeding 100% for uniaxial and biaxial tests and 150% for planar test, had to be used. Figure 11 shows that the agreement between the calculated and measured horizontal stiffness is very good, taking into account that the model has no damping (thus the hysteresis loop connot be reproduced). For the evaluation of the horizontal stiffness at 100% shear strain, the same model for the unscragged rubber, including uniaxial input data up to 150%, biaxial input data up to 120% and planar input data up to 300%, had to be used. In this case also, the agreement between the calculated and measured values was good (see Figure 12), but the unscragged model became too rigid at high deformations, with respect to the isolator, which was subjected to the two cycles at 50% shear strain. For higher shear strains, a 3D FEM and a scragged rubber model (with input data for the hyperelastic model mostly concentrated at large strains) had to be used. We found a good agreement between calculated and measured values to 180% shear strain, then the model became too stiff (partly due to some inaccurancy of the hyperelastic model related to insufficient conditioning of specimens), similar to the case of the vertical stiffness calculation. Anyway, it has been confirmed that the hyperelastic model can be used at large shear strains to analyse the stress distribution (Figure 13) and identify the most stressed parts of the isolator. To this aim, some parametric calculations have been performed in order to evaluate the effects of the attachment system, shape factor, steel plate thickness, central hole diameter, etc., on the rubber stress. The first results of this analysis (which is still in progress) show that the 'recess' attachment system is less stiff than the 'bolted' system (which is in agreement with the experimental results) and that the central hole significantly decreases the stress on the rubber, but increases that in the steel plates. More details will be reported by Forni et al. (1995a & b).

CONCLUSIONS AND FUTURE WORK

This paper has summarized the main features of numerical activities which are in progress for the development and validation of finite-element models of steel-laminated high damping rubber bearings. An example of validation has been presented. Such a work will be completed by including damping models and will be extended to all the isolators considered in the tests of Martelli et al. (1995a), namely to optimized isolators with different sizes, rubber compounds, attachment systems, and shape factors. Updated results will be presented by Forni et al. (1995a & b).

The availability of reliable isolators' models will allow the number of quite costly experimental tests on complete bearings to be considerably limited, not only as regards the analysis of the effects of some important parameters (e.g. temperature, ageing, vertical load on horizontal stiffness, etc.), but also for complicated experiments like for instance, failure tests and analysis of the effects of defects.

Should the models developed be sufficiently reliable, they may be used for bearing qualification, as stressed by Martelli et al. (1995b).

Finally, as soon as the experiments of Martelli et al. (1995a) on structure mock-ups isolated by means of the bearings under consideration will be completed, numerical analysis will also be performed to analyse these tests.

REFERENCES

ABAQUS User's Manual - Version 5.3. Pawtucket: Hibbit, Karlsson & Sorensen, Inc.

Forni, M. & A. Martelli 1995a. Finite-element models of rubber bearings and guidelines development for isolated nuclear facilities in Italy. *Proc. Post-SMiRT Conf. Seminar on Seismic Isolation, Passive Energy Dissipation and Active Control of Structures, Santiago, 21-23 August 1995.*

Forni, M., Martelli, A., Dusi, A. and G. Castellano 1995b. Hyperelastic models of steel-laminated rubber bearings for the seismic isolation of civil buildings and industrial plants. *Proc. ABAQUS User's Conf., Paris, 31 May - 2 June 1995.*

Marioni, A., Martelli, A., Forni, M., Bonacina, G., Bettinali, F. & C. Mazzieri 1995. Progress in applications and experimental studies for isolated structures in Italy. *Proc. Post-SMiRT Conf. Seminar on Seismic Isolation, Passive Energy Dissipation and Active Control of Structures, Santiago, 21-23 August 1995.*

Martelli, A., Forni, M., Spadoni, B., Marioni, A., Bonacina, G. & G. Pucci 1995a. Progress of Italian experimental activities on seismic isolation. *Proc. 13th Int. SMiRT Conf., Porto Alegre, 13-18 August 1995.* Rotterdam: Balkema.

Martelli, A., Forni, M., Bergamo, G., Bonacina, G., Cesari, G.F., Di Pasquale, G. & M. Olivieri 1995b. Proposal for design guidelines for isolated nuclear reactors. *Proc. Post-SMiRT Conf. Seminar on Seismic Isolation, Passive Energy Dissipation and Active Control of Structures, Santiago, 21-23 August 1995.*

Rebelo, N. 1991. Analysis of rubber components with ABAQUS. *Proc. of 2° National Congress of ABAQUS Users' Group Italia, Bologna, Italy, March 21-22.*

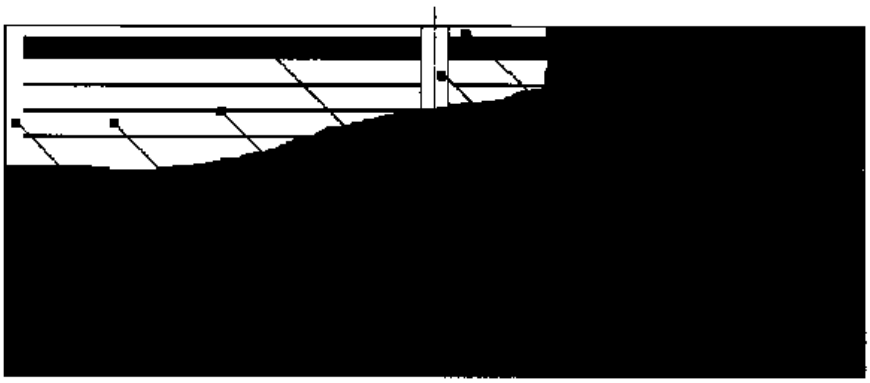

Figure 1. Sketch of the full-scale HDRB

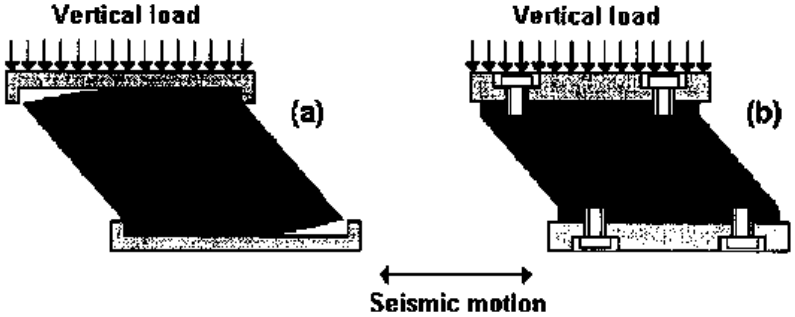

Figure 2. 'Recess' (a) and 'bolts' (b) attachment systems.

Figure 3a. Compression test performed on SISTEM on HDRB.

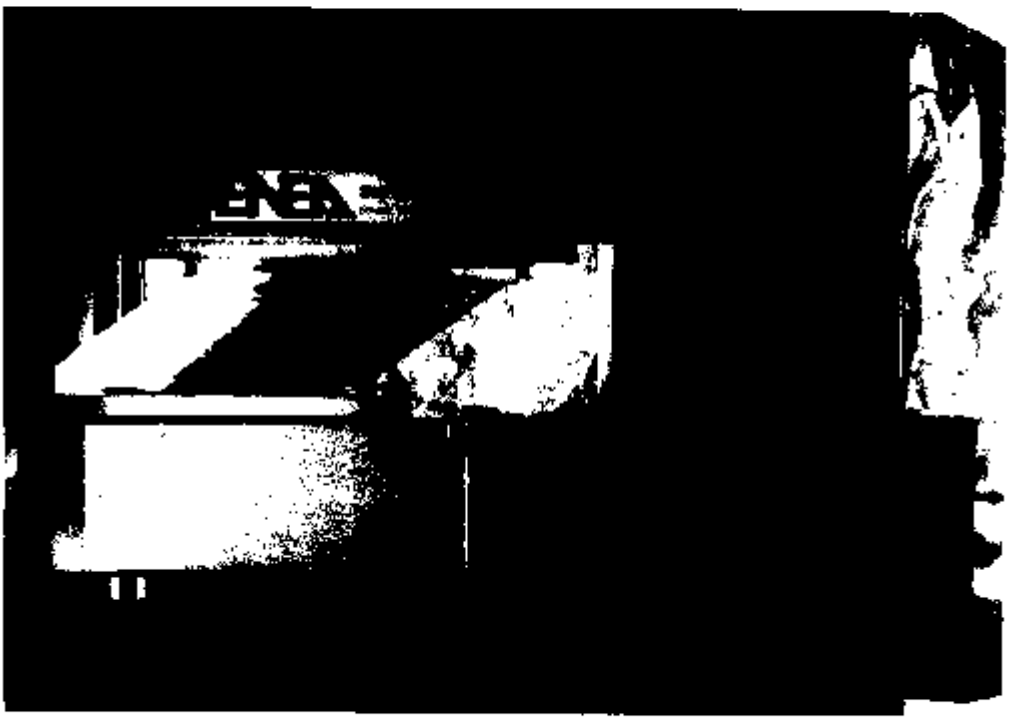

Figure 3b. Combined compression & shear test performed on SISTEM on HDRB.

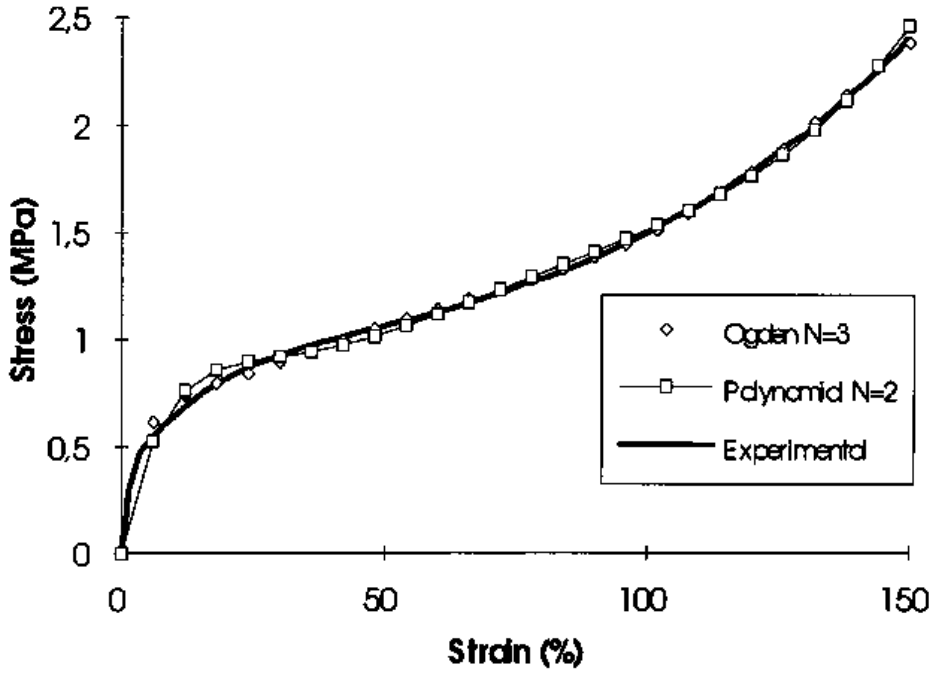

Figure 4. Comparison between measured and calculated stress-strain values for a tensile test on unscragged rubber compound

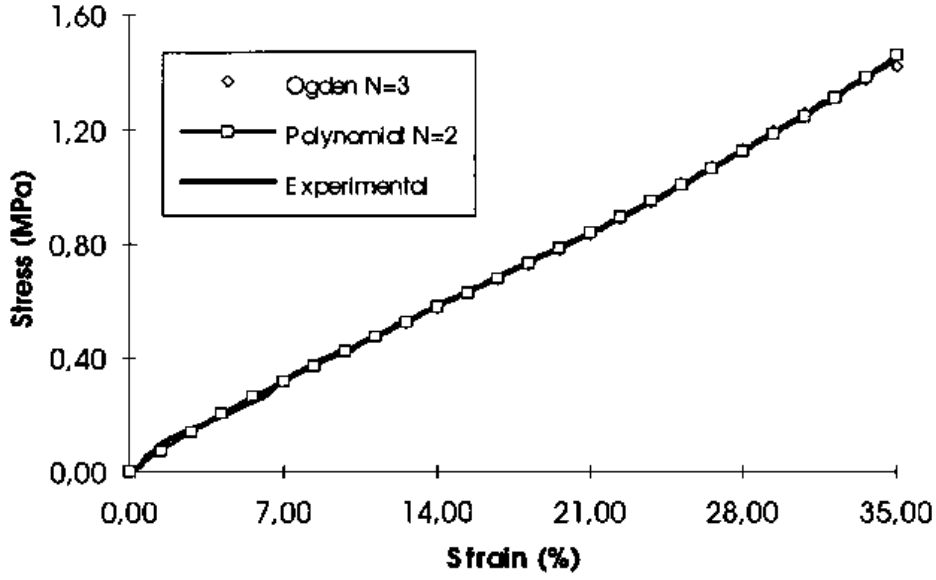

Figure 5. Comparison between measured and calculated stress-strain values for a compression test on unscragged rubber compound

Figure 6. Execution of an equibiaxial (no shear) test

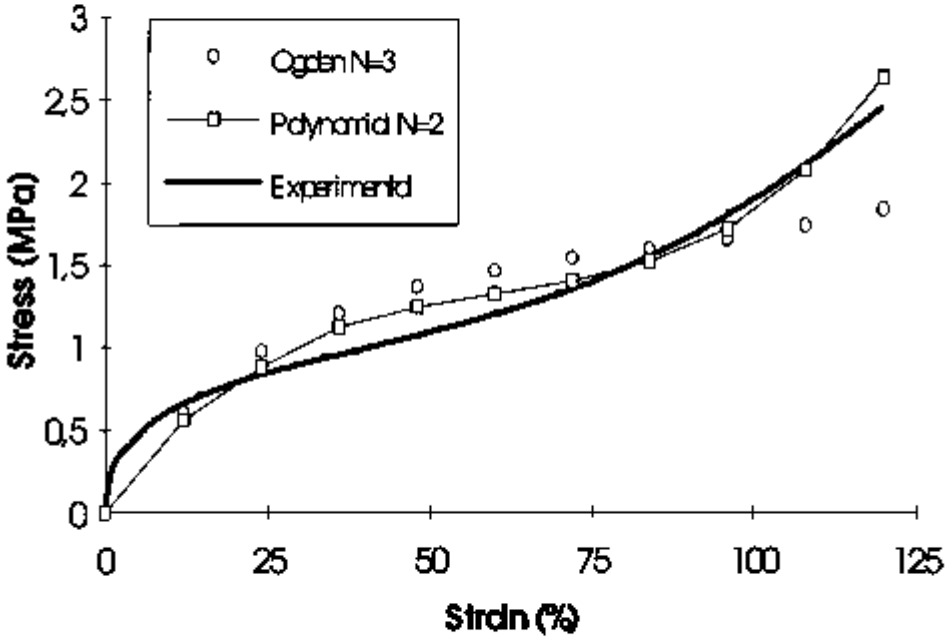

Figure 7. Comparison between measured and calculated stress-strain curves for an equibiaxial test on unscragged hard rubber compound

Figure 8. Execution of a planar (pure shear) test

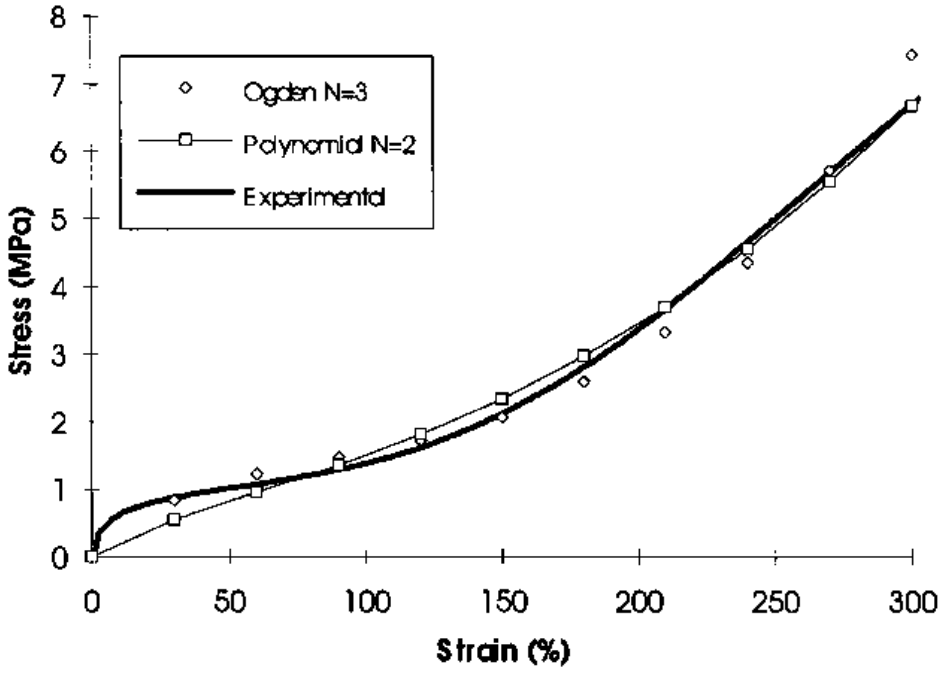

Figure 9. Comparison between measured and calculated stress-strain curves for a planar test on unscragged hard rubber compound

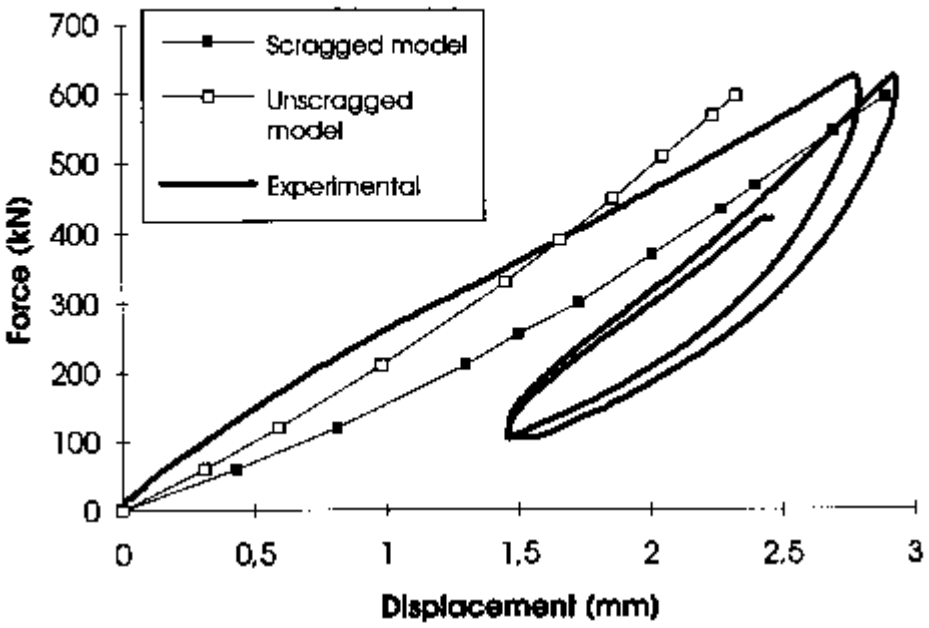

Figure 10. Comparison between measured and calculated force-displacement values for a compression test at 150% design vertical load of a complete bearing

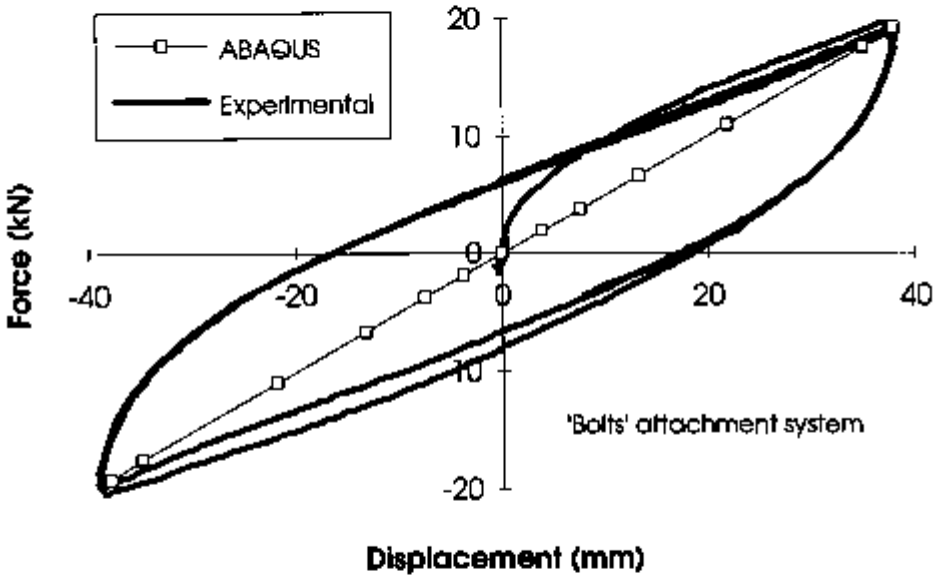

Figure 11. Comparison between measured and calculated force-displacement values for a combined compression & 50% shear strain test of a complete bearing

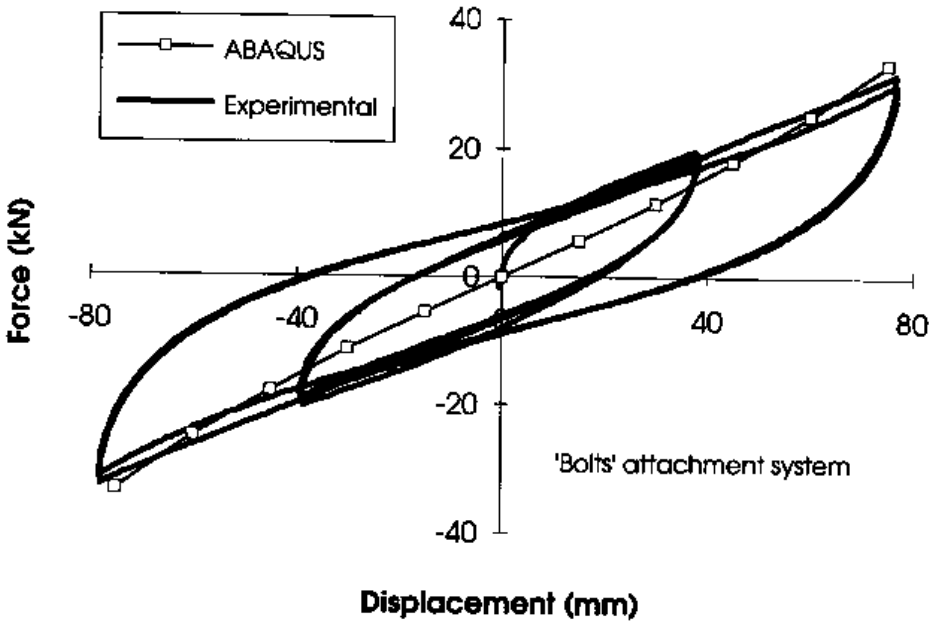

Figure 12. Comparison between measured and calculated force-displacement values for a combined compression & 100% shear strain test of a complete bearing

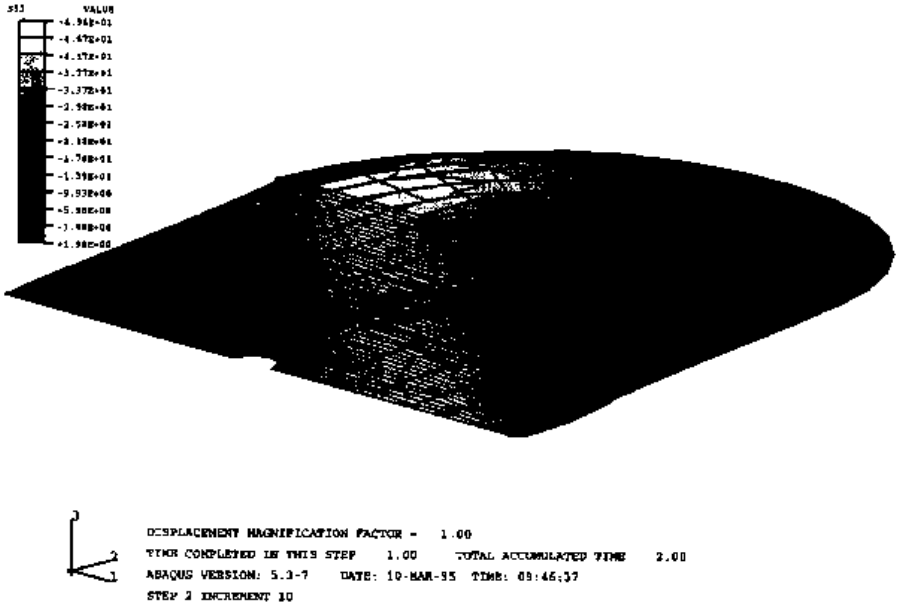

Figure 13. Stress distribution in the 3D model of the 'bolted' isolator at 200% shear strain under the design vertical load

Transactions of the 13th International Conference on Structural Mechanics in Reactor Technology (SMiRT 13), Escola de Engenharia - Universidade Federal do Rio Grande do Sul, Porto Alegre, Brazil, August 13-18, 1995

Seismic testing of models and fragments of seismic isolated structures of NPS buildings

Beliayev, V.S., Vinogradov, V.V., Sirro, V.A.
Scientific Research Center, St. Petersburg, Russia

ABSTRACT: The modern practice in Russia shows the feasibility of simulation of the real non-stationary effect of seismic waves on large constructions with the aid of underground explosions. This report states the bases of original methodology and results of model and full-scale seismic testing on 3-component seismic platforms (load-carrying capacity up to 500 t). For simulation of loads and shakes of elements of structures of seismic isolated buildings on the structure of the stands the technology of buried underground explosions was used.

1 INTRODUCTION

Bench and proving ground investigations of seismic stability of structures and systems are among the most important and expensive components when creating a trouble-free nuclear power objects. Specialists from different countries carry out such investigations i essentially with the aid of seismic platforms, the largest of which (dimensions of test table 15x15 m) successfully operates in Japan. Special problems when designing and testing large-sized and large-capacity objects are connected with necessity to reproduce a multicomponent (in a general way) motion of seismic platform which corresponds with high-intense (up to magnitude 10 as per MSK-64 scale and more) vibrations of NPS buildings foundations at earthquake and especially with the vibrations of high buildings marks under these conditions. The expediency to preserve a real substantially non-stationary nature of seismic effect of earthquakes in this case is to be specially noted.

Quantity of seismic platforms which are used at present in Russia and enable to reproduce non-stationary processes of high-intense seismic and shock loading is rather limited, and their load-carrying capacity is relatively low (less than 30-50 tf). A unique position among test facilities occupies the complex of seismic explosive stands of Research and test center (RTC), which is intended for check of seismic and shock stability of large-sized fragments of building constructions and equipment of special structures.

2 BASIC SPECIFICATIONS OF SEISMIC TEST COMPLEX

Existing RTC seismic test complex includes a series of facilities which are grouped in one place on the opened site near the city of Vyborg. The main characteristics of mass and overall dimensions of the facilities - soil seismic explosive stands are presented in the table 1.

Operation of the facilities is based on original technology which had been ubder investigation for more than 20 years.

The main element of this stands is a supporting steel structure, installed on a layer of sandy soil on the rock, and a movable test table which is cross-connected with the structure with the help of transforming members. The building fragments and the equipment under test are either sited on the table or, if necessary, they are suspended to the portals of the stand.

Table 1

Stand Brand	Rated load-capacity, tf	Dimensions*) of test table	
		length, m	width, m
VSS-300	300	30.0	14.0
VSS-100	100	16.0	8.0
VSS-40 (2 stands)	40	7.6	4.7
VSS-20	20	5.6	5.6

*) Dimensions of the object under testing are not limited by the height.

At the end of 1994 a special facility VSS-500-VOK was incorporated into the complex structure, the facility is designed for testing the seismic isolated structures of nuclear power objects. It includes a rectangular steel fragment of building with dimension 22x6x7 m and mass 400 tf, which is supported with the aid of removable seismic insulators on movable bearings. The bearings are located on a layer of sandy soil similarly to the supporting structure of the stands.

The motion of supporting structure of stands and bearings of the facility VSS-500-VOK is carried out due to explosions in the ground under the bottom and/or sidewise. The monitoting of parameters of the test table space motion is produced by way of selection of location of the charges and their values, as well as of the characteristics of transforming elements and the parameters of initial displacement of the test table.

3 PARAMETERS OF BENCH EFFECTS

On each of facilities the realization of three main modes of testings is ensured:

"shock-seismic" mode, reproducing the shakes of building constructions and fixing units of equipment at the effect of nearby industrial explosions, for example;

"severe-seismic" mode, simulating, among the other things, seismic vibration on high (12.0 m and higher) marks of buildings and structures, as well as in accordance with similarity laws of real structures models;

"soft-seismic" mode, simulating the ground and foundations motions under the conditions of earthquakes of various rate.

In this case the motion of support blocks of an object under study in conformity with testings purposes has type of space, flat or one-dimensional non-stationary vibrations. The limits of changes of characteristic peak values, reproduced on the load applications stands in the frequency range [0; 200 Hz] are presented in the table 2.

Besides the observance of amplitude-time limitations in ranges, specified in the table 2, in the processes realized there is ensured the performance of requirements to amplitude-frequency composition of vibrations of test table of the stand, for example, filling of standard spectrum or special prescribed spectra. The fig. 1-3 show the typical experimental reaction spectra for testing conditions, here too several domestic and foreign standard spectra are given for comparison purpose.

4 SEISMIC TESTINGS

Complex of facilities is equipped with a system of control, collection, primary processing and analysis of the results of experiment. A control system ensures the programmatic explosion of explosive charges. A specialized instrumental and computing complex permits to register kinematic parameters (accelerations, speeds, displacements) and deformation of the structures of the objects under investigation in

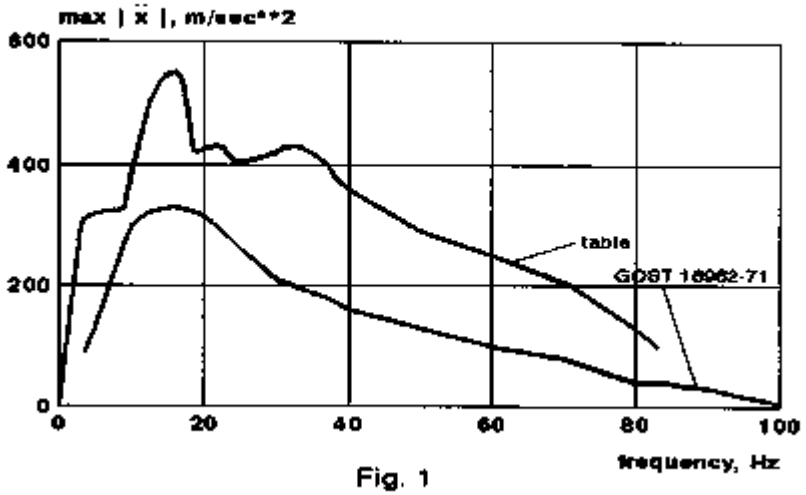

Fig. 1

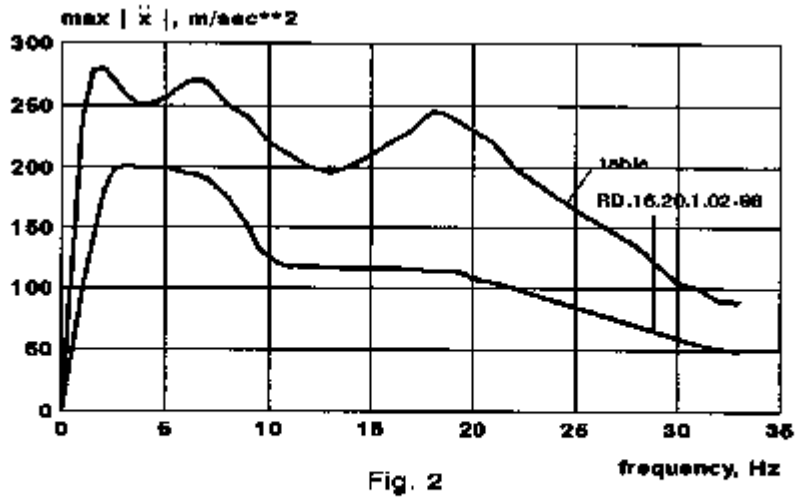

Fig. 2

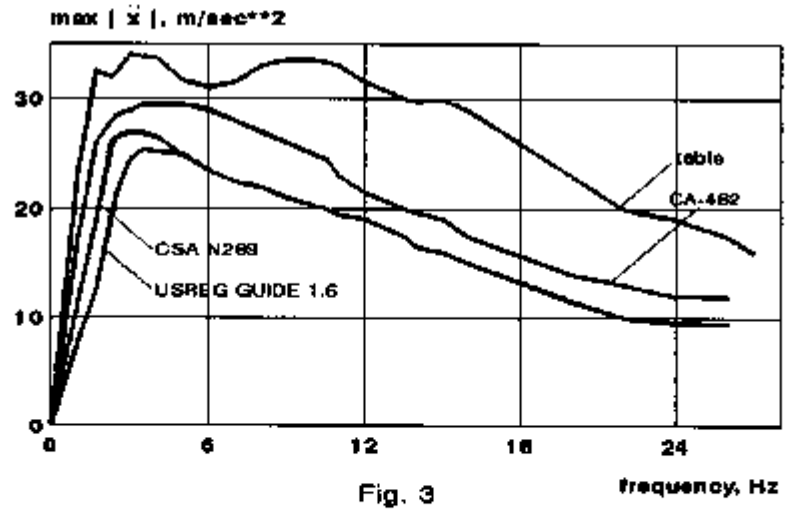

Fig. 3

Table 2

Type of loading mode	Accelerations (g) about the axes		Speeds (m/s) about the axes		Displacements (m) about the axes		Durations of loading, s
	oz	ox(oy)	oz	ox(oy)	oz	ox(oy)	
Shock-seismic	+30/ −10	±40	+3/ −1	±3	+0.5/ −0.2	±0.5	to 1.0
Severe-seismic	±10	±10	±2	±2	±0.5	±0.5	to 5.0
Soft-seismic	±2	±2	±1	±1	±0.7	±1.0	to 30.0

real time and to conduct automatic processing of experimental data with simultaneous amplitude-frequency analysis. The systems ensure visual and graphical display of received data and storing them in a database.

Bench facilities function both separately and jointly, for example if it is necessary to determine the seismic stability of long-size (50-70 m and longer) objects. On the facilities of the complex, among the other things, testings of full-scale fragment of a multicomponent low-frequency seismic protection system of NPS reactor building with VVER-640 had been carried out, these testings were logical completion of experimental investigations of large-scale (1:7.5) model of seismic isolated building which were performed earlier on this complex.

5 CONCLUSION

Seismic explosive technology of seismic testings permits to expand substantially (in comparison with seismic platforms which have mechanical drive) the possibilities to reproduce the parameters of effects of severe earthquakes, especially for high buildings marks.

The efficiency of the technology in question, including the economical efficiency, is confirmed during the testings of a new type of seismic protection for NPS reactor building with VVER-640.

Transactions of the 13th International Conference on Structural Mechanics in Reactor Technology (SMiRT 13), Escola de Engenharia - Universidade Federal do Rio Grande do Sul, Porto Alegre, Brazil, August 13-18, 1995

Study on ultimate behavior and fragility of Seismic isolated FBR plant in Japan

Kato, M.[1], Watanabe, Y.[1], Kato, A.[1], Tomura, H.[2], Shirahama, K.[2], Somaki, T.[2]
1) The Japan Atomic Power Company, Tokyo, Japan
2) Obayashi Corporation, Tokyo, Japan

1. INTRODUCTION

Regarding the design of a Fast Breeder Reactor (FBR) building, it is essential to reduce the seismic load, since the thermal load during operating is larger than the Light Water Reactor. The seismic isolation system is an effective method to do so. However, it is very important to grasp the ultimate behavior of the seismic isolation layer from the viewpoint of the assurance for the seismic safety margin of the seismic isolation system. If several isolators with small strength relatively were to rupture, the torsional response of the isolation layer would occur, and it is thought that such a torsional response would influence the ultimate behavior and the fragility (seismic safety margin) of the isolation layer.

This paper describes the results of the fragility analyses and the ultimate behavior of the seismic isolated building by three-dimensional (3-D) seismic response analyses considering the rupture phenomenon of isolators.

2. ANALYTICAL PROCEDURE

Analytical Model: As shown in Fig. 1, the object is the seismic isolated FBR building. The seismic isolation device consists of a laminated rubber bearing (hereafter "Isolator": the design vertical load of 500 tons) and the steel damper[1]. Regarding the basic characteristics of the isolation layer, the natural periods are 1.0 second before yielding of the damper and 2.0 second after yielding in the horizontal direction, and 0.05 second in the vertical direction. The yielding strength is 0.10W (W:the sum total weight of the superstructure).

Two types of the analytical model are considered, which are the one-lumped mass models consisting of the superstructure and the isolation springs. *Model A* having 367 isolators installed in the isolation layer, which is equivalent to the actual building, is used for evaluating the fragility and the ultimate behavior of the isolation layer (the propagating rupture phenomenon to other isolators). The randomness of the rupture strength of isolators is considered. *Model B* having 25 elements (one element corresponds to 12 isolators in Model A) for investigating the torsional response is a reduced and simplified model rather than Model A.

MSS (Multi Shear Spring) model is employed for each isolator/element, which has 8 springs arranged at uniform intervals on the plane, and is possible to consider the two-directional interaction.

Mechanical Properties: Fig. 2 shows the one directional hysteresis rules of the isolator and damper. The skeleton curve slides according to the maximum response displacement in the past, and the behavior after rupture phenomenon of isolators are considered based on the experimental results[2),3)].

Rupture Criteria: As shown in Fig. 3, the rupture limit of the isolator is defined by a three dimensional rupture surface with shear and vertical strains. Rupture of the damper is not considered. As for Model A, the variation is considered as randomness of rupture criteria to be the COV (Coefficient of variation) of 10%, assuming that it is based on the Gaussian distribution. As for Model B, elements with small rupture strength are installed along the edge concentrically to increase the torsional response.

It is remarkable that the rupture phenomenon does not occur in the linear region of the isolator/element (see Fig. 2), and in this paper the unbalanced forces generated by rupture of isolator/element are converged within the current time step.

Input Ground Motion: The input ground motion "S_2" (see references 4)) contains relatively long period contents, of which the maximum acceleration and the maximum velocity are 830.94 gal and 200 kine respectively.

Analytical Parameters: List of parameters is shown in Table 1. The scaled-up intensity of the abovementioned input motion as to Model A and the input direction as to Model B are considered as parameters. Furthermore, the fragility is evaluated by employing the Monte Carlo simulation technique using 50 samplings.

3. RESULTS

3.1 Ultimate Behavior and Fragility (Model A)

The results in comparison with the two dimensional(2-D) analyses, in which the same randomness and the same input level are used, are the following:

- The response acceleration wave at the center of gravity by the 3-D analyses is a little greater than by the 2-D ones, and it is considered that the difference is attributable to the influence of modeling between 2-D and 3-D. However, as for the response displacement wave (see Fig. 4) and the velocity wave, both 2-D and 3-D results are almost the same.
- As shown in Fig. 5, the rupture phenomenon occurs at roughly 14.8, 19.2 and 24.7 seconds. It is also proved obviously by analyses that the propagating rupture phenomenon, which might cause all isolators to rupture, is not observed[3], even if several isolators were to rupture.
- As the input level is increased, the torsional response becomes greater. However the maximum torsion is insignificant, since the average relative displacement between the corners of the base-mat (68 m) is 5 cm (even the maximum value is at most 19 cm) at the input level of 2,100 gal ($2.53S_2$).
- The fragility of the isolation layer is shown in Fig. 6. The fragility curves are estimated based on the relationship between the maximum input acceleration and the rupture ratio (in the range 10% to 50%). As it is observed that there is little difference between the rupture patterns of 2-D and 3-D as shown in Table 2, it is shown that the influence of the torsion is insignificant. Furthermore, the isolation system has a very large seismic safety margin against the design-base earthquake(S_2).

3.2 Torsional Response (Model B)

- The torsional response becomes greater, as the degree of the input direction is larger (see Fig. 7). At the input level of 2,200 gal ($2.65S_2$), the element rupture phenomenon propagates to other elements, the displacement at the corner is forced to enlarge by the torsional response, as shown in Table 2. However, it is not observed that the partial rupture phenomenon causes the propagating rupture of the isolation layer in such a case, since there is some different phase between the displacement response of the superstructure and the torsional response of the isolation layer as shown in Fig. 8.
- Regarding the influence on the floor response spectra due to the torsional response, as shown in Fig. 9, the increase of the floor response at the corner (Element No.25) is observed to be large, but at the center to be small in comparison with results by the 2-

D, where the torsional response is not considered. The floor response at the corner (Element No.5) is smaller than at the other corner (No.25), though the displacement response at Element No.5 becomes larger than at Element No.25. It is considered that the response acceleration at Element No.5 becomes small, as the derivative (secondary) acceleration due to the torsion might cancel the response acceleration of the building (at the center), as shown in Fig. 10.

- The results of the input direction of 0 degree reaches all the rupture, in which the torsional response does not occur (see Table 2). Therefore, it is remarkable that the rocking response of the building has a significant influence on the ultimate behavior (safety margin) rather than the torsional response of the isolation layer.

4. CONCLUSIONS

From the results of the seismic response analyses considering the rupture phenomenon of isolators, the torsional response occurred by the partial rupture, the ultimate behavior, and the fragility of the isolation layer are estimated. Conclusions are as follows.

- In the case that the rupture criteria is given randomly to each isolator (Model A), the torsional response value is clarified to be insignificant. Accordingly, the influence on the ultimate behavior (propagating rupture phenomenon) and the fragility curve of the isolation layer are recognized to be inconsiderable. Furthermore, it is confirmed that the isolation layer of the FBR building has an appreciable seismic safety margin against the tentative design-base earthquake(S_2).
- Even if the torsional response becomes greater due to the partial and concentrative rupture (Model B), neither the drastic increase of the displacement response nor the propagating all rupture phenomenon by the torsion are observed, since there is some different phase between the displacement and the torsional response. Regarding the influence on the response of the superstructure, the floor response spectra at the corner is greater or less than at the center. However the influence on the spectra at the center due to the torsional response is insignificant. Furthermore, it is proved that the rocking response of the building has a significant influence on the ultimate behavior (safety margin) rather than on the torsional response of the isolation layer.

5. ACKNOWLEDGMENT

This study was carried out as a part of the FBR common research of the electric power companies in Japan, entitled "Technical Study on Actualization of Isolated FBR Plant (Part I)"

REFERENCES

1)Kato, M., Watanabe, Y., et al. 1993. EXPERIMENTAL STUDY ON A LARGELY DEFORMABLE STEEL DAMPER. *12th SMiRT, Vol.K2:* 261-266.

2)Kato, M., Watanabe, Y., et al. 1993. MULTI DIRECTIONAL EARTHQUAKE INPUT TEST AND SIMULATION ANALYSIS OF BASE ISOLATED STRUCTURE. *12th SMiRT, Vol.K2:* 237-242.

3)Kato, M., Watanabe, Y. et al. 1993. DYNAMIC BREAKING TESTS ON BASE-ISOLATED FBR PLANT. *12th SMiRT, Vol.K2:* 267-278.

4)Kato, M., Watanabe, Y., et al. 1993. STUDY ON ULTIMATE BEHAVIOR OF BASE ISOLATED REACTOR BUILDING. *12th SMiRT, Vol.K2:* 315-320.

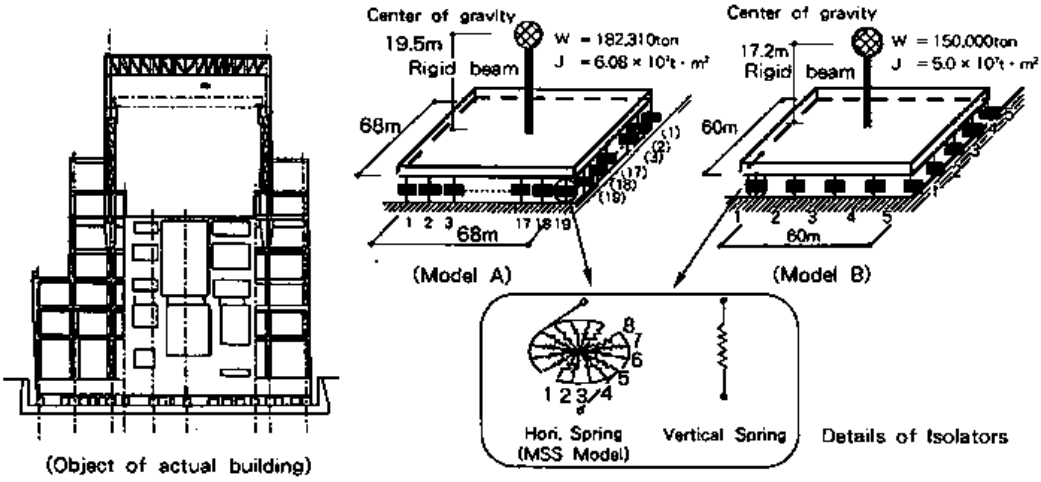

Fig. 1 Analytical model.

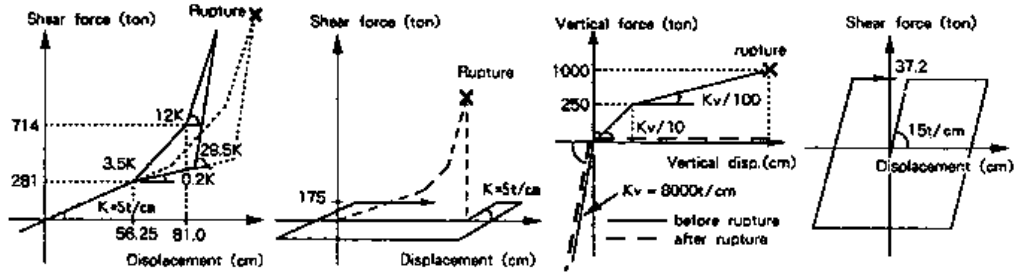

(a) Horizontal rule for isolators (b) Horizontal rule after rupture for isolators (c) Vertical rule for isolators (d) Horizontal rule for dampers

Fig. 2 Mechanical properties of isolation device.

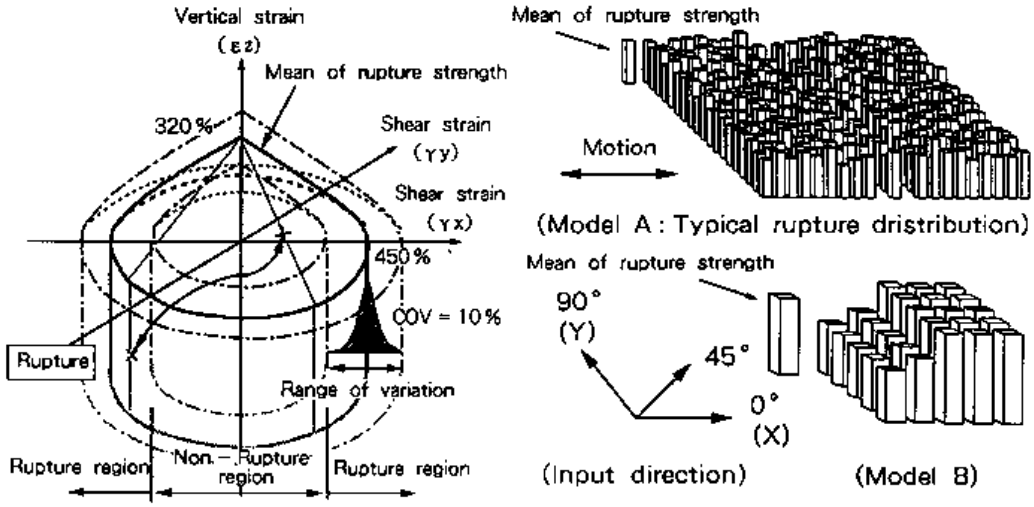

Fig. 3 Rupture criteria.

Table 1 List of parameters

Case No.	Input acceleration (gal)	Input direction (degree)	Remark
X170	1,700	0	Model A (50 Samplings)
X180	1,800	0	
X190	1,900	0	
X200	2,000	0	
X210	2,100	0	
T100	1,900	0	Model B
T145	1,900	45	
T190	1,900	90	
T200	2,000	0	
T245	2,000	45	
T290	2,000	90	

(Note) Two dimensional analyses with the same condition as three dimensional analyses are conducted, in which the torsional response is not considered.

Table 2 Typical Rupture Patterns

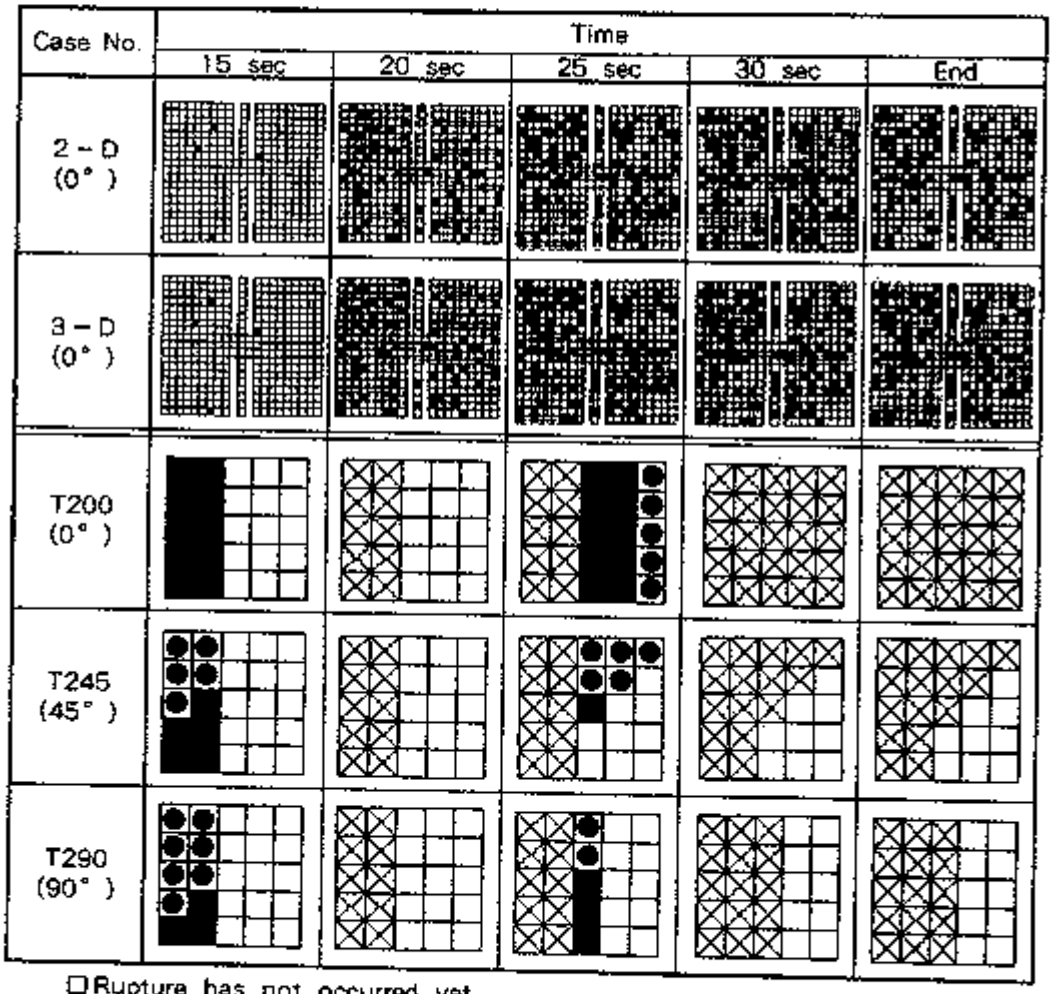

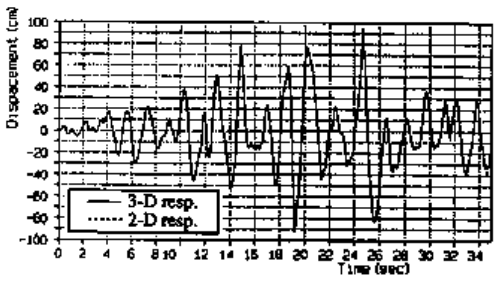

Fig. 4 Comparison of diplacement response between 2-D and 3-D.

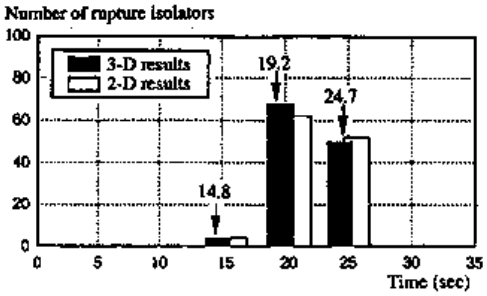

Fig. 5 Occurrence time of rupture and rupture number

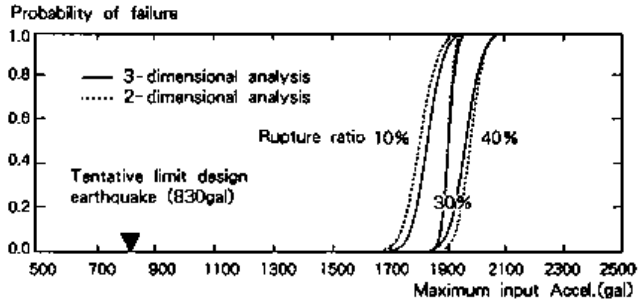

Fig. 6 Fragility curve of isolation layer.

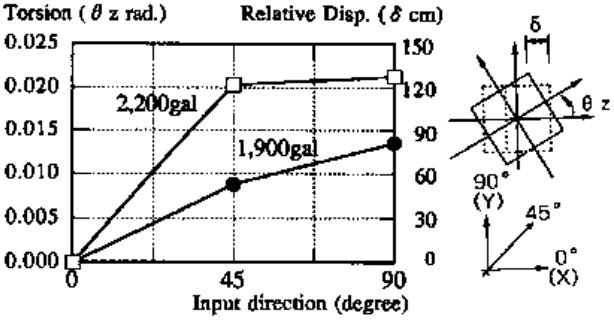

Fig. 7 Relationship of input direction and maximum torsional response.

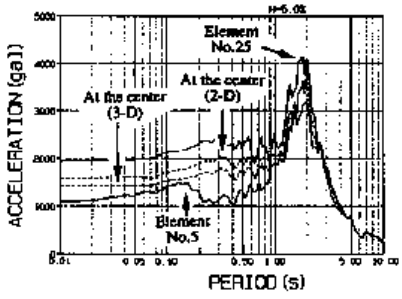

Fig. 9 Comparison of floor response spectrum between the center and the corner.

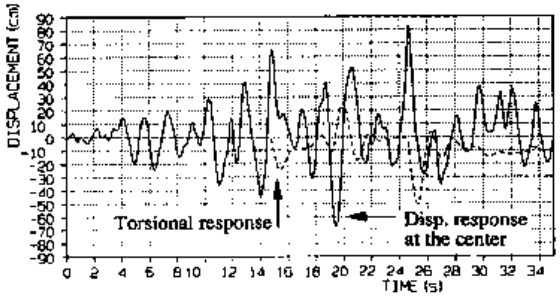

Fig.8 Comparison between displacement response and torsional response at the center.

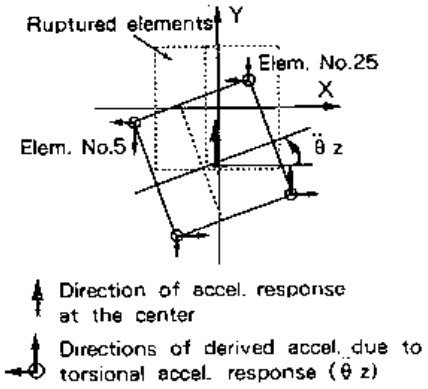

Fig.10 Concept of derivative acceleration due to the torsion.

Transactions of the 13th International Conference on Structural Mechanics in Reactor Technology (SMiRT 13), Escola de Engenharia - Universidade Federal do Rio Grande do Sul, Porto Alegre, Brazil, August 13-18, 1995

Effects of high damping rubber bearing on seismic response of superstructure in base isolated system

Yoo, B.[1], Lee, J.H.[1], Koo, G.H.[1], Kim, Y.-H.[2]
1) Korea Atomic Energy Research Institute, Taejon, Korea
2) Korea Advanced Institute of Science and Technology, Taejon, Korea

ABSTRACT : The seismic responses of a base isolated Pressurized Water Reactor(PWR) are investigated by using the mathematical model of which expresses the superstructure by a linear lumped mass-spring and the seismic isolator as an equivalent spring-damper. Time history analyses are performed by using the 1940 El Centro earthquake with linear amplification. In the analysis 5% structural damping is used in the superstructure. The four stiffness model types and varying isolator damping ratios from 2% to 100% are used to evaluate the effects of high damping rubber bearing on seismic response of the superstructure in base isolated system. The acceleration responses in base isolated PWR superstructure with high damping rubber bearings are much smaller than those in fixed base structure. However, when the damping ratio of the isolation system is above certain level, the peak acceleration at the superstructure starts to increase.

1. INTRODUCTION

The seismic isolation system used for the reduction of the seismic response of the structures is now promising device to be applied thru the world where large earthquakes are expected to occur. The seismic isolation systems are usually designed to lower the frequency of structure in the range of 0.5Hz to 0.7Hz, which prevents the structural damage from strong earthquakes having the high energy frequency range of 1.0 Hz to 10Hz. One of the seismic isolation system commonly used is a high damping laminated rubber bearing(HLRB). Since HLRB has a comparably large damping, both accelerations in superstructure and displacements between lower mat and upper base mat are remarkably reduced. However increasing damping ratio of the rubber bearings above certain level gives undesirable effects for the response of structural systems and components in superstructure[1]. The superstructural responses with varying the isolation damping are affected on the frequency contents of the excitation, the flexibility

and the damping of the superstructure[2].

Time history analyses for a typical PWR superstructure with a high damping rubber bearing isolation system were performed to understand the effects of various stiffness models for isolator and of flexibility for superstructure on seismic response and to determine damping ratio which gives the minimum seismic response in superstructures.

2. MATHEMATICAL MODEL

The model used in the analysis is shown in Fig.1. The isolated system considered in this paper consists of the isolator, base mat and the superstructure (containment vessel part and internal structure part). The computer program used in analysis is ABAQUS version 5.3[3]. The 2-dimensional beam element(type=B21) and mass element (type=MASS, type=ROTARYI) are used for the superstructure, and non-linear spring element (type=JOINTC) for the isolator.

In the model, the nodes from 1 to 10 represent the containment vessel part and the nodes from 11 to 17 represent internal structure part. The nodes 18, 7 and 11 represent the base mat, the polar crane support and the horizontal reactor vessel support respectively. The total weight of the superstructure is about 150,000 kips. The structural damping of the superstructure is assumed to be viscous damping with 5% damping ratio for all modes. It is converted into Rayleigh damping for the mathematical model.

Fig.2 shows the test results of the isolator which is scaled down 1/8 size. In modelling of the isolator which has severe hardening characteristics in large strain regions as shown in Fig.2, a simple equivalent viscous damping is applied for the damping model and the equivalent stiffnesses of the isolator are modelled with 4 types as shown in Table 1 and Fig.3.

Table 1. Spring models of the isolator

Spring models		Equivalent stiffness values
model 1 : linear spring 1	:	Keq = 46.283 x 10^6 lb_f / ft
model 2 : linear spring 2	:	Keq = 70.639 x 10^6 lb_f / ft
model 3 : bi-linear spring	:	K1 = 46.283 x 10^6 lb_f / ft, K2 = 174.130 x 10^6 lb_f / ft
model 4 : multi-linear spring	:	K1 = 46.283 x 10^6 lb_f / ft, K2 = 53.426 x 10^6 lb_f / ft, K3 = 112.14 x 10^6 lb_f / ft

The Keq's of model 1 and 2 are determined by an extreme equivalent stiffness. In model 3, K1 is same as the model 1 in the range of the displacement response from 0.0 ft to 2.23 ft, equivalent to strain 230% and K2 acts in the range from 2.23 to 2.755 ft,

equivalent to the maximum strain 300%. In model 3, the stiffness is jumped from K1 to K2 which is about four times of K1. To reduce the transition effects between K1 and K2, another intermittent spring is considered in model 4.

3. EFFECTS OF STIFFNESS MODELING TYPES OF HLRB

The fundamental natural frequencies of the containment vessel and internal structure for fixed base[4] are 5.39 Hz and 15.73 Hz respectively, and for base isolated system are 5.94 Hz and 16.17 Hz respectively. The first frequency of the isolated system is 0.5 Hz. Fig.4 shows the first three mode shapes of the base isolated model.

The structural responses of the base isolated system having four different stiffness models of isolators but having identical viscous damping(12%) are analyzed and compared with those of fixed base structure. The isolated system is assumed to be subjected to horizontal ground motion of the linearly amplified 1940 El Centro earthquake up to the seven times. In the Fig.5 the zero period acceleration at the superstructure for the isolated system, of which represents rigid body motion, are remarkably reduced to 0.68g. It is noteworthy that the acceleration at the crane support for the fixed base system is 3.8g and that at reactor support is 2.4g respectively when it is subjected to five times El Centro earthquake. Figs.6 and 7 show the results of numerical simulation of the floor response spectrum at the polar crane support(node 7) and the reactor vessel support(node 11) of the superstructure, associated with the four stiffness models. The results essentially envisage that the responses depend on the flexibility of the superstructure and how one models the stiffness of the isolator.

From Figs.6 and 7, one can see that the models 3 and 4 which have large stiffness components in large strain ranges of the isolator, produce higher maximum peak accelerations by about 20% than models 1 and 2. This can be translated as that models 1 and 2 which have only one equivalent stiffness may not adequately represent the hardening phenomena of the rubber bearing at large strain. The resonant responses of the isolated system using the model 2 are slightly shifted to high frequency region and amplified around 0.7 Hz to 3 Hz to some extent, compared with other models. This is due to the fact that the equivalent stiffness for model 2 is higher by 1.5 times than the first stiffness for other models.

The model 3 having the highest stiffness value in high strain range has the higher value of the maximum peak acceleration in the range above 2.0 Hz than the Model 4 which has slowly increasing three different stiffnesses. The acceleration responses at the polar crane support of the containment vessel are slightly amplified around 6 Hz, and are also larger than those of the reactor vessel support of the internal structure because the

flexible structure can be excited larger than the stiff structure when subjected to an earthquake having lower frequency content excitation.

4. EFFECTS OF ISOLATOR DAMPING

In this paper, the effects of the isolator damping ratios on the superstructural responses are investigated by using the numerical simulations and the flexibility effects of the superstructure on the responses are also investigated.

The response locations of major concern are a polar crane support (node 7) in containment vessel part and the reactor vessel support (node 11) in internal structure part. Figs.8 and 9 show the results of the numerical simulations for the isolator damping ratio versus the floor response spectra at nodes 7 and 11 respectively. From these results one can see that the responses of the superstructure are decreased as increasing the damping ratio of the isolator but increasing the isolator damping beyond some level enlarges the maximum peak values of the superstructural accelerations. Figs.10 and 11 show the results of the numerically simulated damping effects. Fig.10 essentially demonstrates that maximum peak acceleration of both the flexible structure(polar crane) and stiff structure(reactor support) does not depend linearly on damping; their minimums occur at 40% and 65% respectively. An increase of flexibility of superstructure tends to lower the damping ratio to obtain the minimum peak acceleration of the superstructure. In the meanwhile, as illustrated in Fig. 11, the relative displacements between lower mat and upper base mat decrease monotonously as increase of damping ratio of isolator.

5. CONCLUSIONS

Based on this study, the followings are concluded

The acceleration responses in base isolated PWR superstructure subjected to linearly amplified 1940 El Centro earthquake are much smaller than those in fixed base superstructure.

In the higher strain region where stiffness behaves non-linearly, the acceleration responses modelled by one equivalent stiffness are smaller than those in nonlinear spring model, and the higher stiffness spring model of isolator exhibits larger peak acceleration response at superstructure in the frequency range above 2.0 Hz, when subjected to linearly amplified 1940 El Centro earthquake.

Peak accelerations at the certain level of the base isolated superstructure decrease

sharply as increase of damping ratio of the isolator up to 15%, and minimum peak acceleration can be obtained by 40 % damping ratio of the isolator for flexible containment vessel and by 65 % for stiff internal structure. However as increase of damping ratio of the isolator above this value in each structure, peak accelerations at both structures increase, and peak accelerations at flexible structure increase more than those at stiff structure. This means that the secondary components and systems at flexible structure may have more unfavorable effects than those at stiff structure. The relative displacements between lower mat and upper base mat decrease monotonously as increase of damping ratio of isolator.

REFERENCES

1. Tsai, H.C. and Kelly, J.M. 1993. Seismic response of heavily damped base isolation systems: Earthquake engineering and structural dynamics. Vol.22: 633-645.
2. Inaudi, J.A. and Kelly,J.M. 1993. Optimum damping in linear isolator system: Earthquake engineering and structural dynamics. Vol.22: 583-598.
3. ABAQUS Version 5.3, Standard user's manual I,II.
4. Yun, C.H. et al. 1994. A study of major seismic safety issues for nuclear power plants(1): Report No. KINS/GR-067 (in Korea).

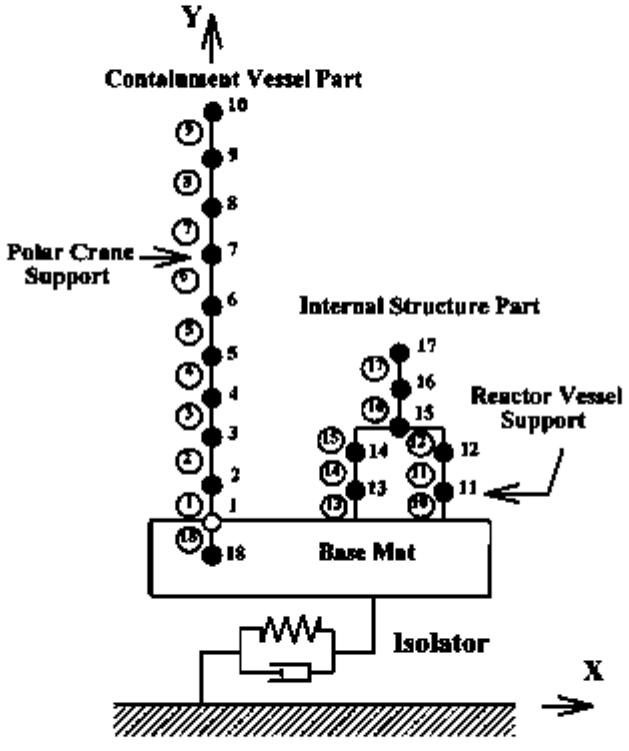

Fig. 1. Analysis model of base isolated system

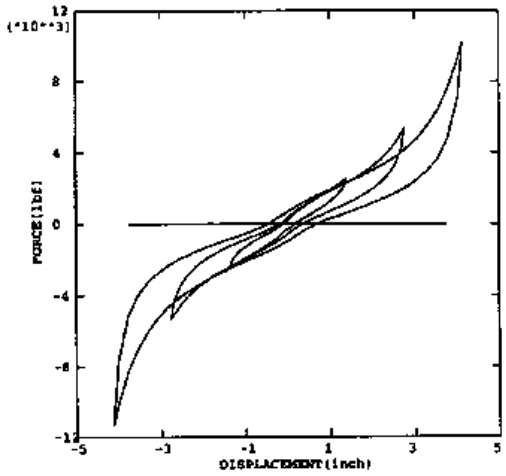

Fig. 2. Hysteretic curve of the 1/8 scale rubber bearing test

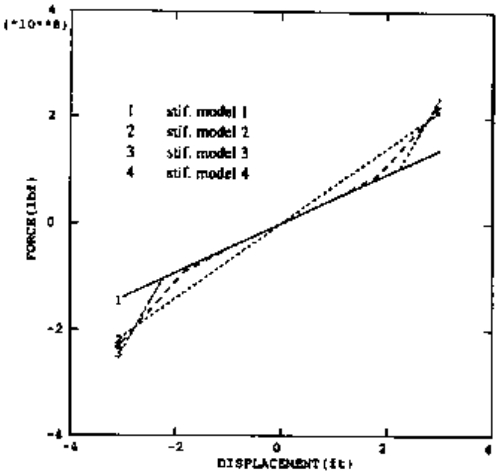

Fig. 3. Horizontal equivalent stiffness models of isolator

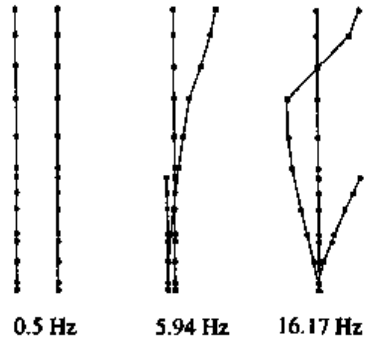

Fig. 4. Mode shapes of base isolated superstructure

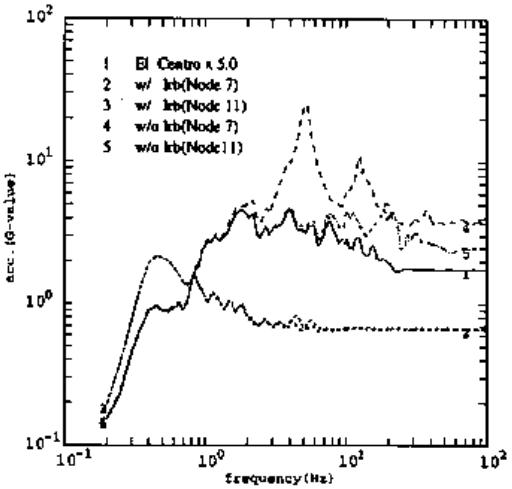

Fig. 5. Acceleration response spectra of base isolated and fixed base superstructure

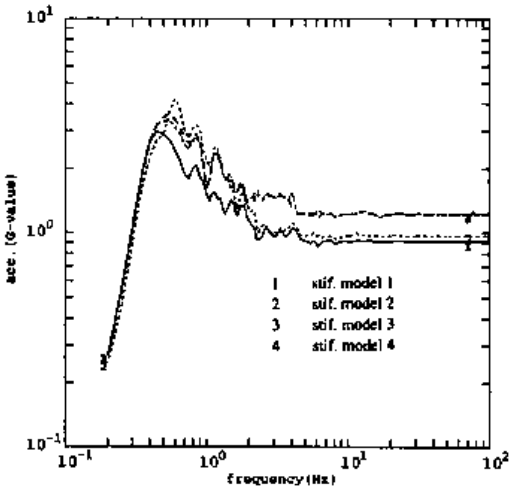

Fig. 6. Effects of equivalent stiffness model at polar crane support (node 7)

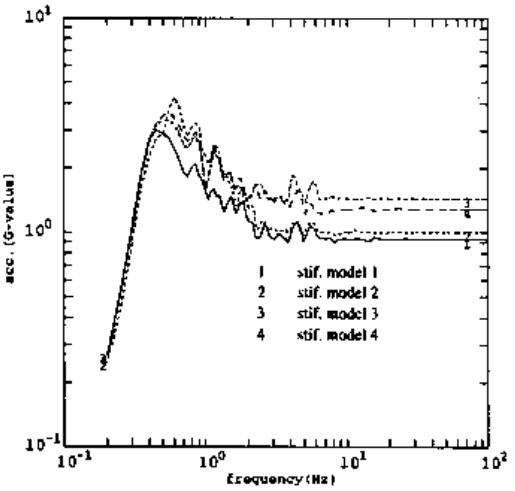

Fig. 7. Effects of equivalent stiffness model at reactor vessel support (node 11)

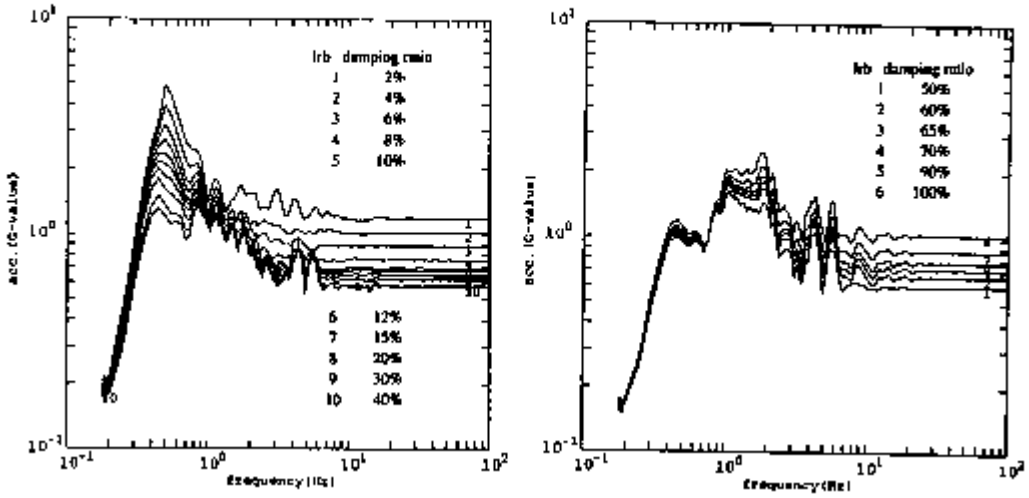

Fig. 8. Effects of isolator damping at polar crane support (node 7)

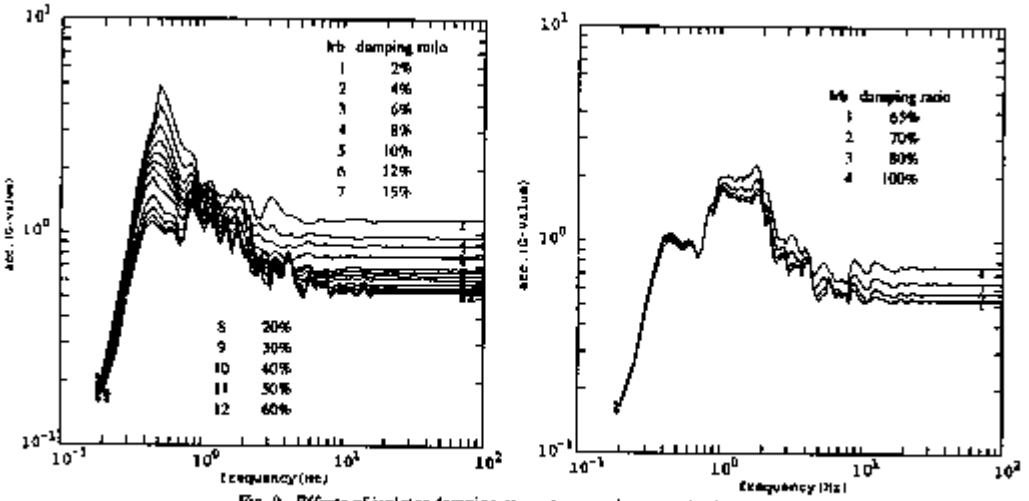

Fig. 9. Effects of isolator damping at reactor vessel support (node 11)

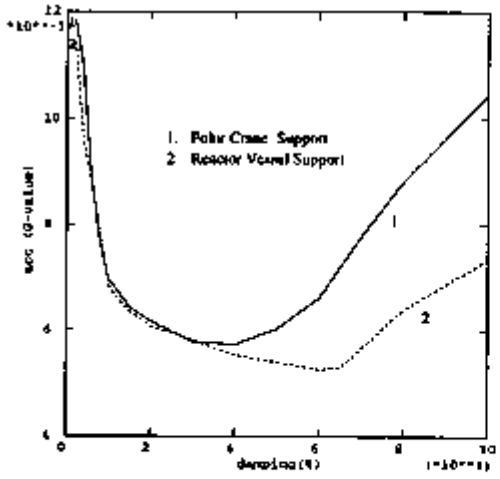

Fig. 10. Maximum peak accelerations vs. isolator damping

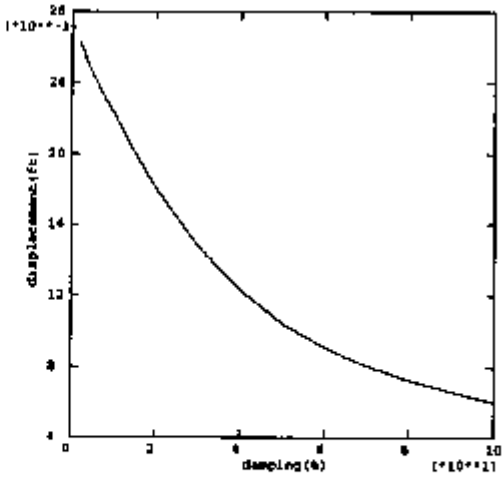

Fig. 11. Maximum relative displacements vs. isolator damping

Transactions of the 13th International Conference on Structural Mechanics in Reactor Technology (SMiRT 13), Escola de Engenharia - Universidade Federal do Rio Grande do Sul, Porto Alegre, Brazil, August 13-18, 1995

Influence on seismic response of base-isolated building by different phase spectrum of input wave

Kato, M.[1], Watanabe, Y.[1], Kato, A.[1], Suhara, J.[2], Hirotani, T.[2]
1) Civil Engineering and Architectural Dept., The Japan Atomic Power Co., Tokyo, Japan
2) Power & Energy Project Division, Shimizu Corp., Tokyo, Japan

ABSTRACT: In a seismic response analysis for nuclear facilities such as reactor building, simulated earthquake motion has been used as input ground motion. It is made using site-specific response spectrum and phase spectrum. There are two methods to determine the phase spectrum, one is using a phase spectrum of actual major earthquake and another is produce it by random process.

Under design level input, the ordinary seismic-resistant building responds almost linearly, though the response of base-isolated building shows a non-linear tendency based on the combination of isolator and damper. It is supposed for base-isolated building that the uncertainty of response under design level input would be increased compared with seismic-resistant building owing to its non-linear characteristics.

This paper examines the influence of the phase spectrum of input ground motion on the response of base-isolated building.

1 GENERATION OF SIMULATED EARTHQUAKE MOTION

In generating the simulated earthquake of the design basis earthquake S_2, the target spectrum which had the velocity level of 200 cm/s for slightly long-period domain and the acceleration level of 2,000 cm/s^2 for short-period domain in a response spectrum of 5% damping was employed(Kato,M.,1991).

For the phase spectrum of the simulated earthquake, phase spectra of following eight recorded earthquake motions are used

(1)La Union records on Mexico Earthquake(1985) NS, EW
(2) Taft records(1952) NS, EW
(3) Records at Hachinohe harbor on Tokachi-oki earthquake(1968) NS, EW
(4) El Centro records(1940) NS, EW

In addition, three motions with random phases and time dependent amplitude envelopes corresponding to Magnitude (MJ) 8.0 are generated. The simulated motion can be generated by an iterative procedure using superposition of sinusoidal waves. The agreement between the target spectrum and the response spectrum of the simulated motion can be improved by modifying an amplitude of spectrum according to the ratio of a calculated spectrum to a target spectrum. Fig. 1 shows the time histories of generated eleven acceleration waves. Fig. 2 shows an example of the agreement between the target spectrum and the spectrum of the generated motion in a response spectrum of 5% damping .

2 ANALYSYS CONDITIONS AND MODEL

An analysis model for seismic response of a base-isolated FBR plant is shown in Fig. 3. A single-stick lumped mass model with bending and shear stiffness is used for the superstructure.

Stiffness of seismic-resistant walls of reinforced concrete are evaluated by beam elements with bending and shear deformation, and the relation between shear deformation and shear force is modeled by the maximum point oriented tri-linear model to consider non-linear characteristics. Both the upper and lower basements are assumed to be rigid for out-of-plane direction.

The isolation story of building is modeled by a combination of laminated rubber bearings and steel dampers. Laminated rubber bearings are represented by a horizontal spring and vertical springs. Horizontal spring is concentrated to the center of the basement and its hysteresis characteristics has a tri-linear skeleton considering hardening of stiffness and effect of repeated deformation. Vertical springs of laminated rubber bearings are substituted to 19 springs distributed horizontally on the basement. The hysteresis characteristics of a vertical spring is modeled by a tri-linear skeleton that shows softening in the tension region and its response doesn't describe any loops. (Kato,M.,1993) These springs represent rotation of the isolation story and can evaluate the shift of the neutral axis caused by rocking of building.

Steel dampers are represented by a horizontal spring gathered to the center of the basement. They have perfect elasto-plastic hysteresis characteristics

Horizontal and rotational soil springs represent soil-structure interaction. Geometric non-linearity due to uplift is assumed for the rotational spring. The damping coefficient, however, is constant even if the basement is uplifted.

Two input levels for the seismic response are considered. One is the design level equal to S_2 and another is the seismic safety margin level equal to S_2 amplified by 2.

3 ANALYSIS RESULTS AND EVALUATION

3.1 Maximum Response of Superstructure

Fig. 4 shows the maximum acceleration response of the superstructure. From this figure, it is found that the coefficient of variation(COV) in the response obtained by the eleven input motions is about 0.1 for S_2 and 0.2 for $2 \times S_2$.

The maximum response of the lowest seismic resistant wall on shear force-shear strain relation is shown in Fig. 5. COV of the maximum shear force is 0.15 for S_2 and 0.24 for $2 \times S_2$.

3.2 Maximum Response of isolation Story of Building

Fig. 6 shows the maximum response of the isolation story. From this figure, it is found that COV in the response is roughly 0.15 for S_2 .

For $2 \times S_2$ COV of the maximum response displacement of the isolation story is 0.07 and COV of the maximum response shear force is 0.2. The variations of seismic response obtained by using phase property of the actual earthquake records are larger than those obtained by random phases.

The seismic safety margin of the isolation story of the building which is designed to have a low center of gravity can be generally assessed in terms of horizontal displacement. Since variation of response at the seismic safety margin level ($2 \times S_2$) is roughly half of that of design level (S_2), it is found that the seismic safety margin of base-isolated building is hardly affected by the phase of the input ground motion.

3.3 Floor Response Spectra

The floor response spectra at the reactor vessel supporting floor under S2 input is shown in Fig. 7. This figure shows that the floor response spectrum around the isolation frequency (1-2 seconds) varies so widely that COV becomes from 0.3 to 0.4. On the contrary, the variation in the short period range less than 0.2 seconds that is influential for equipments is similar to that of the maximum acceleration response of the building.

3.4 Consideration

Since the agreement between the target spectrum and spectrum obtained by simulated motion is verified in the 5% damping spectrum (see Fig. 2), COV of 0.15 for response under S2 is seemed to be large. An equivalent coefficient of viscous damping which is evaluated by the horizontal hysteresis loop of the isolation story is about 17% as shown in Fig. 8. Fig. 9(a) shows the acceleration response spectrum of 5% damping. COV of the spectrum is approximately 0.05, indicating good agreement with the target spectrum. Fig. 9(b) shows the acceleration response spectrum with an equivalent coefficient of viscous damping of 17%. The target spectrum of 17% damping is modified by 5% damping target spectrum. COV of the ratio of a target spectrum to the spectrum obtained simulated motion is roughly 0.1 in 17% damping. Since COV of 17% damping spectrum is nearly twice as much as COV of 5% damping spectrum, it is considered that the variation of seismic response of isolated building is caused by the variation of a high damping spectrum of input motion which is significant for isolation.

4 CONCLUSION

From the analysis of non-linear seismic response obtained by simulated input ground motions generated using eleven different phases, the following results are obtained.

(1) COV of the response during design level input shows a roughly 0.15.
COV in input motions with a response spectrum of 5% damping is roughly 0.05. COV in input motions with a response spectrum of 17% damping, which is equivalent viscous damping of the isolation system, is approximately 0.1.

(2) The variations of seismic response by phases of actual earthquake records is larger than those by random phases.

(3) The variation of the response in isolation story for the seismic safety margin level is roughly half of that for the design level input.

5 ACKNOWLEDGMENT

This study was carried out as a part of the FBR common research of the electric power companies in Japan, entitled "Technical Study on Actualization of Isolated FBR Plant (Part I)".

REFERENCE

Kato, M. et al. 1991. *STUDY ON THE SEISMIC BASE-ISOLATED REACTOR BUILDING FOR DEMONSTRATION FBR PLANT IN JAPAN*. 11th SMiRT, Vol.K2

Kato, M. Watanabe, Y.,et al. 1993. *STUDY ON ULTIMATE BEHAVIOR OF BASE ISOLATED REACTOR BUILDING. 12th SMiRT*, Vol.K2

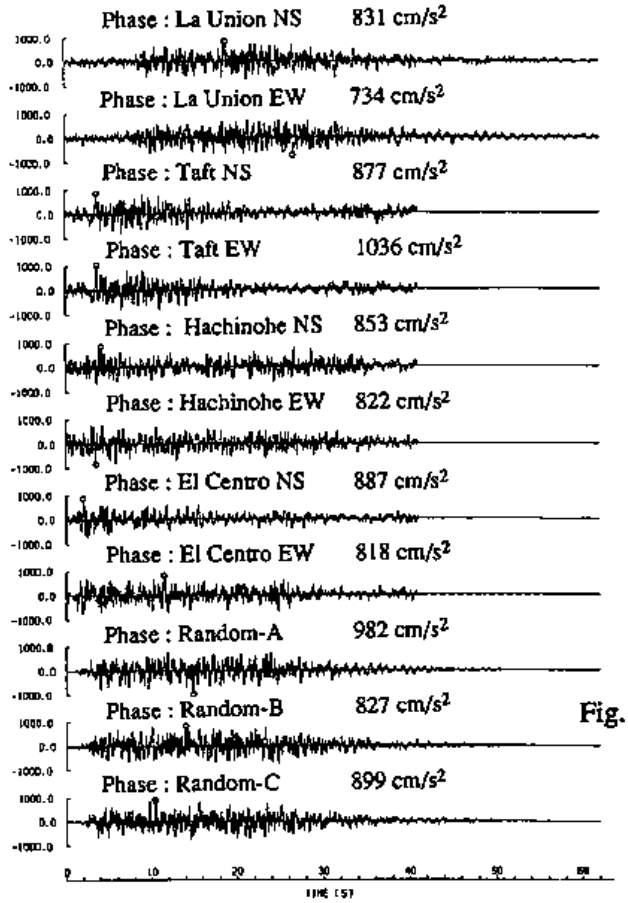

Fig. 1 Time Histories of generated eleven acceleration waves

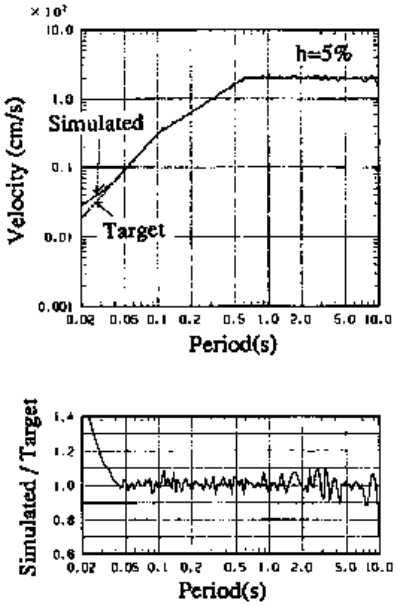

Fig. 2 Target Spectrum and Spectrum of Generated Motionin in 5% damping Response Spectrum(Taft NS)

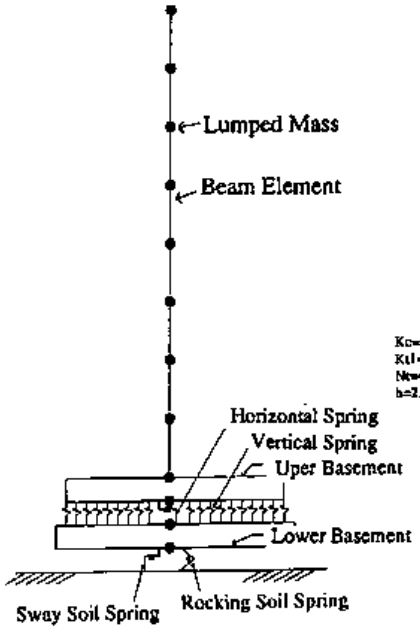

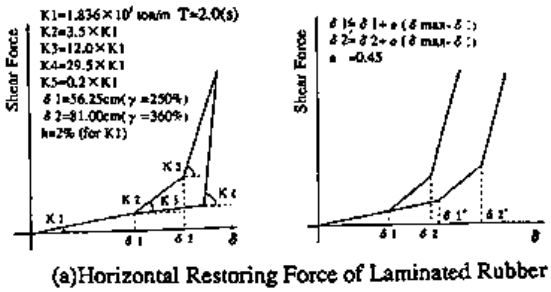

(a)Horizontal Restoring Force of Laminated Rubber

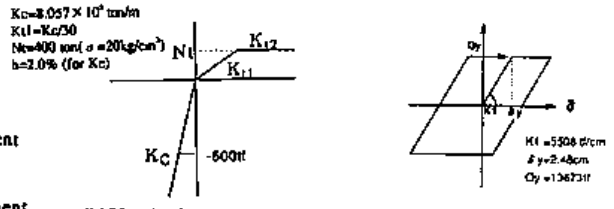

(b)Vertical Restoring Force of Laminated Rubber (c)Horizontal Restoring Force of Steel Damper

Fig. 3 Analyses Model for Seismic Response

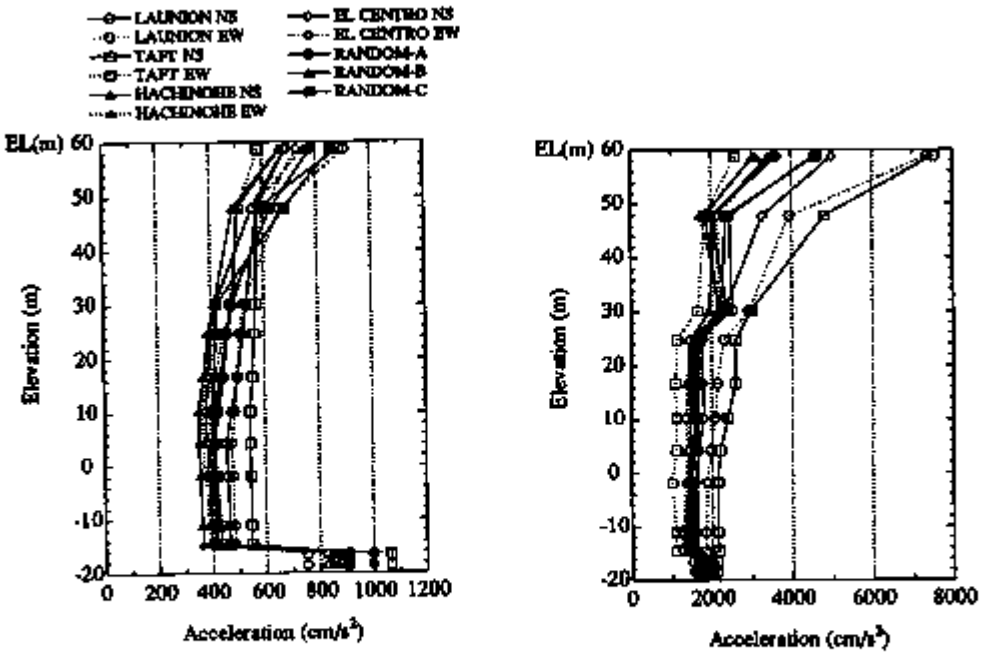

Fig. 4 Maximum Acceleration Response of Superstructure

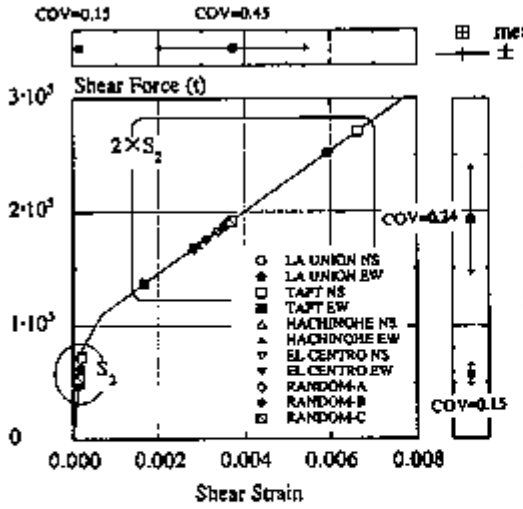

Fig. 5 Maximum Response of Superstructure

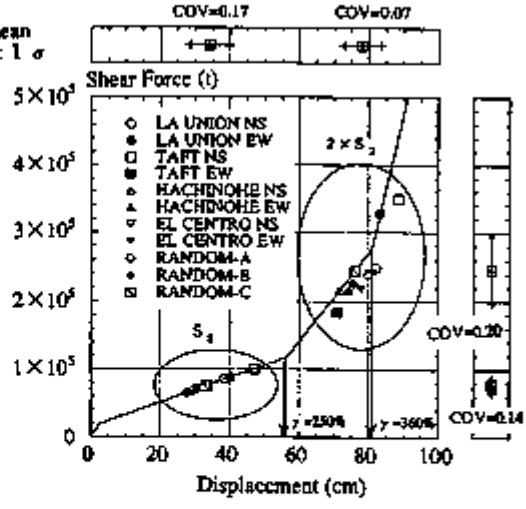

Fig. 6 Maximum Response of Isolation Story

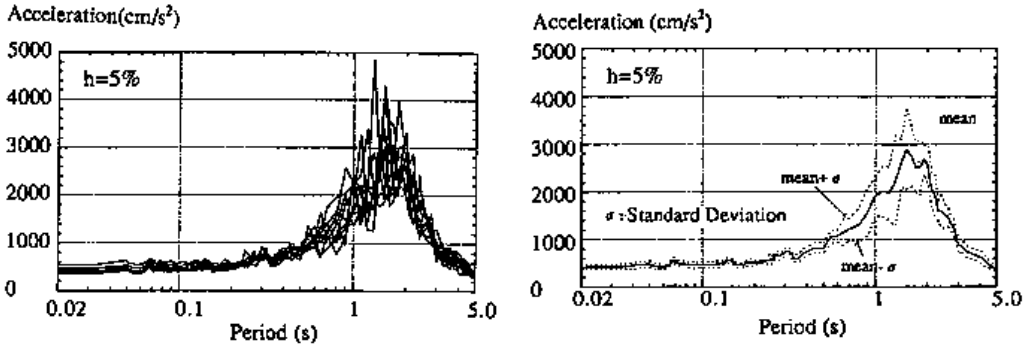

(a) FRS of 11 input motions (b) Variation of FRS

Fig. 7 Floor Response Spectra at Reactor Vessel Supporting Floor for S2

$$h_{eq} = \frac{\Delta W}{2\pi W} + \frac{h_0\sqrt{K1}}{\sqrt{K_{eq}}} = 17\%$$

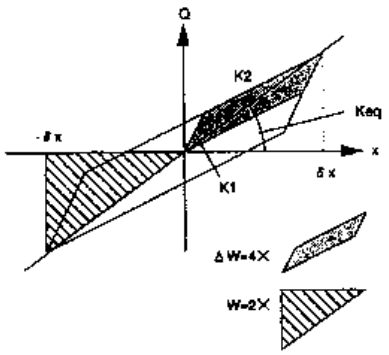

Fig. 8 Evaluation of Equivalent Damping Ratio

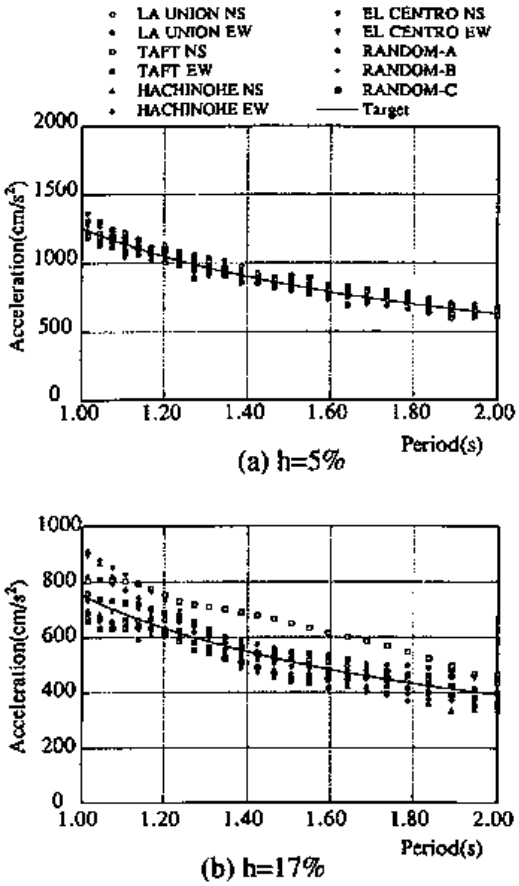

Fig. 9 Response Spectra for Slightly Long Periods

Transactions of the 13th International Conference on Structural Mechanics in Reactor Technology (SMiRT 13), Escola de Engenharia - Universidade Federal do Rio Grande do Sul, Porto Alegre, Brazil, August 13-18, 1995

Seismic analysis of base isolated spent fuel storage structures

Lee, D.-G.[1], Chung, W.-J.[1], Kim, N.-S.[2], Lee, S.-G.[3]
1) Korea Advanced Institute of Science and Technology, Taejon Korea
2) Hyundai Engineering & Construction Co., Ltd., Seoul, Korea
3) Chonnam National University, Taejon, Korea

ABSTRACT : An extensive series of experiments was conducted to evaluate the mechanical characteristics of laminated rubber bearings. The pseudo-dynamic test method was employed in this study to predict the seismic response of a base isolated spent fuel storage system. The numerical analyses on the base isolated spent fuel storage structures were conducted using the various numerical models obtained from test results. It is shown that the numerical results obtained using the analytical model are in an excellent comparison with the test results. Thus, the proposed method is considered to be efficient and reliable for evaluation of the seismic response of a base isolated spent fuel storage system.

1. INTRODUCTION

The safety of spent fuel storage structures is extremely important, because the failure of the structures, containing cooling water and spent fuel which are of high level in radioactivity, may have disastrous consequences on lives and environments. An alternative to increase the seismic resistance of the spent fuel storage structure and its anchorages is to reduce the seismic forces to which the structure is subjected by incorporating base isolators. In general, a linear vicously damed model, roughly defining the characteristics of base isolators, can not accurately represent the isolated system in which the structure is affected by the hysteresis and the strain hardening induced from base isolators. Therefore, it would be desirable to conduct experimental studies on the isolated systems.

The base isolated spent fuel storage structures were tested by the Pseudo-dynamic(PSD) test method using a substructuring technique in which the isolated system is devided into the tested and computed parts. The experiments were performed to evaluate the mechanical characteristics og base isolator, and the seismic analyses on the base isolated spent fuel storage structures were conducted using the various numerical models obtained from test results. The numerical results using several hysteresis models and experimental results are in good agreements. Thus, the proposed method is considered to be efficient and reliable for evaluation of the seismic response of a base isolated spent fuel storage system.

2. MODELLING OF A FLUID-STRUCTURE SYSTEM

2.1 *Rectangular liquid storage structures*

The rectangular structure is mounted onto the base isolators on the ground and partially filled with fluid shown in Fig 1. The behaviors of the stuctures during earthquake are basically 3-dimensional. However, for the complicity, the 2-dimensional structure as shown in Figure 2 is considerd in this study. The wall of the structures are modelled by using beam elements. In the actual analysis, only a half of the fluid-structure system is considered, because the motion of the system under horizontal earthquake loading is anti-symmetric with respect to the vertical plane at the center.

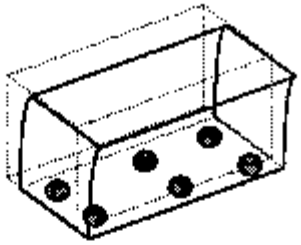

Fig. 1 Base-Isolated Liquid Storage Structure

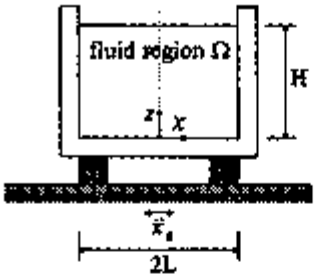

Fig. 2 Model of Rectangular storage structure

2.2 *Velocity potential and hydrodynamic forces*

For the irrotational flow of an incompressible inviscid fluid, the velocity potential, $\phi(x,z;t)$, satisfies the Laplace equation in the fluid region.

$$\nabla^2\phi(x,z;t)=0 \quad in\ \Omega \tag{1}$$

Then, the fluid-wall boundary conditions can be expressed as follows:

$$\phi_{,x}(\pm L,z;t)=\dot{W}(z;t) \tag{2}$$
$$\phi_{,z}(x,0;t)=0 \tag{3}$$
$$\phi_{,z}(x,H;t)=\dot{\xi}(x;t) \tag{4}$$
$$\rho\dot{\phi}(x,H;t)+\rho g\xi(x;t)=0 \tag{5}$$

where $\xi(x;t)$ is the elevation of the free surface over the mean surface level; $W(z;t)$ is the horizontal displacement of the wall; $\phi_{,x}$ represents $\partial\phi/\partial x$; ρ is the mass density of fluid; and g is the acceleration of gravity. The general solution for the Eq. (1). which satisfies the boundary condition on the tank wall, Eq. (2), can be expressed as,

$$\phi(x,z;t)=\sum_{n=1}^{\infty}A_n(z;t)\sin\lambda_n x+x\dot{W}(z;t) \tag{6}$$

where $\lambda_n=(2n-1)\pi/2L$ and $A_n(z;t)$ is the time varying coefficients of the n-th term in the sine series which is to be determined using the other boundary conditions. The free surface elevation can be also expressed in terms of the sine series as,

$$\xi(x;t)=\sum_{n=1}^{\infty}\eta_n(t)\sin\lambda_n x \tag{7}$$

where $\eta_n(t)$ represents the generalized free surface amplitude associated with $\sin\lambda_n x$.

Substituting Eqs. (6) and (7) into Eqs. (1), (3), (4) and (5), one can obtain expressions for $A_n(z;t)$ in terms of $\dot{W}(z;t)$ and $\eta_n(t)$. The horizontal displacement of the wall is represented by the using third order polynomial of z within each beam element. Once the solution for $A_n(z;t)$ is obtained, substituting it into the free surface boundary conditions, one can obtain the relationship between $\{\eta\}$ and $\{\ddot{d}\}$ as,

$$[M_g]\{\ddot{\eta}\}+[K_g]\{\eta\}=[S]\{\ddot{d}\} \tag{8}$$

where diagonal matrices $[M_g]$ and $[K_g]$ can be interpreted as mass and stiffness matrices associated with the free surface motion; and $[S]$ is the coefficient matrix of the exciting force associated with the wall motion. The hydrodynamic pressure exerted on the wall can be expressed in terms of velocity potential. Then, the nodal hydrodynamic force vector, $\{F\}$, can be obtained as,

$$\{F\} = -[M_a]\{\ddot{d}\} - [S]^T \{\eta\} \tag{9}$$

where $[M_a]$ is the hydrodynamic added mass matrix associated with the horizontal movement of the liquid; and $[S]$ is the matrix relating the horizontal force on the wall with the free surface motion.

2.3 *Equation of motion for the base isolated spent fuel storage system*

Combining Eqs. (8) and (9), the equation of the fluid structure system can be obtained as,

$$\begin{bmatrix} M_w + \overline{M}_a & 0 \\ -\overline{S} & M_{ff} \end{bmatrix} \begin{Bmatrix} \ddot{d} \\ \ddot{\eta} \end{Bmatrix} + \begin{bmatrix} K_w & \overline{S}^T \\ 0 & K_{ff} \end{bmatrix} \begin{Bmatrix} d \\ \eta \end{Bmatrix} = \begin{Bmatrix} 0 \\ 0 \end{Bmatrix} \tag{10}$$

where $\{d\}$ is the nodal horizontal displacement vector of the wall; $[\overline{M}_a]$ and $[\overline{S}]$ are the matrices corresponding to $[M_a]$ and $[S]$ but with proper dimensions. By expressing the displacement vector of the free nodes, $\{d\}$, as the sum of the ground movement, $\ddot{x}_g$, and the relative displacement to the ground movement, $\{x_r\}$, i.e.,

$$\{d\} = \{1\}x_g + \{x_r\} \tag{11}$$

Decomposing the displacement vector $\{x_r\}$ into the components at the base isolator $\{x_b\}$ and at the nodes on the wall $\{x_w\}$, Eq. (11) can be rewritten as,

$$\begin{bmatrix} M_{bb} & M_{bw} & 0 \\ M_{bw}^T & M_{ww} & 0 \\ -\overline{S}_b & -\overline{S}_w & M_{ff} \end{bmatrix} \begin{Bmatrix} \ddot{x}_b \\ \ddot{x}_w \\ \ddot{\eta} \end{Bmatrix} + \begin{bmatrix} K_{bb} & K_{bw} & \overline{S}_b^T \\ K_{bw}^T & K_{ww} & \overline{S}_w^T \\ 0 & 0 & K_{ff} \end{bmatrix} \begin{Bmatrix} x_b \\ x_w \\ \eta \end{Bmatrix} = -\begin{bmatrix} M_{bb} & M_{bw} \\ M_{bw}^T & M_{ww} \\ -\overline{S}_b & -\overline{S}_w \end{bmatrix} \begin{Bmatrix} 1 \\ 1 \end{Bmatrix} \ddot{x}_g \tag{12}$$

or $\quad [M]\{\ddot{x}\} + [K]\{x\} = -[M^r]\{1\}\{\ddot{x}_g\}$

where K_{bb} is the stiffness coefficient for the base motion which can be expressed as the sum of the stiffness coefficient associated with the tank wall, K_{bb}^w and the base isolator, K_{Isol}. Decomposing Eq. (12) into the substructure of isolation system and superstructure of storage tank, Eq. (12) can be simply expressed as Eq. (13).

$$[M]\{\ddot{x}\} + [C^I]\{\dot{x}\} + [K^I]\{x\} + \{R^E\} = -[M^r]\{1\}\{\ddot{x}_g\} \tag{13}$$

where :

$$[C^I] = \begin{bmatrix} 0 & 0 & 0 \\ 0 & c_w & 0 \\ 0 & 0 & c_f \end{bmatrix}, \quad [K^I] = \begin{bmatrix} K_{bb}^w & K_{bw} & \overline{S}_b^T \\ K_{bw}^T & K_{ww} & \overline{S}_w^T \\ 0 & 0 & K_{ff} \end{bmatrix}, \quad \{R^E\} = \begin{Bmatrix} c_b\dot{x}_b + K_{Isol}x_b \\ 0 \\ 0 \end{Bmatrix} = \begin{Bmatrix} R_{Isol} \\ 0 \\ 0 \end{Bmatrix}$$

3. PSEUDO-DYNAMIC TESTS OF BASE ISOLATED SPENT FUEL STORAGE STRUCTURES

3.1 *Pseudo-dynamic test method*

The Pseudo-dynamic test method is a relatively new experimental technique for evaluating the seismic performance of structural models in a laboratory by means of on-line computer controlled simulation. Thus, in fundamental PSD technique, the structural model is represented as a discrete system and solved for its seismic response by using the direct integration, while their restoring forces are not numerically modeled but directly measured from a test conducted in parallel with the direct integration.

On behalf of evaluating the seismic performance of base-isolated spent fuel storage tanks as a base isolation system, the PSD test incorporating a substructuring technique, which have been mostly developed and applied by Dermitzakis et al. and Nakashima et al., was employed in this study. Thus, the base-isolators would be only tested on the tested part whose hysteretic behavior was complicated and not well-defined, whereas the liquid tanks as the computed part would be numerically treated in a computer with the mechanical model. For this purpose, as an integration method adaptable to the PSD test, an implicit-explicit method proposed by Hughes et al. was used. This method combined with the general Newmark method and an explicit predictor-corrector method is to apply an explicit method to the tested part and an implicit method to computed part. Implementation scheme of the PSD test can be described as three main operations: (a) numerical integration, (b) displacement control, (c) data acquisition.

3.2 *Description of test models*

The base-isolated reinforced concrete structure for the storage of spent fuel is investigated. The width (2L) and the wall thickness(h) are taken as 12m and 1.2m, respectively. The fluid is assumed to be filled upto 13m above the base. The material properties of the concrete storage structure are: Young's modulus(E)=19.6 GPa, Poisson's ratio(ν)=0.2 and mass density(ρ_s)=2.4×10^3Kg/m^3. The properties of fluid elements are: bulk modulus(K)=2.0 GPa, mass density(ρ)=1.0×10^3Kg/m^3. The test models were subsequently tested using the El Centro 1940 NS accelerogram. The vascous damping ratio of convective and impulsive modes were assumed to be 5% and 0.5% respectively. The frequencies associated with convective and impulsive modes of fixed base spent fuel storage structure are illustrated in Table 1.

Table 1. Frequencies of fixed-base storage structure (Hz)

	1st	2nd	3rd	4th
Convective mode	0.255	0.442	0.570	0.675
Impulsive mode	3.276	17.880	43.047	124.064

The base isolators, shown in Fig. 3, were loaded horizontally along transverse direction. The tests were performed using the test apparatus which exerted two hydraulic actuators on horizontal and vertical directions simultaneously as shown in Fig. 4. Vertical loads and horizontal displacements exerting on a pair of base isolators are controlled by each actuator from which the displacements and restoring forces of the isolators are measured immediately.

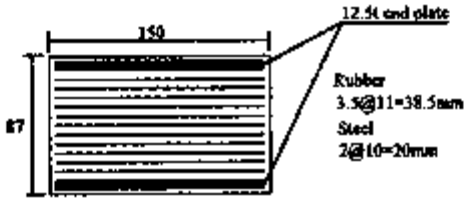

Fig. 3 LRB base isolator

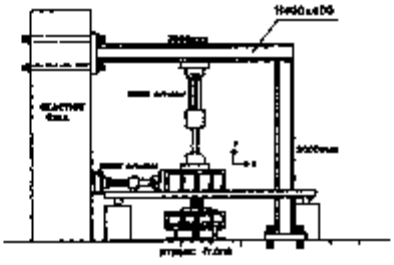

Fig. 4 Test layout

3.3 *Test result*

The Pseudo-dynamic tests incorporating a substructuring technique were performed on the test models subjected by seismic excitations. The seismic response obtained by the PSD tests of the test model are shown from Fig. 5 to Fig. 6. From Fig. 5, it can be observed that the base shear force associated with impulsive component exerting on the tank wall would be well reduced by an effect of base isolation. However, the base shear forces associated with convective components would be slightly increased as using base isolation system. Fig. 6 shows the max. base shear forces and max. wave

heights for isolation frequency, f_b, obtained from the test of the isolated tank. In the isolated tank, the convective forces, partly attributed to the tank wall, are almost not reduced but slightly increased. On the other hand, the impulsive forces more dominant rather than the convective forces are reduced to much lower ones due to energy dissipation of base isolators. Thus, it is shown that base isolators have more effect on the impulsive force and lead to much lower resultant seismic forces. Moreover, from Fig. 6, it can be observed that the the max. wave height associated with free surface motion would be increased by an effect of base isolation.

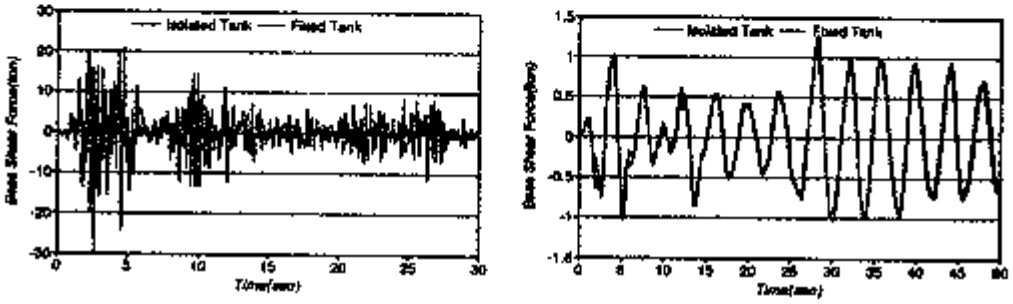

(a) Impulsive mode (b) convective mode

Fig. 5 Base shear force in fixed-base and isolated structure under input ground motion.

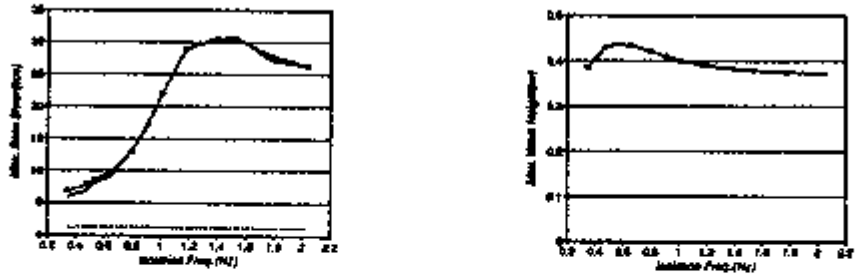

Fig. 6 Relationships of max. base shear forces and max. wave height for isolation frequency on isolated storage structures.

4. HYSTERESIS MODEL PARAMETER OF BASE ISOLATOR

Fig. 7 shows the hysteresis loops for various shear strains, from 10 to 50mm. From this result, hysteretic restoring force characteristics of the base isolator are modelled by the bi-linear model and Bouc-Wen model.

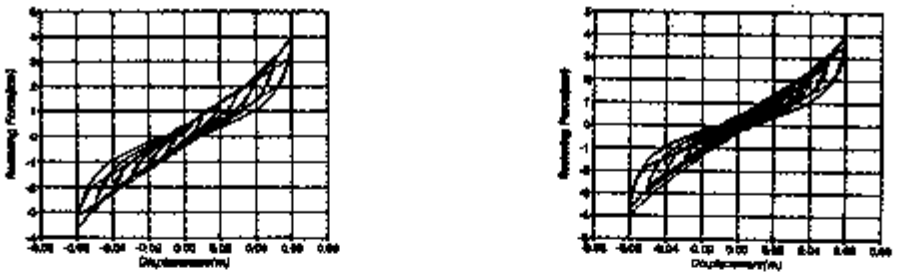

(a) Bi-linear Model (b) Bouc-Wen Model

Fig. 7 Comparison of numerical models with test results

Bi-linear model

From experimental results, the parameters of test piece used in the numerical analysis are determined as follows,

Q_d=0.395 ton, K_f=144.96ton/m K_d=46.10 ton/m

Bouc-Wen model

$$R=\alpha kd+(1-\alpha)kz$$
$$\dot{z}=A\dot{d}+\beta|\dot{d}||z|^{n-1}z-\gamma\dot{d}|z|^{n}$$

From experimental results, the parameters for this model are obtained as follows, K=36.08 ton/m, α=0.96, A=80.5182, β=161.787m^{-1}, γ=-185.2024m^{-1},

5. SIMULATION ANALYSIS

The numerical analysis results are shown in Fig. 8 compared with the experimental results. From the comparison, it has been indicated that the bi-linear model and the Bouc-Wen model reproduce the experimental result very well. One can note that the Bouc-Wen Model gives better agreements with the experimental results than the bi-linear model, while the bi-linear model is much simpler in computation viewpoint than the Bouc-Wen model.

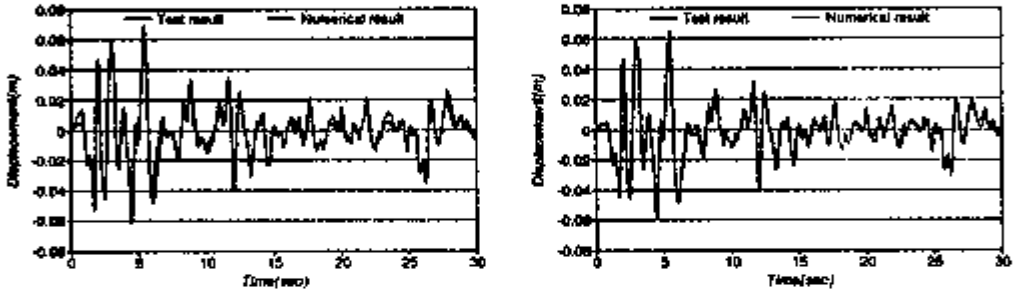

(a) Bi-linear Model (b) Bouc-Wen Model

Fig. 8 Comparison of analytical results with test results for response time history of the base isolated structure

6. CONCLUSIONS

A number of Pseudo-dynamic(PSD) tests and the numerical analyses have been conducted on the spent fuel storage structure supported by base isolators under earthquake loadings. The seismic performances of the base isolated spent fuel storage structure have been evaluated by using the PSD test method incorporating a substructuring technique. From the test results, it can be considered that the resultant seismic forces exerting on the tank wall would be well reduced by using the isolation system.

Since the numerical results obtained using the proposed model show excellent comparisons with the test results, the proposed test method is considered to be efficient and reliable for evaluation of the seismic response of a base isolated spent fuel storage system.

ACKNOWLEDGMENTS

This work was supported by the Hyundai engineering & construction Co., Ltd. The support would be gratefully acknowledged.

REFERENCES

R.H.Sues, S.T.Mau & Y.K.Wen, 1988. System Identification of Degrading Hysteretic Restoring Forces. *J. of Engineering Mechanics, Vol. 114, No. 5*: 833-846

C.B.Yun, Y.S.Kim & J.M.Kim 1992. Fluid-structure interaction analysis for spent fuel storage stuctures. *Proc. 10th World conference on Earthquake Engineering* : 4975-4980

Nam-Sik Kim & Dong-Guen Lee, 1993. Pseudo-dynamic Test of Base-Isolated Liquid Storage Tanks With a substructuring Technique. *The 4th East Asia-Pacific Conference on Structural Engineering and Construction.*

Transactions of the 13th International Conference on Structural Mechanics in Reactor Technology (SMiRT 13), Escola de Engenharia - Universidade Federal do Rio Grande do Sul, Porto Alegre, Brazil, August 13-18, 1995

Design study of the seismic-isolated reactor building of demonstration FBR plant in Japan

Kato, M.[1], Watanabe, Y.[1], Kato, A.[1], Suhara, J.[2], Shirahama, K.[3], Fukushima, Y.[4], Murazumi, Y.[5], Yoneda, G.[6]
1) Civil Engineering and Architectural Dept., The Japan Atomic Power Co., Tokyo, Japan
2) Power & Energy Project Division, Shimizu Corp., Tokyo, Japan
3) Structural Engineering Dept. Nuclear Facilities Div., Obayashi Corp., Tokyo, Japan
4) Nuclear Structures Engineering Dept., Kajima Corp., Tokyo, Japan
5) Nuclear Facilities Dept., Taisei Corp., Tokyo, Japan
6) Office of Energy and Nuclear Engineering, Takenaka Corp., Tokyo, Japan

ABSTRACT: In the design of FBR demonstration plant that has been developed in Japan, it is important to make the plant comparable to LWRs in terms of construction cost by introducing all kinds of innovative technology. An adoption of seismic isolation system that can reduce seismic load is necessary to compromise contradicting design conditions that are unique in FBR plant; large thermal load and seismic load. For this purpose, common research works among electric power companies have been carried out since 1989 on subjects necessary to realize a seismic-isolated FBR plant. In 1993, preliminary design of seismic-isolated FBR plant reflecting results of these researches is performed. This paper shows the result of the design study.

1 DESIGN OF SEISMIC-ISOLATED REACTOR BUILDING

1.1 *Fundamental Design Principle*

The principal specifications of the demonstration FBR are as follows:
Reactor type: loop type reactor with top entry system (3 loops)
Capacity: approx. 660,000 kWe

In studying a seismic-isolated plant the fundamental principles taking into consideration the features of a demonstration FBR are as follows:
(1) The seismic isolation design would be of horizontal seismic base-isolation with a seismic-resistant design for the vertical direction.
(2) There should be an outlook for the design to be realized under the maximum probable earthquake ground motions(S_2) in Japan.
(3) There should be seismic safety compatible to that of seismic-resistant LWR.

1.2 *Earthquake Ground Motion for Design*

With regard to earthquake ground motions, since a frequency characteristic of a period of about 2 seconds would be of importance in seismic isolation design, earthquake motions of long periods 2 seconds to about 10 seconds which are longer than stipulated in Regulatory Guide for Aseismic Design of Nuclear Power Reactor Facilities of Japan are taken into consideration. Standard earthquake ground motions (S_1-D, S_2-D) and the maximum probable earthquake ground motion in Japan (S_2-M) are set out in this study (Fig. 1). Designing is done using S_2-D while the S_2-M is used for evaluating feasibility on critical parts. As for vertical earthquake ground motion, 0.6 times the horizontal ground motion is taken.

1.3 *Design of Seismic Isolation Device*

Of the basic characteristics of the seismic isolation device what mainly govern responses are the isolated natural period T_2 and the ratio of yield force to building weight β. In this case, T_2 is taken to be 2 seconds (Kato,M.,1991). As for β, it is made 0.1 for S_2-M motion, and 0.05 for S_2-D motion since input level is small.

Preliminary response analyses are performed based on the basic characteristics selected, and seismic isolation devices are designed. The two points below are considered for allowable deformation of seismic isolation devices.

(a) Deformation in an S_2 earthquake is not to be more than 1/1.5 of displacement at the beginning point of hardening.

(b) Deformation in a $2S_2$ earthquake is not to be more than the rupture limit displacement.

The seismic isolation systems are laminated natural rubber bearing + steel damper system, leaded laminated rubber bearing system, and high-damping laminated rubber bearing system, but here, the laminated natural rubber bearing + steel damper system will be mainly discussed.

The design of seismic isolation devices are shown in Fig. 2 and Table 1.

1.4 *Layout Plan and Structural Plan of Seismic-Isolated Reactor Building*

The principles for the basic layout of the reactor building are taken as follows:

(a) It is necessary to provide a stable building configuration which will not cause the seismic isolation device to rupture in tensile and shear forces from overturning moment during earthquake.

(b) Since the amount of response of the superstructure would be reduced compared with an seismic-resistant design reactor building, it is to be aimed to reduce weight by making base mat thickness and shear wall thickness thinner.

(c) The arrangement of seismic isolation devices should be well balanced giving thorough consideration to weight distribution to match locations of center of gravity and center of rigidity so that torsional response will not occur.

(d) Equipment delivery routes, access routes, etc. in relation with adjacent buildings should be thoroughly taken into consideration, along with which space from adjacent buildings should be secured in order that functions of seismic isolation system will not be lost.

1.5 *Design of Seismic-Isolated Reactor Building*

The plan and sectional drawings of the nuclear reactor building are shown in Fig. 3. The ratio of the foundation width to gravity center height of the superstructure is 3.5, and it is confirmed that the superstructure is stable against both S_2-D and S_2-M motion. The reactor building possesses ample rigidity with its fundamental period 0.2 second at the fixed base.

The arrangement of seismic isolation devices is shown in Fig. 4. Laminated rubber bearings are laid out well balanced giving thought to arranging them under shear walls and columns in order that vertical axial forces would act uniformly on the individual laminated rubber bearings, with the center of gravity of the building and the center of rigidity of the seismic isolation story to coincide so that torsional vibration would not occur.

2 SEISMIC RESPONSE ANALYSIS RESULTS

2.1 *Integrity Assessment for Superstructure*

The maximum shear stress of the reinforced concrete walls under S2-D motion is 4.3 kgf/cm^2, while under S2-M motion the maximum value is 12.1 kgf/cm^2. The superstructure can be seemed to be linear from these results, and the superstructure is sufficiently sound.

2.2 *Integrity Assessment for Seismic Isolation Story*

The response of a laminated rubber bearing at an end portion satisfies the allowable limit set for a state of composite stress of shear strain and axial stress (Fig. 5). As a result of calculating cumulative fatigue damage rate Dk(n) of steel bar dampers by Miner's law, the value of Dk(n) is 0.0082 in case of S2-D and 0.0188 in case of S2-M, and smaller compared with 1.0 at which rupture would occur.

2.3 *Floor Response Spectra*

The floor response spectra at the reactor supporting floor in a seismic-isolated plant and an seismic-resistant plant are compared as shown in Fig. 6. The horizontal floor response accelerations of the seismic-isolated plant are greatly reduced in the fundamental period domain of equipment design. On the other hand, the vertical response accelerations are increased more than those of the seismic-resistant plant in the frequency range around 10 Hz that is influential on equipment design, it is considered to be mainly due to amplification at the seismic isolation story.

3 SEISMIC SAFETY MARGIN

Seismic response analyses whose input levels increase are performed to grasp the response characteristics until the superstructure or seismic-isolated device reaches the ultimate state. The maximum responses of the shear wall and laminated rubber bearing at input of S2-M amplified by factor are shown in Fig. 7.

It may be seen from these results that in case of S2-M the ultimate state is not reached up to S2 amplified by 2.25. As for S2-D, it is ascertained that the ultimate state is not reached up to input of S2 amplified by 3.0 . On the other hand, from the fact that a typical existing seismic-resistant LWR retains an allowance of double the S2-M until ultimate state, the seismic-isolated nuclear reactor building composed in this study possesses seismic safety equal to or greater than the seismic-resistant design reactor building.

4 PHYSICAL PROTECTION (PP) FOR SEISMIC ISOLATION PLANT

PP facilities of the seismic isolation plant are required to be capable of absorbing relative displacement during earthquake along with being of a sound construction. The concept of PP facilities taking these into consideration is shown in Fig. 8. The PP facilities are composed of a concrete pent roof provided in the vicinity of ground level at the exterior wall, a peripheral wall of concrete rising up from the retaining wall, and a seal between the pent roof and wall.

5 FIRE PROTECTION

The frequency of fire breaking out at the seismic isolation story of the building is extremely low, but because of the fact that the laminated rubber bearings are not flame retardants, a cover structure having fire-resistant efficiencies around rubber bearings is considered as the measure of fire protection assuming that a fire breaks out at the seismic isolation story. The fire-resistant cover is a blanket placed over the laminated rubber bearing, which would be capable of following displacements during earthquake, while also being detachable for inspection (Fig. 9). Furthermore, from the points of view of fire detection and fire extinguishing, fire detectors and water extinguishing and other fire extinguishing facilities are provided.

6 QUALITY CONTROL AND MAINTENANCE CONTROL

Seismic isolation devices are controlled for scatter in device characteristics to be within the specified ranges by inspections at the time of manufacture. While in service, it is confirmed that the functions of the seismic isolation device are secured through daily inspections, periodic inspections, and temporary inspections

Further, assuming a case of serious irregularities occurring with the seismic isolation device, the construction and arrangement of seismic isolation devices are to be such that replacement would be possible.

7 CONCLUSION

Conceptual design of a seismic-isolated FBR plant, which would be realized in earthquake country Japan, is studied. As a result of an analytical study on seismic safety which is important in realization of the concept, it was found that it would be possible to secure seismic safety equivalent to an existing seismic-resistant LWR.

Following this, a study is to be made for optimization of reactor buildings, seismic isolation devices, and equipment and facilities aiming for realization of a horizontal seismic base-isolation system whose technological progress is steadily being made.

8 ACKNOWLEDGMENT

This study is carried out as a part of the FBR common research of the electric power companies in Japan, entitled "Conceptual Design Study of DFBR ".

REFERENCE

Kato, M. et al. 1991. *STUDY ON THE SEISMIC BASE-ISOLATED REACTOR BUILDING FOR DEMONSTRATION FBR PLANT IN JAPAN.* 11th SMiRT, Vol.K2

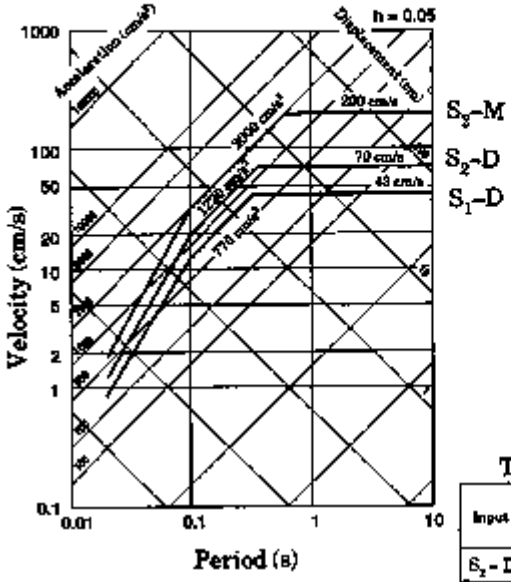

Fig. 1 Response Spectra of Horizontal Design Earthquake Ground Motions

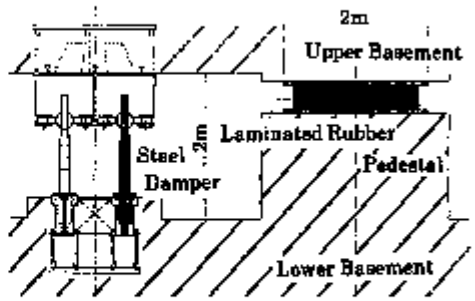

Fig. 2 Concept of Seismic - Isolation System

Table 1 Design of Laminated Rubber Bearings

Input	Supporting Load(ton)	Diameter (cm)	Thickness of Rubber (cm)	Deformation of S_2 (cm)	Axial Stress (kg/cm²)	Rupture Displacement (cm)
S_2 - D	750	160	15.3	14	37.9	68.9
S_2 - M	500	160	22.5	40	25.3	101.3

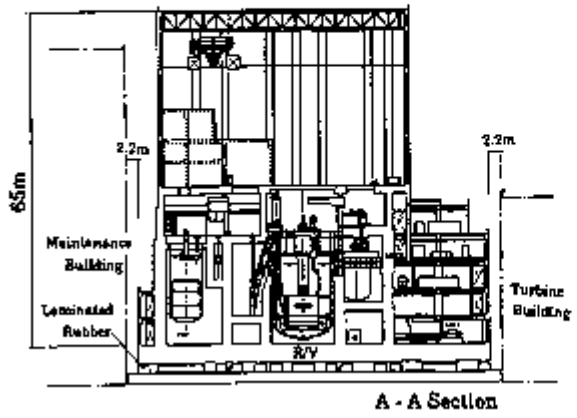

Fig. 3 Seismic Base Isolated Reactor Building for FBR

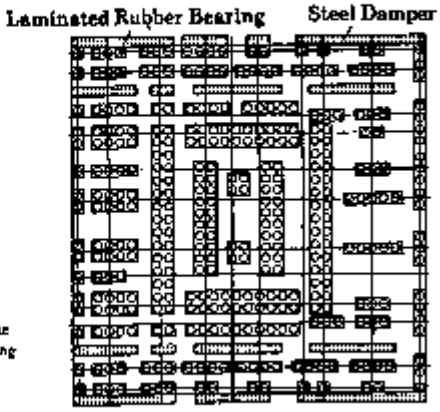

Fig. 4 Arrangement of Seismic Isolated Devices for S_2-M

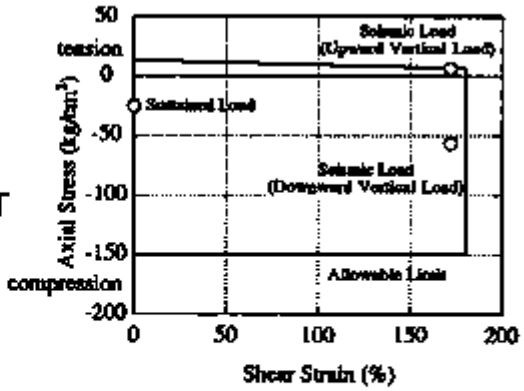

Fig. 5 Maximum Response of Laminated Rubber Bearing for S_2-M

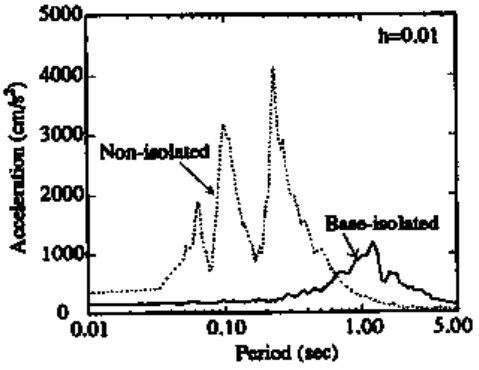

a) Horizontal FRS for S_2-M

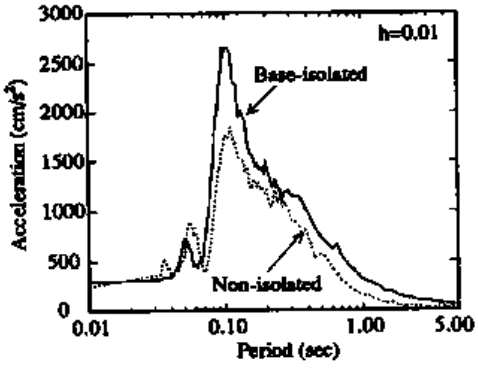

b) Vertical FRS for S_1-D

Fig. 6 Floor Response Spectra at Reactor Vessel Support

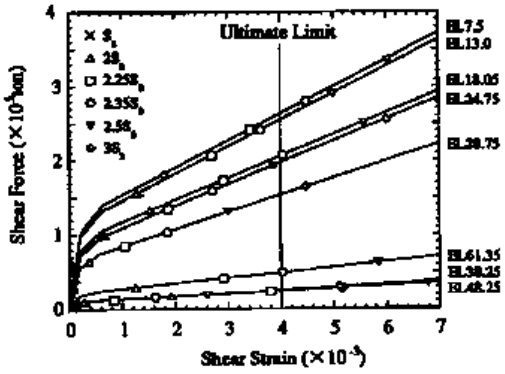

a)Shear Wall

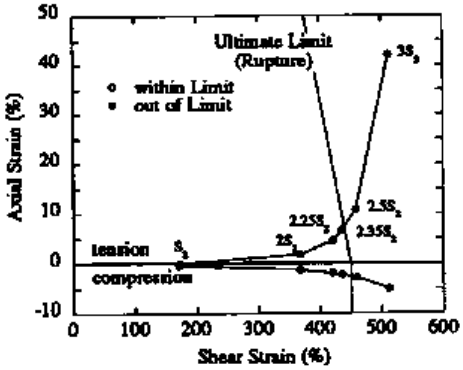

b)Laminated Rubber Bearing

Fig. 7 Maximum Response for Amplified S_2-M

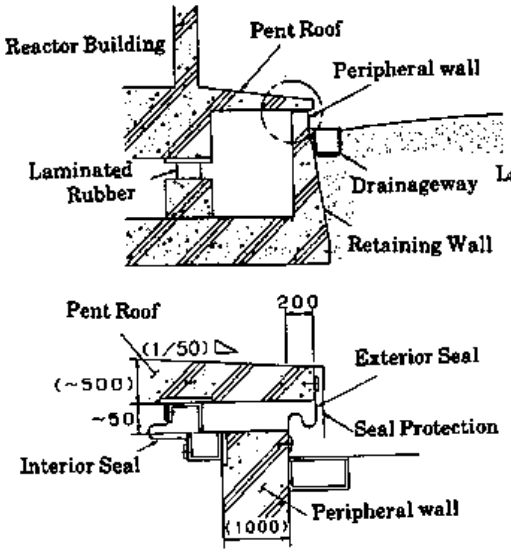

Fig. 8 Concept of PP Facilities

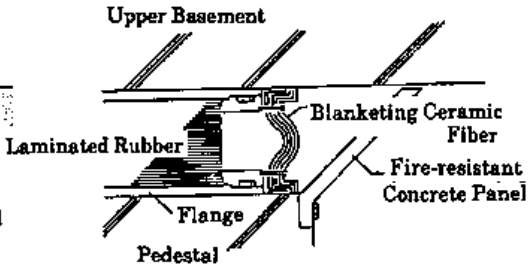

Fig. 9 Concept of Fire-resistant Cover

Transactions of the 13th International Conference on Structural Mechanics in Reactor Technology (SMiRT 13), Escola de Engenharia - Universidade Federal do Rio Grande do Sul, Porto Alegre, Brazil, August 13-18, 1995

Proposal for design guidelines for isolated nuclear facilities

Martelli, A.[1], Forni, M.[1], Bergamo, G.[2], Bonacina, G.[2], Cesari, G.F.[3], Di Pasquale, G.[4], Olivieri, M.[5]
1) ENEA, Energy Department, Nuclear Fission Branch, Bologna, Italy
2) ISMES S.p.A, Bergamo, Italy
3) Nuclear Engineering Laboratory, University of Bologna, Italy
4) ANPA, Roma, Italy
5) ANSALDO-Ricerche, Genova, Italy

ABSTRACT: A proposal for design guidelines for seismically isolated nuclear reactors and other nuclear facilities has been developed in the framework of a study sponsored by the European Commission. This proposal updates a previous document which focused on the high damping rubber bearings and extends it to most of the other isolation system types of interest.

1 INTRODUCTION, SCOPE AND APPLICABILITY

A proposal for guidelines for seismically isolated nuclear plants was prepared by Forni et al. (1995a) in the framework of a European Commission (EC) study contract, taking into account the most recent information on seismic analysis of nuclear plants in general and the state-of-the-art of engineering design of isolated structures (see, for instance, Martelli and Forni, eds., 1994), and taking advantage of considerable R&D and guidelines development work performed in Italy for seismic isolation (SI) of civil structures (Martelli et al. 1993 & 1995; Forni et al. 1995b).

The document of Forni et al. (1995a) was published in a tentative form to allow for broad review from experts. The qualification procedure specified for the SI devices may lead to a definition of a standard and use of a standardized product for SI design. The document updates and extends that of Martelli et al. (1990). It applies not only to isolated reactors, but also to other nuclear facilities (e.g. spent fuel storage pools) and concerns the horizontal SI systems that - according to the technologies developed in the EC countries, Japan, New Zealand and the USA - may be suitable for application to nuclear structures, namely those formed by high damping rubber bearings (HDRBs), lead rubber bearings (LRBs), low damping natural or synthetic (e.g. neoprene) rubber bearings (LDRBs) with separate elastic-plastic dampers (EPDs) or viscous dampers (VDs), and sliding devices (SDs). Remarks are also provided on simultaneous horizontal and vertical SI systems (3D systems), although the development of such systems or related information available to the authors were insufficient as to enable them to propose detailed guidelines (in particular, no details were available on the 3D pneumocord system which has been developed by Russians and is being considered for application to the VVER-500 reactor project, see Martelli and Forni, eds., 1994).

2 CONTENTS OF THE PROPOSAL

Similar to the proposal of Martelli et al. (1990), that of Forni et al. (1995a) mainly deals with items different from non-isolated systems. Focus is on requirements, analysis methods and qualification procedures of SI system and devices; proposals for design requirements and analysis methods for isolated structures, systems and components are also included. More details are provided for horizontal SI systems using rubber bearings than for horizontal systems formed by other SI devices, or especially, 3D systems, according to the larger application and experimental experiences of the authors on the former. Areas in which experimental data or design experience are not available have been marked (TBD) (To Be Determined). A list of still TBD items is summarized in appendix. When needed, the document provides comments to clarify the guidelines. Information on the SI systems considered in also provided in appendix.

The main structure of the previous proposal of Martelli et al. (1990) has not been modified. Some remarks are reported below on the technical sections of the document, by stressing some modifications and extensions with respect to the previous document.

Sect. 5: Definition of ground motions. Only analysis at Safe-Shutdown Earthquake (SSE) remains mandatory, while that at Operational Basis Earthquake (OBE) is now mandatory only when significant changes of isolator stiffness are expected from OBE to SSE, and the requirement that the minimum OBE value shall be half the SSE has been deleted. The need for special attention to the low-frequency range 0.1-1 Hz (because of the effects on isolated structures) is still stressed, but the requirement that design response spectra in the frequency range to 1 Hz shall be equal at least to that specified by R.G. 1.60 has been changed to a suggestion. Specific requirements concerning the features of design time-histories (t.hs.) have been moved to this section from Sect. 6 and better precised. The need for a characterization of ground motion rotational components, if relevant, has been specified.

Sect. 6: Design requirements and analysis methods for isolated building and isolation support structure. Somewhat improved definitions have been given for the horizontal Reference Displacement D_R, Calculated Displacement D_C, and Design Displacement D: in particular, reference shall be now made to 90% D_R (instead of D_R) for calculating D_C, and account for accidental eccentricity due rotational ground motion component is suggested to determine D_R. Residual Displacement D_F (which is relevant for some sliding systems) has also been defined. While the requirements concerning the stiffness of structural elements located above and below the SI interface and that no resultant tensile loads nor isolator uplift are permitted up to SSE remain unchanged, the safety factors agaist overturning at SSE has been increased from 1.1 to 2. The functions of ultimate vertical and horizontal fail-safe systems have been better pointed out, by also precising the related (previously TBD) values: it has been specified that the vertical system (for which a maximum clearance of 3-5 cm with respect to the structure is now required) and horizontal system shall be used unless it is demonstrated that the isolators can support the structure to 5 and 3 times the SSE, respectively; as regards the horizontal system it has been also specified that - if present - it shall not act until horizontal displacement is lower than 0.85 SF (where SF is a safety factor for which a value larger than 2 is now required) and shall hinder displacements larger than SF times the design value. A somewhat less conservative approach is now required for the definition of the gaps between adjacent isolated and non- or independently isolated structures (according to that mentioned above for D_C), and a specific requirement that they shall remain free in every design condition (e.g. flood) has been added. No major

changes have been made as regards the rules concerning inspectability and replacement capability of isolators, and recentring of the structure if necessary. For soil-structure interaction analysis the maximum damping ratio which can be assumed at SSE has been increased from 5% to 15%. For design analysis (use of t.hs., applicability of simplified methods, features of parametric calculations) some requirements have been implemented, namely the need for taking into account the contribution of input motion rotational components if they are larger than 10% of that due to translational components, need for at least 4 t.hs. (6 to 8 for sliding systems) when using t.h. analysis, and that for also considering damping (or friction) of the SI devices - in addition to soil, device and structure stiffnesses - when performing parametric analysis.

Sect. 7: Design and performance requirements of overall seismic isolation system. The horizontal design force has been defined, consistent with the design displacement, for sliding systems also. Maximum and minimum vertical loads V_{max} and V_{min} (resulting from the combination of vertical design load with the vertical earthquake component) have also been defined. The values concerning some previously TBD safety factors to be used in the design have been specified, by requiring that systems shall have a safety factor 1.7 for V_{max} and for 1.7 of D applied statically and simultaneously, and a safety factor 1.7 for D at 0.6 V_{min} (the minimum safety factor 3 was kept unchaged for V in the laterally underformed state of SI system). For SI systems using rubber bearings with or without separate EPDs the permissible range for horizontal isolation frequency has been extended to 0.33-1 Hz, and the requirement that vertical stiffness shall be sufficiently high to reduce any tendency of amplification refers now not only to vertical motion, but also to rocking. For such systems the minimum equivalent viscous damping ratio has been lowered from 10% to 8%, variations of +/- 30% and +/- 15% of the mean values have been specified as permissible for stiffness and damping, respectively (considering the external and environmental conditions and ageing - these ranges were TBD), and the need for investigating the effects of minor earthquakes has been specified, while requirements concerning self-centring with a minimum offset of 10% of the design displacement and wind resistance remain unchanged. Similar requirements have been specified separately, where applicable, for the sliding systems and systems including VDs. For the former a permissible range of +/- 30% of the mean value has been specified for friction coefficient; for the latter the need for accounting in the design for the dependance of damping on vibration velocity and internal fluid temperature resulting from ambient temperature and the number of applied vibration cycles has been specified; for both systems the presence of recentring devices in the SI system has been required, should not the devices be self-centring.

Sect. 8: Design requirements and analysis methods for isolated structures, systems and components. Should the OBE analysis be performed, the minimum number of OBEs to be accounted for in the analysis (in addition to one SSE) has been increased to 5 for components remaining in the plant during the entire life, although a minimum of 2 OBEs is frequently recommended. The rules previously provided for the analysis of secondary components, evaluation of floor response spectra and static analysis remain unchanged. As to sloshing, reference to simplified rules has been added in comments, and the requirement that the loss of liquid shall be prevented has been specified.

Sect. 9: Design requirements and analysis methods for interface components. Besides defining the displacements to be accomodated by both safety and non-safety related components and systems which cross the isolation interface (piping, cables, etc.), prescribing the effects to be considered and pointing out the need for experimental

qualification (accounting for the multidirectional nature of seismic motion, and the actual values of pressure and temperature when relevant), the present document includes more specific requirements concerning interface piping. These were derived from those applicable to usual nuclear piping, and concern design prescription, design analysis, the supports and their location, bellows, expansion joints, fittings and flanged joints. In particular, it has been stated that bellows should be avoided in all safety-related piping until their reliability has not been fully demonstrated.

Sect. 10: Design requirements for individual isolation devices. The use of previous experimental experience, instead of performing specific tests on prototypes, has been permitted to evaluate the basic parameters for the design (stiffnesses, damping, friction coefficient). The requirements concerning the vertical load capacity and design load, maximum horizontal displacement capacity, design displacement D and stability, and damping have been made consistent with those related to the overall SI system (Sect. 7). In addition, it has been specified that vertical load capacity and safety factors shall account for buckling effects and respectively, for roll-over if relevant. The definitions and requirements concerning vertical and horizontal stiffnesses, stiffness-strain relationship, dependence of horizontal stiffness on vertical load and maximum scatterings of stiffness and damping (+/- 10% from the mean value) have been confirmed, together with the need for specifying maximum and minimum stiffness, friction and damping values within the ranges mentioned in Sects. 7 and 12 and the possibility of using simplified formulas for estimating stiffnesses for rubber and steel devices. For damping the requirement that it shall be calculated as an average of the last 5 cycles has been removed, although conditionning before tests is still recommended for rubber bearings (it is suggested that 2 cycles are sufficient for them). Specific requirements have been added for LRBs (sufficiently high shape factor as to confine the lead plug, vertical load to be supported only by the rubber), for SDs (need for tests to evaluate friction coefficient dependence on sliding velocity, vertical load and temperature) and for VDs (evaluation of their stiffness contribution depending on frequency and temperature). As regards the effects of cycling and related degradation (fatigue), it has been specified that the characteristics of SI devices shall not vary more than 15% between the 2nd the the 10th cycle performed at the isolation frequency and at the displacement D after 50 cycles at OBE (all these items were TBD). Requirements concerning the environmental effects have been also much better precised, in particular by including the need for SI devices of withstanding chemical and biological attacks, by requiring that adequate engineering solutions are adopted to prevent and mitigate the various attacks, by providing information on radiation effects, by limiting temperature effect to +/-15%, and by requiring resistance to exposition to a temperature of 150°C for 2 hours, direct exposition to fire for a TBD time, and replacement after a fire. The limit value for creep vertical deformation has been increased from 20% of the dead load deflection during the isolator life (which shall be equal to at least that of the plant) to 30%. It is now specified that SI devices shall survive the faulted conditions at the end of their design life and that periodic (TBD) replacement is permitted for internal fluid of VDs. Experiments have been required to evaluate maximum offset unless previuos experience is available. The requirements concerning absence of resultant tensile loads, limit tensile capacity of isolators and absence of disengagement of monolateral bearing connections to SF times D have been confirmed. Finally. the requirements concerning design tolerances have been extended to SI devices other than the HDRBs.

Sect. 11: Qualification of seismic isolation device and isolation system. It has been specified that seismic qualification by test is mandatory unless finite-elements (f.e.)

models are available which have been previously qualified for the relevant test conditions (see Forni et al. 1995b). Reference to IEC standards has been introduced as regards non seismic aspects, together with the requirement that the manufacturing process of SI devices shall be qualified. The static and dynamic tests required on materials, complete bearings and SI system proposed by Martelli et al. (1990) have been updated and specified for all horizontal SI systems considered, taking into account subsequent experience and the requirements mentioned in previous sections (see also Martelli et al., 1995a). The minimum number of each device type to be manufactured for qualification tests has been specified (4 for isolators and 2 for dissipators). As regards SI device tests, the concept has been introduced that qualification is necessary every time that devices with new features are used; accordingly, criteria for keeping previous tests valid, in spite of somewhat different values of some parameters have been specified, together with those allowing for tests on scaled devices. Repetition of some tests on ageed bearings at the maximum and minimum design temperatures has been required. As regards the SI system the shake table tests which are required (unless previous detailed experience is available) have been somewhat simplified according to test experience, by permitting two- or even one-dimensional shake table tests if they aim at simply evaluating the self-centring or re-centring capability of SI system (to this purpose free-vibration tests are generally not adequate). The usefulness and limits of in-situ dynamic tests on actual structures have been outlined.

Sect. 12: Acceptance testing of isolation devices. Similar to qualification tests, those required to provide the quality control of SI devices have also been updated and extended to the various systems considered. As regards rubber bearings, while the compression tests to confirm vertical stiffness and sustained compression tests shall be still performed for all isolators, the destructive tests have been limited to 2% of those to be installed (minimum 2 isolators) and combined shear and compression tests shall be carried out for a minimum between 20 and 20% of isolators. With regard to sustained compression tests the duration of 24 hours has been specified, and the limit of 20% of the dead load deflection has been confirmed for total height variation (taking into account temperature and ageing effects as evaluated during qualification). The criteria to be adopted for rejecting bearings in the case that controls are out of tolerances have been better precised. Finally, the importance of reliable bearing identification has been better stressed and the required documentation concerning acceptance tests has been specified.

Sect. 13: Seismic isolation reliability. No major changes have been made as to the Quality Assurance program and bearing life-time (only the reference to f.e. analysis as to the evaluation of phenomena affecting the bearing reliability has been deleted). On the contrary, in-service inspection tests have been updated and extended to all SI devices considered, based on criteria consistent with those adopted for qualification and acceptance tests, and the requirement concerning submission of the in-service inspection program to the Licensing Authorities has been deleted. The previously TBD numbers of devices to be tested, time intervals between subsequent testing and related procedures have been precised (3 full-scale or scaled devices per each outage, kept in actual vertical compression load and environmental conditions, every 6 months; 10 or 10% of full-scale devices every two years; 10 or 10% of actual devices, temporarily removed at random from the plant, after an OBE).

Sect. 14: Seismic safety margins. This section has been considerably shortened, because it was unnecessarily too detailed. Reference is now made to relevant documents as regards the description of Probabilistic Risk Assesment (PRA) and Seismic Margin

Evaluation (SME) procedures (which are alternative options), and requirements have been limited to specific issues related to the adoption of SI, namely to the definition of seismic input (earthquake level for SME, maximum displacement at the ground and spectral content) and SI effects on the response to beyond SSE earthquakes (scaling issues, possible closure of gaps, evaluation of the seismic capacity/fragility of the SI system taking into account various non-linear effects).

Sect. 15: Seismic safety and monitoring systems. No significant changes were made for the requirements concerning these systems. The document still specifies the need for a detailed monitoring system, capable of recording seismic motions during time in the free-field and on the structure, partly in short time, and points out that dispacements between the structure base and SI system support base must be recorded, besides acceleration at various elevations.

4 CONCLUSIONS

This paper has summarized the main features of an updated proposal for design guidelines for seismically isolated nuclear plants, applicable to most horizontal isolation systems of interest, by stressing the improvements with respect to a previous document, which was limited to the use of HDRBs and for which several issues were still unresolved. The document will be periodically updated by ENEA to include comments and to reflect the advances in seismic isolation technology development. Future R&D work shall focus on establishing a data base which will support the development of specific rules for items which are still "To Be Determined" (TBD).

REFERENCES

Martelli, A., Carpani, B., Forni, M., Di Pasquale, G., Sanò, T., Bonacina, G., Olivieri, M., Marioni, A. & G.F. Cesari 1993. Extension of guidelines to seismically isolated reactors. *Proc. 12th Int. SMiRT Conf., Stuttgart, 15-20 August 1993*. K2: 333-338. Amsterdam: North Holland.

Forni, M., Martelli, A., Bergamo, G., Bonacina, G., Cesari G.F., Di Pasquale, Marioni, A. & M. Olivieri 1995a. *Proposal for design guidelines for seismically isolated nuclear plants. EC-ENEA Contract ETNU-0031-IT*. Bologna: ENEA for EC.

Forni, M., Martelli, A., Dusi, A. & G. Castellano 1995b. F.E. models of steel-laminated rubber bearings for seismic isolation of nuclear facilities. *Proc. 13th Int. SMiRT Conf., Porto Alegre, 13-18 August 1995*. Rotterdam: Balkema.

Martelli, A., Masoni, P., Di Pasquale, G., Lucarelli, V., Sanò, T., Bonacina, G., Gluekler, E.L. and F.F. Tajirian 1990. Proposal for Guidelines for Seismically Isolated Nuclear Power Plants - Horizontal Isolation Systems Using High Damping Steel-Laminated Elastomer Bearings. *Energia Nucleare*. 1: 67-95.

Martelli, A. & M. Forni, eds., 1994. *Isolation, energy dissipation and control of vibrations of structures. Proc. of the Post-SMiRT Conf. Seminar, Capri, 23-25 August 1993*. Bologna: ENEA for GLIS.

Martelli, A., Forni, M., Spadoni, B., Marioni, A., Bonacina, G. & G. Pucci 1995. Progress of Italian experimental activities on seismic isolation. *Proc. 13th Int. SMiRT Conf., Porto Alegre, 13-18 August 1995*. Rotterdam: Balkema.

Transactions of the 13th International Conference on Structural Mechanics in Reactor Technology (SMiRT 13), Escola de Engenharia - Universidade Federal do Rio Grande do Sul, Porto Alegre, Brazil, August 13-18, 1995

Progress of Italian experimental activities on seismic isolation

Martelli, A.[1], Forni, M.[1], Spadoni, B.[1], Bettinali, F.[2], Marioni, A.[3], Bonacina, G.[4], Pucci, G.[4], Cesari, F.[5]

1) ENEA, Energy Department, Nuclear Fission Branch, Bologna, Italy
2) ENEL, Hydraulic and Structural Research Center, Milano, Italy
3) ALGA S.p.A., Milano, Italy
4) ISMES S.p.A., Bergamo, Italy
5) Nuclear Engineering Laboratory, University of Bologna, Italy

ABSTRACT: Detailed studies have been performed in Italy since 1988 to verify the applicability of seismic isolation to high risk structures such as nuclear plants. These include experiments, development and validation of numerical models, and design guidelines development. This paper deals with the first item. In particular, information is provided as to the most recent progress concerning static and dynamic tests of high damping rubber specimens and bearings, and shake table tests of isolated structures.

1 INTRODUCTION

Large efforts are going on in Italy for the development, validation and application of seismic isolation (SI) techniques for civil and industrial structures. These are being performed in framework of both collaborative activities of the Italian Working Group on Seismic Isolation (GLIS), and international co-operative projects with other European and U.S. partners. As regards the applications to industrial structures, ENEA is particularly interested in those to nuclear reactors and other nuclear facilities (e.g. spent fuel storage pools), while the main interest of other Italian partners (e.g. ENEL) is at present mainly in conventional energy production plants (Bonacina et al. 1994). Very close co-operation among partners with different application objectives has been justified by the great potential of SI for both civil and industrial structures, and among the latter, for both nuclear and non-nuclear plants (Forni et al. 1993).

Studies relevant to nuclear and other industrial applications of SI began in Italy in 1988, and include experiments, numerical modelling and development of design guidelines. This paper focuses on the recent developments concerning the first item, while those related to the last two items are presented separately by Forni et al. (1995) and by Martelli et al. (1995).

2 EXPERIMENTS IN PROGRESS

Forni et al. (1993) described the experimental campaigns which had been carried out in Italy for SI development prior the 12th SMiRT Conference. These concerned the use of High Damping Rubber Bearing (HDRB) as isolator, and comprised laboratory tests on rubber specimens, individual isolators, isolated structure mock-ups, and actual isolated

buildings (in-situ tests).

The above activities have been jointly continued by ENEA, ENEL, ALGA (which is the manufacturer of HDRBs in Italy), ISMES, the Nuclear Engineering Laboratory (LIN) of the University of Bologna and ANSALDO Ricerche. Again, experiments have been mainly based on the HDRBs, although some tests have also been performed and a new research project already defined concerning other SI and energy dissipation systems. With respect to previous studies, however, the analysis of the effects of different parameters affecting the HDRB behaviour, and their combinations, has been considerably extended: in particular, various types of attachment systems between bearings and steel end-plates (recess, bolts, central dowel, combined use of central dowel and bolts, and direct bonding), rubber compounds and shape factors (S) have been considered. The most relevant recent activities which have already been completed or are in progress concern: (a) uniaxial, equibiaxial and shear tests on high damping rubber specimens; (b) static and dynamic tests of single isolators; (c) shake table tests of a half-scale isolated mock-up of electric equipment. In order to allow for such tests special purpose testing equipment was designed and fabricated (Forni et al. 1995). Further tests will begin soon.

3 TESTS ON RUBBER SPECIMENS

Uniaxial (tension and compression) and equibiaxial tests of rubber specimens have been performed at ENEL for both a rather hard rubber compound used in the U.S. Advanced Liquid Metal Reactor (ALMR) Project (shear modulus G = 1.4 MPa) and new medium hardness (G = 0.8 MPa) and soft (G = 0.4 MPa) compounds. Tests concerning the ALMR rubber have been carried out in the framework of a co-operation with GE Nuclear Energy. Special equipment designed by ENEA and ENEL and manufactured by ENEL has been used for equibiaxial tests. Shear tests have also been carried out at ENEL for specimens of the aforementioned rubber compounds, again using a new testing equipment, which was designed by ENEA and manufactured by LIN.

Figure 1 shows examples of test results. Tests data were used by Forni et al. (1995) to validate and calibrate hyperelastic models of the rubbers considered, then adopted in the detailed analysis of related HDRBs. Evaluation of temperature and ageing effects will soon begin at ALGA and ANSALDO-Ricerche.

4 TESTS ON ISOLATORS

The experimental campaigns in progress for the HDRBs are being jointly carried out by ENEA, ENEL, LIN and ISMES using both SISTEM (Seismic ISolation TEst Machine) - after this equipment was improved by ENEA to allow for easier testing of different size isolators and for real time visualization of the measured data (Figure 2) - and the new CAT (Creep and Aging Tests) machine (Figure 3). These experiments concern HDRBs characterized by: (a) various sizes (125 mm, 250 mm, 500 mm and 600 mm diameters); (b) both medium hardness and soft compounds mentioned in Sect. 3; (c) shape factors S = 12, S = 16 and S = 24; (d) all the attachment systems mentioned in Sect. 2. Some bearings (including the 600 mm diameter HDRBs with soft compound and S = 16) were tested in support of the evaluation of SI benefits for electric equipment, while the other experiments belong to a more recent project for the optimization of HDRBs.

As regards the first tests Bonacina et al. (1994) showed that HDRBs provided with

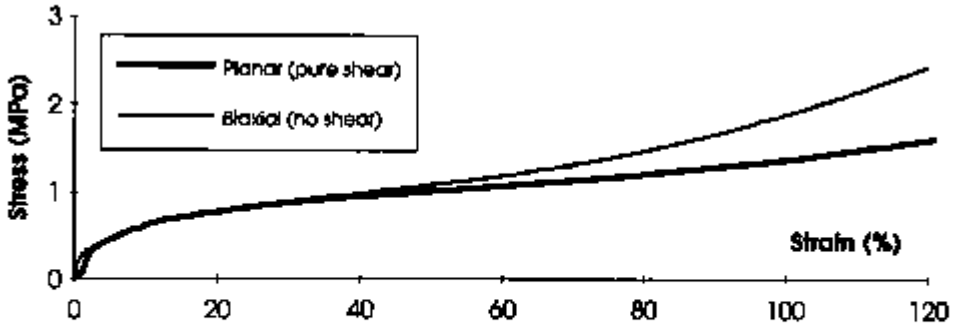

Figure 1. Results of equibiaxial and shear tests of rubber specimens (G = 0.8 MPa).

Figure 2. Compression and compression & shear tests on the SISTEM modified version.

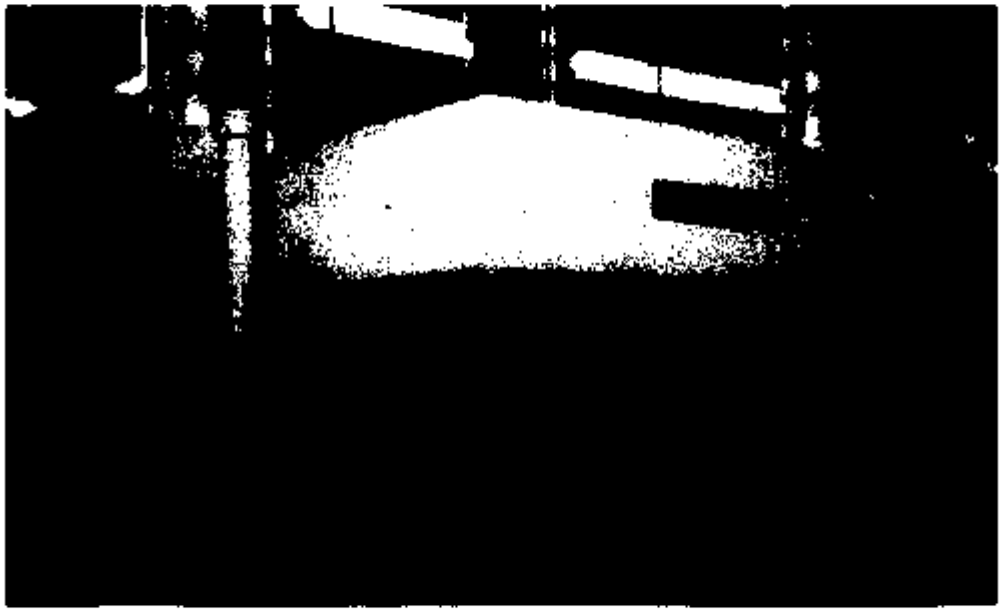

Figure 3. Creep test on full-scale isolators on CAT machine.

central dowel in conjunction with bolts for the attachment system can reach 400% shear strain, in addition to vertical compression load equal to at least 8 times the design value, without failing. Control test performed to 150% shear strain on a 250 mm diameter bearings immediately after the large shear tests showed non-negligible stiffness decrease and damping increase; however, by repeating the same control test 16 months afterwards (prior to shake table experiments of Sect. 5), it was found that damping had recovered its initial value, and that horizontal stiffness was only 7% lower than its original value at 150% shear strain. Thus, the effects of large shear test are to not be attributed to internal damage, but rather to some temporary modification of rubber molecular structure.

The experiments for optimization of HDRBs have been defined based on previous experience of Forni et al. (1993). They comprise, for each relevant combination of the above parameters: (i) quasi-static vertical compression tests for the evaluation of vertical stiffness; (ii) quasi-static shear tests under constant vertical compression load V for the evaluation of static horizontal stiffness at 50%, 100% and 200% shear strain; (iii) quasi-static shear tests at 100% shear strain with different vertical compression loads (from 0.25 V to 2 V) for evaluating the effects of vertical load variation on horizontal stiffness; (iv) dynamic shear tests at various frequencies (0.1, 0.4, and 0.6 Hz), under constant V and at various shear strain values (from 10% to 200%), to evaluate equivalent viscous damping and dynamic effects on the horizontal stiffness; (v) sustained compression tests (from 72 hours at ISMES to some months on the CAT machine at LIN) to evaluate creep effects; (vi) quasi-static failure tests due to compression and shear; (vii) evaluation of temperature and ageing effects on stiffness and damping. These tests are consistent with bearing qualification requirements.

Several experiments have already been performed (March 1995) at room temperature for the 250 mm diameter bearings formed by the medium hardness compound (on which previous experience was deeper), for both shape factors S = 12 and S = 24. Tests for the the evaluation of temperature and ageing effects will begin soon at ANSALDO-Ricerche. Most completed tests concerned bearings with the recess attachment system (for the same reason as above), but some also with that consisting of the central dowel in connection with bolts. Data are already available for the full test series mentioned above. Their processing and implementation in detailed HDRB models are in progress. The good performance of isolators seems to be confirmed, in particular as regards damping which increased (with respect to the HDRBs previously available) from less than 15% to about 20% as desired (Figure 4 shows the results of a shear test).

5 SHAKE TABLE TESTS

Based on the experience achieved in previous tests by Forni et al. (1993), shake table tests have already been performed at ISMES on a rigid mass mock-up of ENEL electric equipment supported by four 250 mm diameter HDRBs designed by ENEA (soft compound, attachment system formed by central dowel and bolts). Three isolators were virgin, while the fourth was that mentioned in Sect. 4 which had been subjected to 400% shear strain. The superstructure, weighting 335 kN, was provided with an eccentric upper part to simulate actual equipment. One-, two- and three directional simultaneous excitations were applied, which corresponded to rigid, medium and relatively soft soil conditions similar to previous tests. The maximum displacement (143 mm, corresponding to 217% shear strain, see Figure 5) was reached for the Calitri record of the 1980 Campano-Lucano (Irpinia) earthquake (relatively soft soil conditions). No damage of

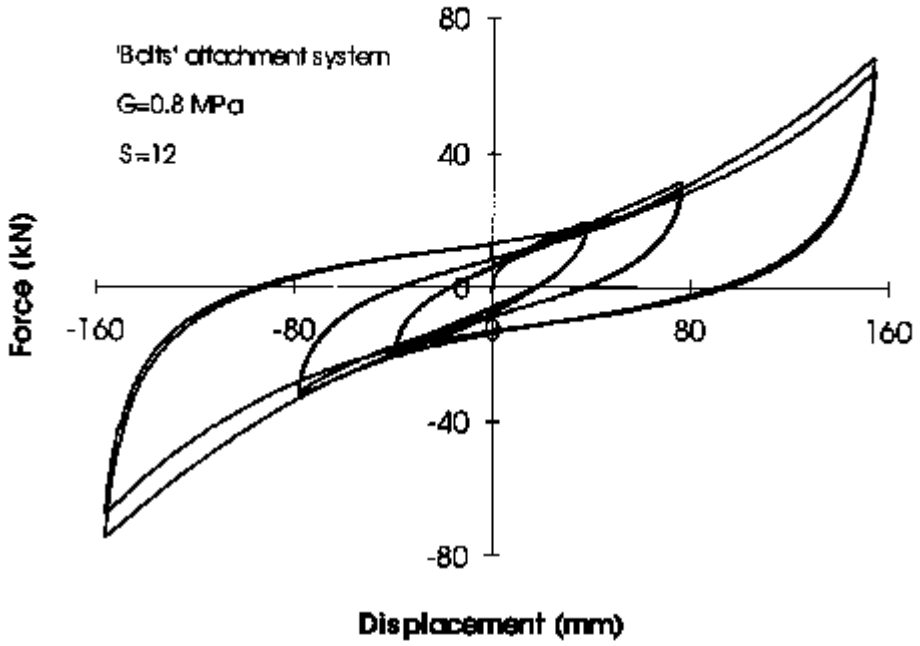

Figure 4. Results of a 200% shear test on a half-scale HDRB.

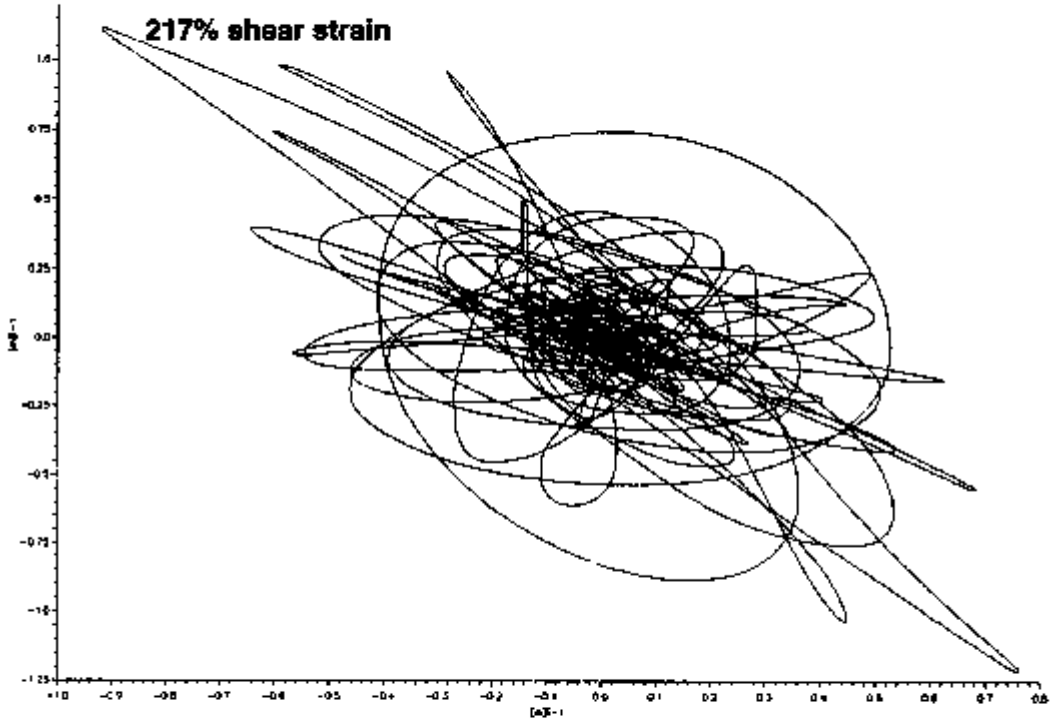

Figure 5. Displacement measured for the isolated electric equipment mock-up (3-directional simultaneous application of the 0 db Calitri record).

bearings was detected at test conclusion, not even on the fourth aforesaid isolator.

Further shake table tests, on a more representative structure mock-up supported by optimized HDRBs, will begin at ISMES as soon as the experiments concerning single bearings are completed. In addition, shake table tests have been planned for isolated nuclear structures at the Casaccia Laboratories of ENEA, partly in the framework of a cooperation with GE (i.e. using the ALMR bearings, which were partly manufactured by ALGA). These tests will concern reactor vessels like that of PRISM, but spent fuel storage pools may be also considered in the future. Finally, a first set of experiments of large structures based on HDRBs, to be performed at JRC Ispra using the pseudodynamic method, has been defined (Renda et al. 1995).

6 CONCLUSIONS

The experiments described above are considerably extending the knowledge previously acquired in Italy on the behaviour of HDRBs and will contribute to the optimization of such bearings. The results already obtained confirm the capability of SI for considerably enhancing the seismic protection of civil and industrial structures, including nuclear plants, and provided relevant input for the design guidelines development of Martelli et al. (1995). Some more details and some extensions of the work will be presented by Marioni et al. (1995) at Post-SMiRT Seminar No. 1.

REFERENCES

Bonacina, G., Bettinali, F. & A. Martelli 1995. State-of-the-art of work in progress on seismic isolation technique for civil structures and industrial plants. *Proc. 10th European Conf. on Earthquake Engineering, Vienna, 28 August - 2 September 1994.*

Forni, M., Martelli, A., Spadoni, B., Vernoni, G., Bettinali, F., Marioni, A., Bonacina, G., Mazzieri, C. & F. Vestroni 1993. Most recent experimental and numerical studies performed in Italy on seismic isolation. *Proc. 12th Int. SMiRT Conf., Stuttgart, 15-20 August 1993.* K2: 225-236. Amsterdam: North Holland.

Forni, M., Martelli, A., Dusi, A. & G. Castellano 1995. F.E. models of steel-laminated rubber bearings for seismic isolation of nuclear facilities. *Proc. 13th Int. SMiRT Conf., Porto Alegre, 13-18 August 1995.* Rotterdam: Balkema.

Marioni, A., Martelli, A., Forni, M., Bonacina, G., Bettinali, F. & C. Mazzieri 1995. Progress in applications and experimental studies for isolated structures in Italy. *Proc. Post-SMiRT Conf. Seminar on Seismic Isolation, Passive Energy Dissipation and Active Control of Structures, Santiago, 21-23 August 1995.*

Martelli, A., Forni, M., Bergamo, G., Bonacina, B., Cesari, G.F., Di Pasquale, G. & M. Olivieri 1995. Proposal for design guidelines for isolated nuclear facilities. *Proc. 13th Int. SMiRT Conf., Porto Alegre, 13-18 August 1995.* Rotterdam: Balkema.

Renda, V., Martelli, A., Verzelletti, G. & L. Papa 1995. Research activities and programmes on seismic isolation at the Joint Research Center of the European Commission. *Proc. Post-SMiRT Conf. Seminar on Seismic Isolation, Passive Energy Dissipation and Active Control of Structures, Santiago, 21-23 August 1995.*

Transactions of the 13th International Conference on Structural Mechanics in Reactor Technology (SMiRT 13), Escola de Engenharia - Universidade Federal do Rio Grande do Sul, Porto Alegre, Brazil, August 13-18, 1995

Input energy spectrum and its application to response prediction considering large deformation characteristics of seismic isolation

Kato, M.[1], Watanabe, Y.[1], Kato, A.[1], Yoshikawa K.[2], Mizukoshi, K.[2], Koshida, H.[2], Fukushima, Y.[2], Nakayama, T.[2]

1) The Japan Atomic Power Company, Tokyo, Japan

2) Kajima Corporation, Tokyo, Japan

ABSTRACT : A method for simple prediction of seismic response was established to evaluate maximum displacement and shear force of a base isolated Fast Breeder Reactor (FBR) plant building, whose foundations incorporated laminated rubber bearings with hardening characteristics and steel dampers with elasto-plastic characteristics.

The general features of the energy spectrum for base isolated buildings were studied and it was found that the seismic response could be estimated easily from the energy spectrum.

1. INTRODUCTION

A simple method of predicting the seismic responses of structures has been studied. This method utilizes the amount of energy applied to a structure during a seismic motion (H. Akiyama 1985). In applying it to the response evaluation of a base isolated structure up to ultimate, an input energy spectrum that takes account of elasto-plastic restoring force characteristics and the hardening stiffness of natural rubber bearings (NRB) was used. The relationships among the input energy, the maximum response displacement and the maximum response base shear coefficient of the isolation layer were examined. Also, a trial was conducted to develop a method for simple prediction of maximum response using the input energy spectrum.

2. SUMMARY OF ENERGY SPECTRUM

The energy spectra indicate the relationships between input energy acting on a structure during a seismic motion and the structure's natural period. The equilibrium of the total energy of a single degree of freedom system is expressed by :

$$1/2M\dot{x}^2 + \int_0^t C\dot{x}^2 dt + \int_0^t F(x)\dot{x}dt = \int_0^t -M\ddot{Z}\dot{x}dt \qquad (1)$$

where,

M : Mass, C : Coefficient of viscous damping, F(x) : Restoring force,

X : Relative displacement, $\dot{X}$: Relative velocity, $\ddot{Z}$: Acceleration of ground motion

The right side of this equation is the input energy acting on a structure from time 0 to time t under a seismic motion. The first term on the left side is the kinetic energy at time t, the second term is the energy absorption of the viscous damping from time 0 to time t, and the third term is the sum of the elastic potential energy at time t and the hysteresis energy absorption from time 0 to time t.

Two kinds of input spectra, the total input energy spectrum and the momental energy spectrum, are used in this paper. The total input energy spectrum is the total input energy acting on the structures till the end of the seismic motion. In this case, the duration of the right side of Eq.(1) is from 0 to the end of the seismic motion. The momental input energy is the maximum input energy incremented during the time span Δ t from time t to time t+Δ t.

In this paper, the equivalent velocity by the transfer of input energy is represented by Ve as:

$$Ve = \sqrt{\frac{2E}{M}} \qquad (2)$$

where, Ve : Equivalent velocity, E : Input energy, M : Mass of single-degree-of-freedom system

3. SEISMIC ANALYSIS MODEL AND INPUT SEISMIC MOTIONS

A non-linear seismic response analysis for the base isolated FBR plant building was conducted by preparing a single degree of freedom system model as shown in Fig.2, that possesses weight, NRB with hardening and viscous damping (and a steel damper with elasto-plastic restoring force characteristics as shown in Fig.3). The energy spectra were analyzed by using two models: one without a damper and the other with a damper. Hereafter, analysis results of the former are represented by 'no damper' and results of the latter by 'damper'. There are 33 kinds of natural vibration period (T) for both models, from 0.3 to 3.5 seconds, that can be determined by K1. The natural periods are used to indicate each vibration period value of the spectra. The values for the hardening point P1,P2 in Fig.2 are assumed to be constant. After K1 is determined, Kd1 is assumed to be such that the natural vibration period of the damper model by (K1+Kd1) becomes 0.5T. Furthermore, the model with the natural vibration period of 2 seconds corresponds to the base isolated FBR building model for the series of studies herein.

Three seismic motions were applied; El Centro 1940(NS), Hachinohe 1968(NS), and Design basis earthquake motion(DBE) which was used in this series of studies (M. Kato et al. 1991). Three input levels, S2 level, two times S2 level(2$\times$S2), and three times S2 level(3$\times$S2), were applied. Also, for the El Centro and Hachinohe waves, the maximum velocity value of 50cm/sec was determined as the S2 level. For the DBE, a maximum acceleration 831 Gal and a maximum velocity 152cm/sec were determined as S2 level.

4. RESULTS OF SEISMIC RESPONSE ANALYSIS

4.1 Total input energy spectrum

The total input energy spectrum obtained from the results of the seismic response analysis is shown in Fig.4. In both cases of with and without the damper, the values of total input energy are about the same. However, in the case with the damper, a considerable smoothing tendency is noticed.

4.2 Relative displacement spectrum

The relative displacement spectrum(DBE) is shown in Fig.5. With the levels of S2 and 2×S2, it is noticed that the relative displacement with the damper is about one half of that without the damper.

4.3 Base shear coefficient spectra

Base shear coefficient spectra(DBE) are shown in Fig.6. At the S2 level, it is noticed that the value with the damper in the long vibration period range is considerably smaller than that without the damper.

4.4 Momental input energy spectrum

A significant correlation was recognized between the maximum response of the isolation layer and the momental input energy (A.I.J 1989). Fig.7 shows the momental input energy spectra (DBE) where Δ t is assumed to be structure's natural vibration period (T). It can be seen that for S2 and 2×S2 the spectra are stable.

4.5 Comparison of total input energy spectra by elastic viscous damping model

The total input energy spectrum can be calculated rather easily by the elastic viscous damping model. If the input energy spectrum by the hysteresis model spectrum can be replaced by the viscous damping model it is possible to make a simple prediction. Fig.8 compares the spectra by the hysteresis model and by the elastic viscous damping model. By adjusting the damping constants of the elastic viscous damping model, it is noticed that the hysteresis model can be approximated. This indicates that the spectra of the no-damper model are approximated by the spectra for damping constant h=2%, and the damper model by the spectra for h=20%

5. RELATIONSHIP OF INPUT ENERGY AND RESPONSE

Regarding the base isolated building as an actual FBR plant, as considered in the series of studies conducted herewith, the review results indicated hereafter are for the case of a damper model whose natural vibration period is 2.0-2.5 seconds.

Fig.9 shows the relationship between the total input energy and the maximum response displacement. Fig.10 shows the relationship between the momental input energy and the maximum response displacement. This shows that the total input energy and the maximum response displacement correlate closely. It also indicates that the momental input energy has a higher correlation than the total input energy. Fig.11 shows the relationship between the total input energy and the maximum response base shear coefficient. Fig.12 shows the relationship between the momental input energy and the maximum response base shear coefficient. From these figures it can be seen that in the case of displacement response, the input energy and the base shear coefficient correlate closely. Also, bilinear relationship is observed. The main reason for this is thought to be that, when the input level is small the base shear coefficient is also small due to the damper effect, but as an input increases, the base shear coefficient becomes larger under the influence of hardening stiffness of the rubber bearing.

6. SIMPLIFIED PREDICTION OF RESPONSE AND ITS APPLICABILITY

The response is predicted by Equation (3) below, which assumes that the total input energy is consumed by repeating the maximum displacement d max of the base isolation layer n times. Wp1 and We are illustrated in Fig.1.

$$n \times Wp1 + We = Eall \quad (3)$$

where,
Eall: Total input energy ($=1/2MVe^2$), Wp1 : Hysteresis absorption energy of 1 cycle at time of maximum displacement d max, We : Elastic potential energy at time of maximum displacement d max, n : Number representing response repetitions

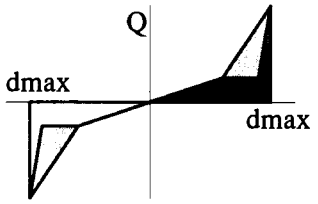

Restoring force characteristics of rubber bearing

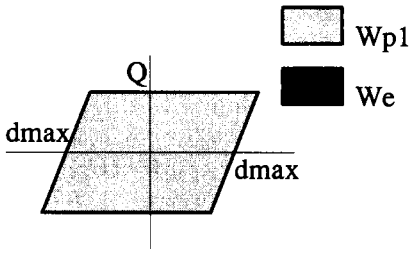

Restoring force characteristics of damper

Fig.1 Hysteresis absorption energy and elastic potential energy

Here, n depends on the seismic motion characteristics. Thus, a small n indicates that a sudden input energy acts on the structures and the energy absorption occurs within a short period of time (few repetitions). If n is determined based on seismic motions in general, and if the hysteresis absorption energy per cycle is obtained from the restoring force characteristics and the elastic potential energy are established, then it becomes possible to predict the response from the total input energy.

Fig.13 shows the response prediction flow. Fig.14 shows the curvilinear relationship between maximum displacement and the total input energy obtained from Eq.(3) when n=2,4,6. The figures correspond to natural vibration periods of 2.0, 2.2, and 2.5 seconds. The figure also shows the response analysis results obtained by the hysteresis model. The maximum base shear coefficient is indicated in the same way. From the figures, if the El Centro wave is considered as approximately n=2, and Hachinohe and DBE(Design basis earthquake) are considered as about n=4, then it is found that the maximum response in general can be predicted.

The energy spectrum is useful in predicting the response. It was found in chapter 4 that if the input is large, the total energy spectrum by the hysteresis model with the damper could approximately equal the spectrum of the elastic viscous damping model (h=20%). That approximation using elastic viscous damping can make it possible to predict the maximum response of the isolation layer. The total input energy of DBE analyzed by the elastic viscous damping model(h=20%) is shown in Fig.14 by a vertical broken line, and the response prediction, which is obtained from the intersection of the vertical line(h=20%) and the curve obtained by Eq.(3), is in good agreement with the analysis results by the hysteresis model.

7. CONCLUDING REMARKS

The response of a base isolated structure with hardening stiffness restoring force characteristics was studied from the stand point of input energy.

First, a total input energy spectrum and momental input energy spectrum that

considers the hardening stiffness of the rubber bearing were derived, and their characteristics were reviewed. The obtained energy spectrum indicated a stable configuration identical to the energy spectrum that is applicable to the non-linear response of non-isolated structures. It was thus verified that the spectrum obtained here can be utilized for base isolated structural design.

Second, it was made clear that the input energy, the response displacement and the response base shear coefficient correlate closely. It was also confirmed that the response could be predicted rather simply from the total input energy and the restoring force characteristics of the base isolation layer.

8. ACKNOWLEDGMENT

The authors wish to express sincere appreciation to Prof. H. Akiyama of University of Tokyo for his valuable advice with this research.

This study was carried out as part of a common research study by the electric power companies of Japan, entitled ' Technical Study on Actualization of Isolated FBR Plant(Part 1) '.

9. REFERENCES

H. Akiyama, *' Earthquake resistant limit state design for buildings '*, University of Tokyo Press, 1985

Architectural Institute of Japan, (1989), *'Recommendation for Design of Base Isolated Buildings'*

M. Kato, Y.Watanabe & A. Kato,(1991), *'Study on the seismic base-isolated reactor building for demonstration FBR plant in Japan'*, 11th SMiRT, Vol.K2, pp97-102

M. Kato, Y.Watanabe, A. Kato et al.,(1993), *'Multi directional earthquake input test and simulation analysis of base isolated structure '*, 12th SMiRT, Vol.K2, PP237-242

M. Kato, Y.Watanabe, A. Kato et al. (1993), *'Dynamic breaking tests on base-isolated FBR plant '*, 12th SMiRT, Vol.K2, PP267-278

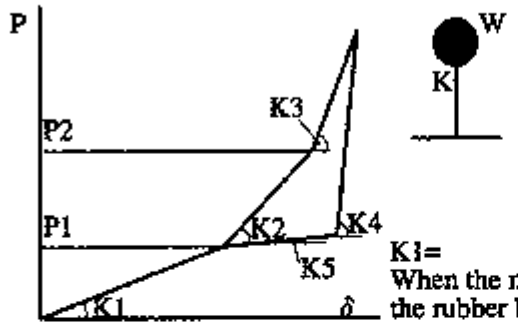

Fig.2 Vibration model and restoring force characteristics of rubber bearing

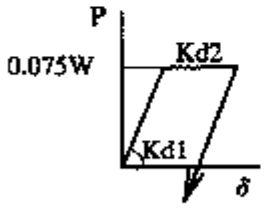

Fig.3 Restoring force characteristics of damper

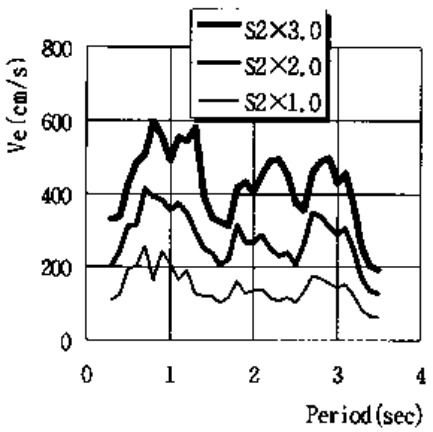

a) El Centro ns (No damper)

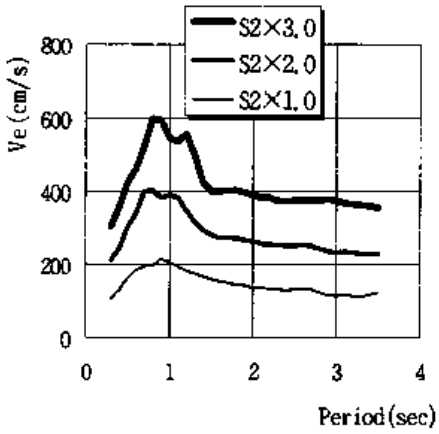

b) El Centro ns (Damper)

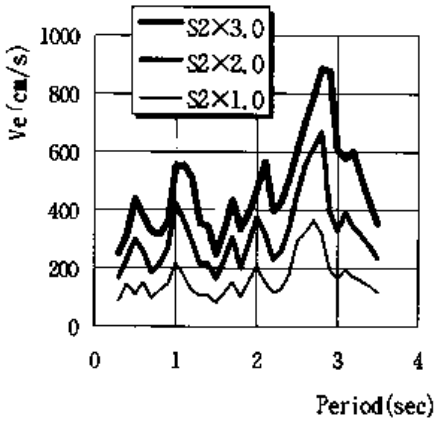

c) Hachinohe ns(No damper)

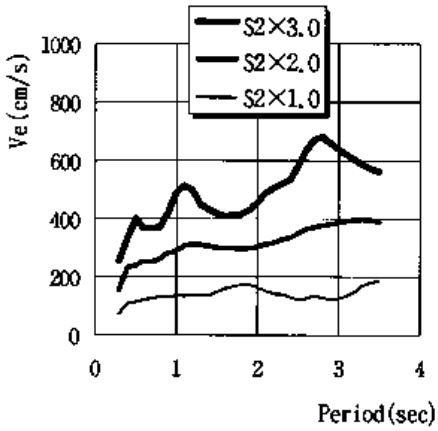

d) Hachinohe ns(Damper)

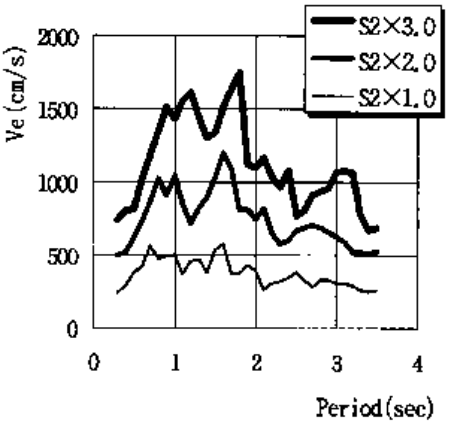

e) DBE (No damper)

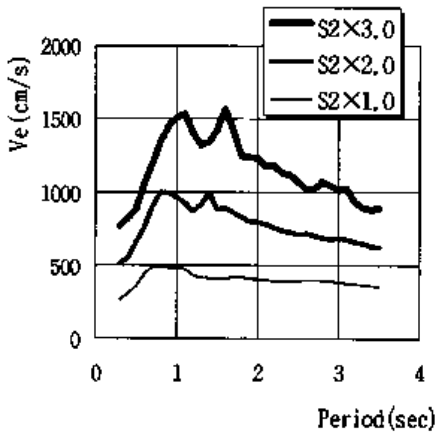

f) DBE (Damper)

Fig 4 Total input energy spectrum

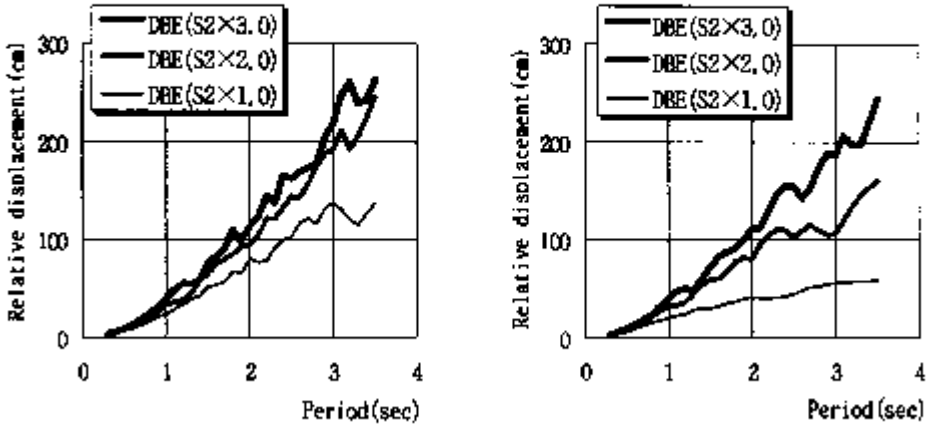

a) No damper b) Damper

Fig.5 Relative displacement spectrum(DBE)

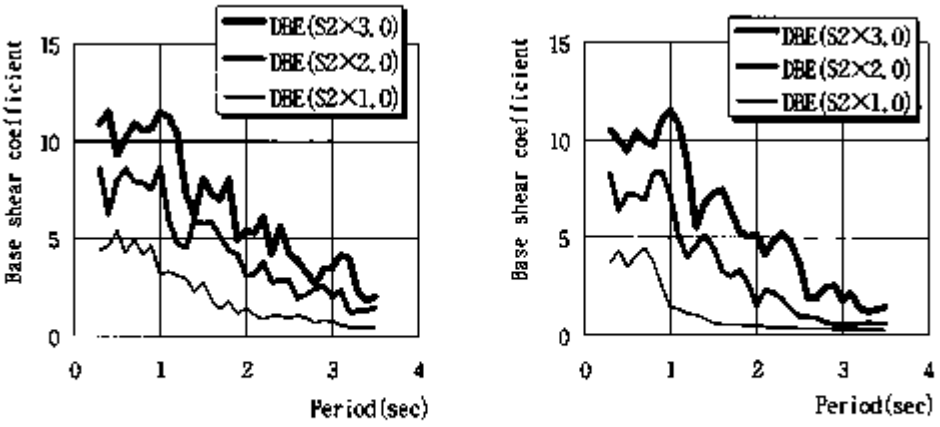

a) No damper b) Damper

Fig.6 Base shear coefficient spectrum(DBE)

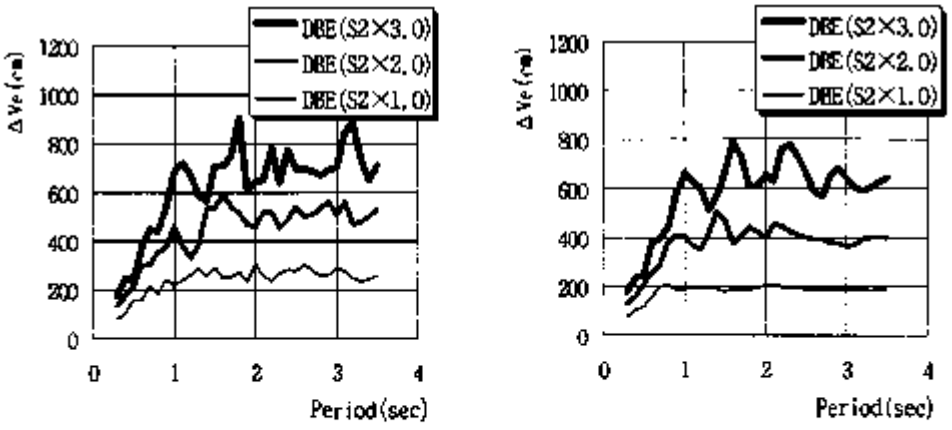

a) No damper b) Damper

Fig.7 Momental energy spectrum(DBE)

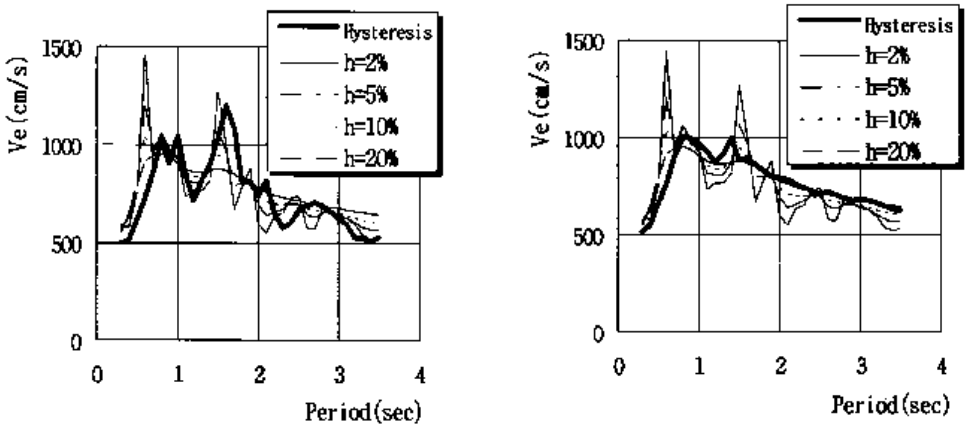

a) No damper DBE S2×2.0 b) Damper DBE S2×2.0

Fig.8 Comparison between the total input energy spectra of the elastic viscous damping model and the hysteresis model

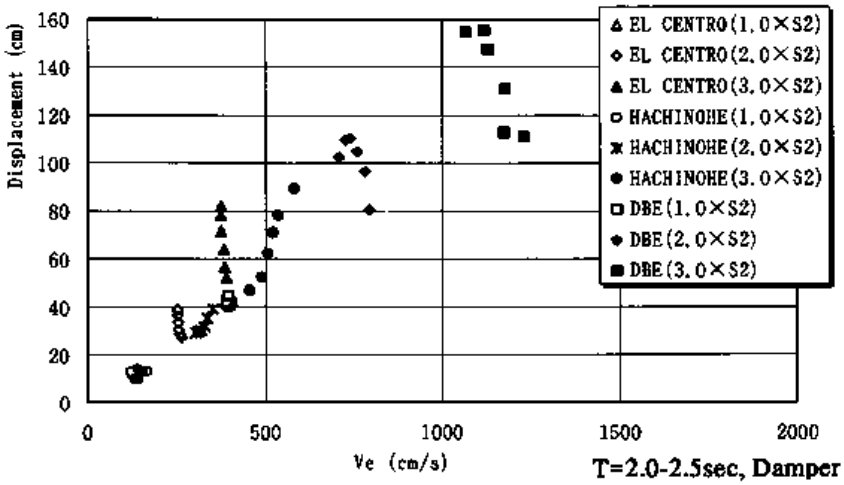

Fig.9 Relationship between total input energy Ve and displacement

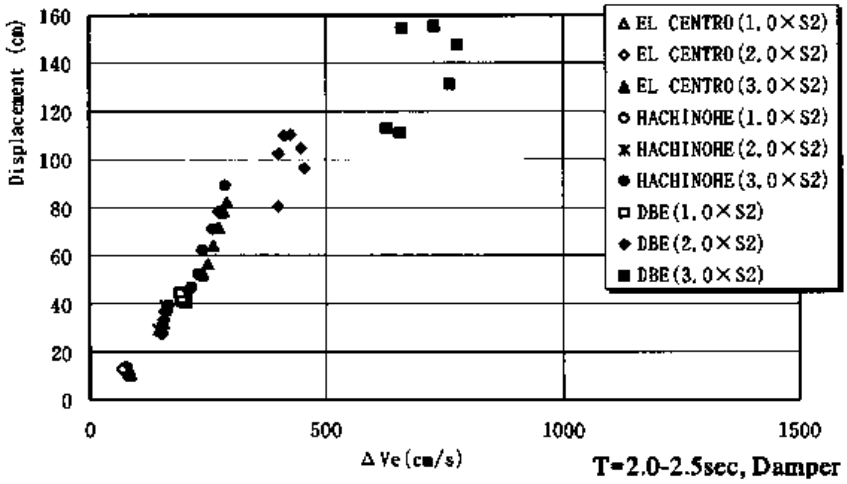

Fig.10 Relationship between momental input energy Δ Ve and displacement

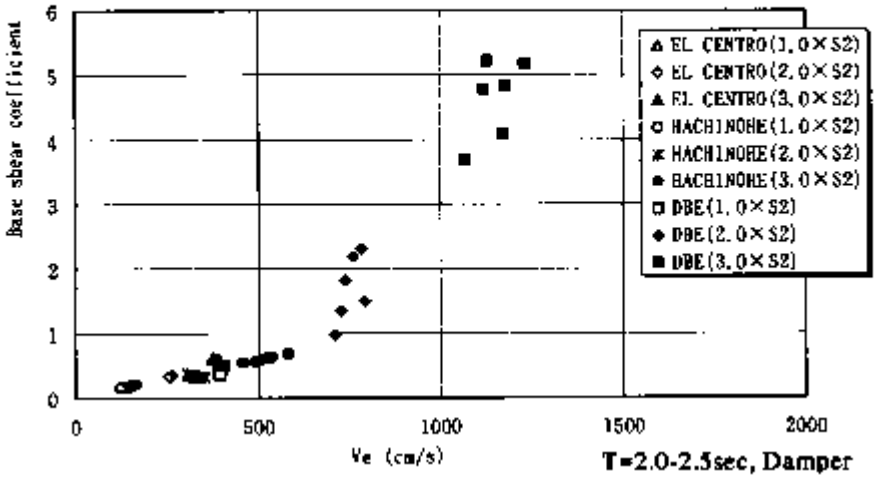

Fig.11 Relationship between total input energy Ve and base shear coefficient

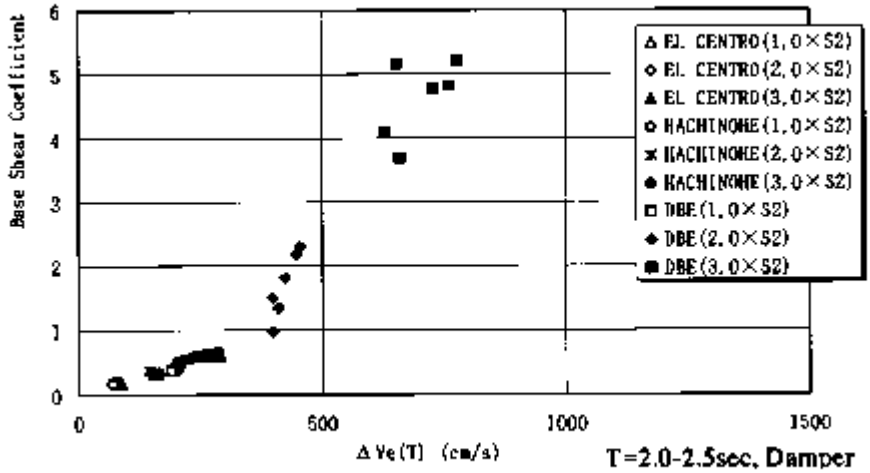

Fig.12 Relationship between momental input energy Δ Ve and base shear coefficien

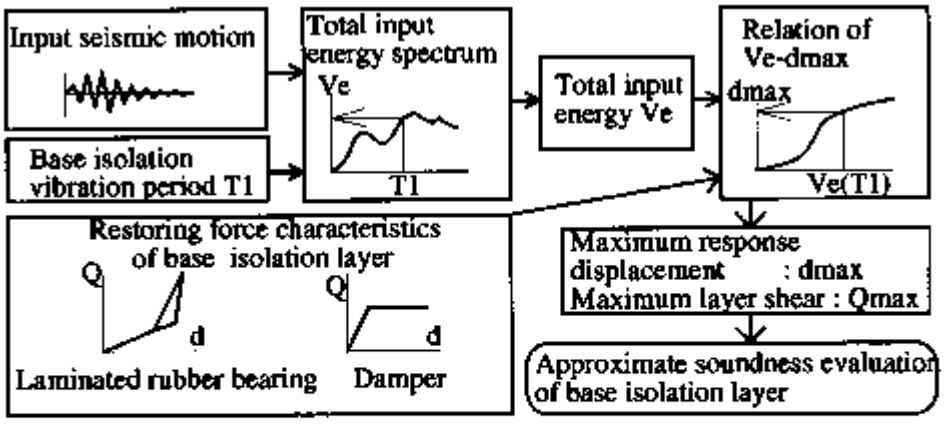

Fig.13 Response prediction flow

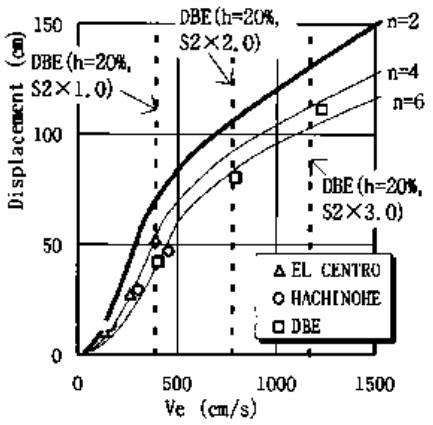

1) Displacement

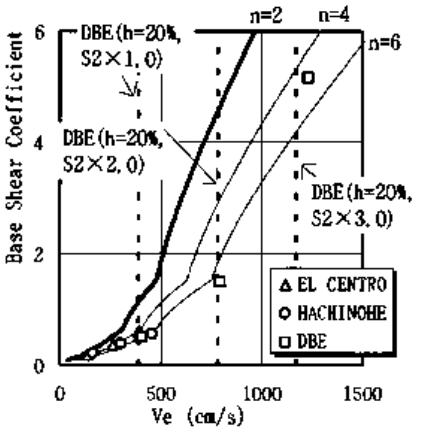

2) Base shear coefficient

a) T=2.0sec(n=2,4,6), Damper

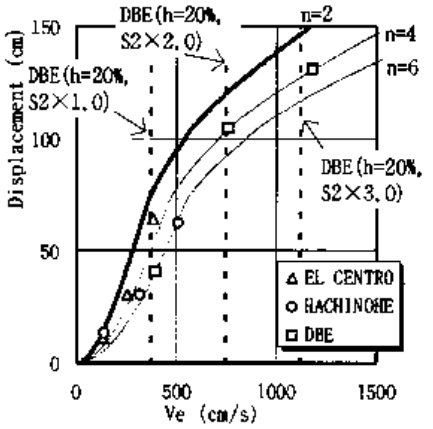

1) Displacement

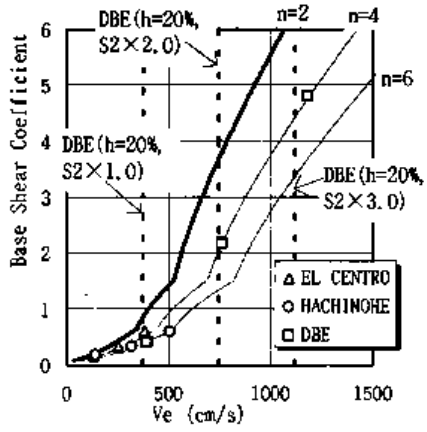

2) Base shear coefficient

b)T=2.2sec(n=2,4,6), Damper

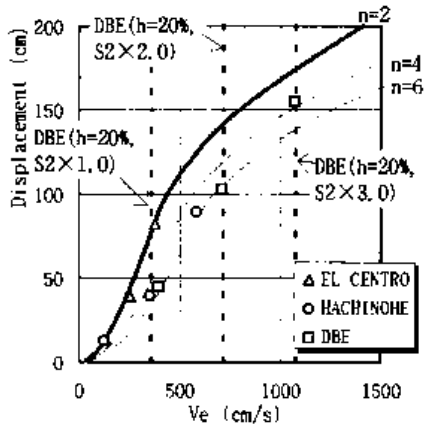

1) Displacement

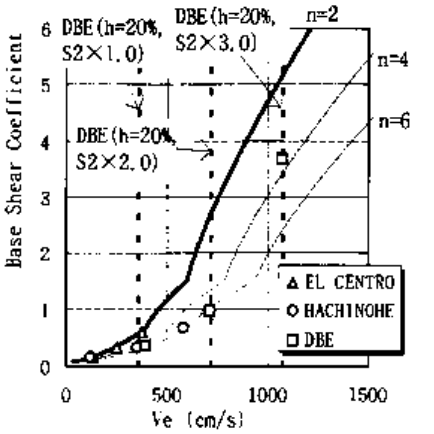

2) Base shear coefficient

c)T=2.5sec(n=2,4,6), Damper

Fig.14 Comparioson of anlysis results and response predictions

Transactions of the 13th International Conference on Structural Mechanics in Reactor Technology (SMiRT 13), Escola de Engenharia - Universidade Federal do Rio Grande do Sul, Porto Alegre, Brazil, August 13-18, 1995

Seismic proving test of process computer system with a seismic floor isolation system

Kondo, H.[1], Fujimoto, S.[1], Niwa, H.[1], Gunyasu, K.[1], Takamatsu, N.[1], Shibata, H.[2], Hara, F.[3], Fujita, T.[4], Kubo, T.[5], Terada, K.[6], Sasaki, Y.[6]
1) Toshiba Corporation, Kawasaki, Japan
2) Yokohama National University, Yokohama, Japan
3) Science University of Tokyo, Tokyo, Japan
4) University of Tokyo, Tokyo, Japan
5) Nagoya Institute of Technology, Nagoya, Japan
6) Nuclear Power Engineering Corp., Tokyo, Japan

1 INTRODUCTION

Role of process computer system has become important to support nuclear power plant operation. The computer system performs various kinds of information processing related to plant operations. Thus its functional capability during earthquakes is highly expected to be maintained for the inportant role in the information management.

One method of improving the seismic capability of a process computer system is to apply seismic isolation to the floor on which the computer system is installed. Using this method, the seismic force up on the computer system can be reduced, which makes it possible to improve the seismic capability of a computer system without modifying its structural system.

This paper presents the results of the seismic proving tests, undertaken at Tadotsu Engineering Center of NUPEC, of three process computer systems installed on a seismic isolation floor. At first, we investigated the function and seismic input conditions required for the seismic floor isolation system. The process computer systems were installed on a large-scale floor seismically isolated in the horizontal direction. Seismic excitation tests were carried out by using the 1000ton shaking table. The isolation performance of the floor and the functional capability of the computer systems were evaluated by the seismic vibration tests. Further, vibration analyses of the isolation floor were carried out and the design method for a process computer system combined with a seismic floor isolation system was evaluated from the test results and the analyses.

Note here that the seismic proving tests were carried out as a NUPEC project sponsored by MITI in Japan.

2 DESIGN OF SEISMIC FLOOR ISOLATION SYSTEM

2.1 Design Input Conditions

The following seismic input waves were used as design input conditions.

1) S1 wave, which is one of the seismic design earthquakes used in Japan for standardized LWR plant design.
2) S1(L) wave, which is made predominant in the long period component in view of

the particularity that a dominant vibration period of the seismic floor isolation system is long.

2.2 Function of a Seismic Floor Isolation System

The function required for the seismic floor isolation system is described as follows:

1) The floor works as a vibration isolator for large earthquake inputs but does not response to small-magnitude ones.
2) The maximum response acceleration of the floor is less than 2.50 m/sec^2 in the horizontal and vertical directions respectively.
3) Floor response spectrum of acceleration is less than the prescribed value shown in Fig.1 in the horizontal direction.

The condition described in item 2 was employed by considering the seismic condition widely used for conventional process computer systems. The response spectrum in item 3 was determined as the interface condition between the computer system and seismic floor isolation system. The conditions described in item 3 and in items 2 and 3 are hereinafter referred to as "design response spectrum" and "seismic design conditions", respectively. The "seismic design conditions" were determined from careful considerations of several types of nuclear power plants, several kinds of site conditions and input waves of design earthquake. The "seismic design conditions" are useful for the following that the method would make it possible to design independently computer systems and seismic floor isolation systems. If the conditions described in items 2 and 3 are satisfied, we are able to use the current design practice of process computer systems without any modification in designing process computer systems and computer related equipments installed on the seismic isolation floor systems.

3 STRUCTURE OF SEISMIC FLOOR ISOLATION SYSTEM

Figure 2 shows an overview of the seismic isolation floor system with three computer systems mounted on the shaking table. This isolation system was composed mainly of a floor frame, ball bearing units, spring damper units and a conventional computer floor. The floor frame was made up from H-section steel beams arranged in a form of wide planar lattice. Each of ball bearing units was equipped with three ball bearings attached to the bottom surface of a circular plate. The floor frame was supported by 25 ball bearing units, allowing it to freely move in any horizontal direction. Figure 3 shows upper and side views of the spring damper unit. Four pre-tensioned coil springs and one oil damper were connected over a pair of sliders which moved in the direction along the long side of the base plate but not moving toward each other from their initial positions. The sliders were installed to the floor frame. Thus the floor frame exhibited a nonlinear restoring force and a damping force in the horizontal direction. The spring constant of the coil spring was designed for the equivalent natural period of the seismic floor isolation system to be 3 seconds. The damping coefficient of the oil dampers was determined in accordance with its damping factor of 0.02. The trigger acceleration level was set at 0.2 m/sec^2 by using pre-tension force of the coil springs.

4 TESTS AND RESULTS

4.1 Static Tests

Static test was performed to confirm the restoring force of the spring system installed in the seismic floor isolation system. The floor frame was pushed and pulled by using two oil hydraulic actuators and we measured the displacement and the force given to the floor. Figure 4 shows the restoring force character against the floor displacement produced in the direction along the one side of the floor.

4.2 Seismic Excitation Tests

Seismic excitation tests were performed for the following items:

1) To confirm that the responses of the seismic floor isolation system for S1 and S1(L) waves are within the "seismic design conditions".
2) To confirm that the computer systems can maintain its required function during seismic excitation tests.
3) To investigate the seismic response property of the seismic floor isolation system with the computer systems.

Accelerations of the floor frame were measured at 24 points for the horizontal direction response and at 25 points for the vertical direction. Figure 5 shows one example of the time history response of the seismic isolation floor and the computer system. Table 1 shows the maximum response magnitude of the seismic isolation floor for S1(L) wave inputs. The response obtained in the case of the horizontal excitation but not including vertical excitation component was the almost same level as that in the case of horizontal and vertical 2d-excitation.

The computer systems installed on the seismic isolation floor maintained its function during the seismic excitation in all of the test cases. Figure 1 shows response spectrum of the isolation floor acceleration in the case of S1(L) wave excitation, where the thick solid line is "design response spectrum".

From the test results, it was confirmed that the maximum response acceleration and the response acceleration spectrum of the seismic isolation floor satisfied the "seismic design conditions" for S1(L) wave input.

5 VIBRATION ANALYSIS

5.1 Analytical Model

We used the following analytical models for the seismic floor isolation system which were modeled based on the results of the vibration tests.

One analytical model was a single degree-of-freedom system (Model A) and the other was 2 degrees-of-freedom system (Model B) shown in Fig.6 and Fig.7, respectively. In Model A, a whole structure on the floor frame was considered as a single rigid body. In Model B, the 1st in-plane vibration mode for the floor frame structure was taken into account in our consideration. In Fig.6, X_0, X and M express the horizontal acceleration for the ground, the relative displacement of the floor frame against the ground and the total mass of the floor frame and a whole structure installed

on the floor frame. C, f and F express the damping coefficient for the oil hydraulic dampers of the spring damper units, the frictional force for the ball bearing units and the restoring force for the spring damper units. The restoring force characteristic for the spring damper units shown in Fig.4 was used to evaluate F and f. In Fig.7, the mass M of Model A was divided into M_1 and M_2. X_1 and X_2 for the mass M_1 and M_2 express the relative displacements for the one side and the center of the the floor frame, respectively. k and C_2 express the equivalent spring constant and damping coefficient for the 1st in-plane vibration mode (about 22Hz) of the floor frame. The value for the 1st mode damping ratio (about 0.09) measured in the vibration tests was used as the value for C_2.

5.2 Analytical Results

Analytical results for the response in the horizontal direction were as follows:

The maximum response acceleration of the center of the floor frame and the maximum response in the relative displacements of the side of the floor frame for various acceleration input levels of S1(L) wave are shown in Fig.8. The acceleration floor response spectra at the center of the floor frame for the same input are shown in Fig.9. In these figures, The analytical results using Model A and Model B agree well with the experimental results. Note here that there is a slight difference in the results between Model A and Model B in the region of high frequency.

6 CONCLUSION

1) Seismic design method is proposed for interfacing seismic isolation floors and computer systems. In this method, the computer system and the seismic isolation floor are designed independently by interfacing the criteria of "seismic design conditions" established in this study.
2) The seismic floor isolation system sufficiently reduced the seismic force for the process computer systems installed on the floor. Specifically, the seismic floor isolation system could satisfy the "seismic design conditions" required to the seismic isolation. Furthermore, the functional capability of the computer systems against S1(L) large earthquake were verified when they were installed on the seismic floor isolation system.
3) In the analytical method for the horizontal direction motion of the isolation floor, it was confirmed that the proposed analytical model, that is, the single degree-of-freedom system or the 2 degrees-of-freedom system holds a sufficient applicability.

Table 1 Maximum response acceleration of floor frame for S1(L) waves

Level	Response Direction	Excitation Direction		
		Horizontal	Vertical	Hor. & Ver.
1/1	Horizontal	1.47 m/s²	0.07 m/s²	1.45 m/s²
	Vertical	0.55 m/s²	2.06 m/s²	2.04 m/s²
2/3	Horizontal	1.31 m/s²	0.06 m/s²	1.28 m/s²
	Vertical	0.54 m/s²	1.53 m/s²	1.44 m/s²
1/3	Horizontal	0.63 m/s²	0.04 m/s²	0.63 m/s²
	Vertical	0.23 m/s²	0.77 m/s²	0.64 m/s²

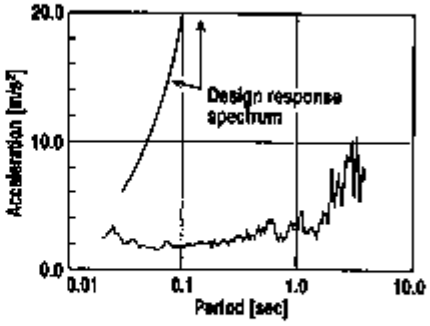

Fig. 1 Response spectrum of the floor frame in the horizontal direction for S1(L) wave input

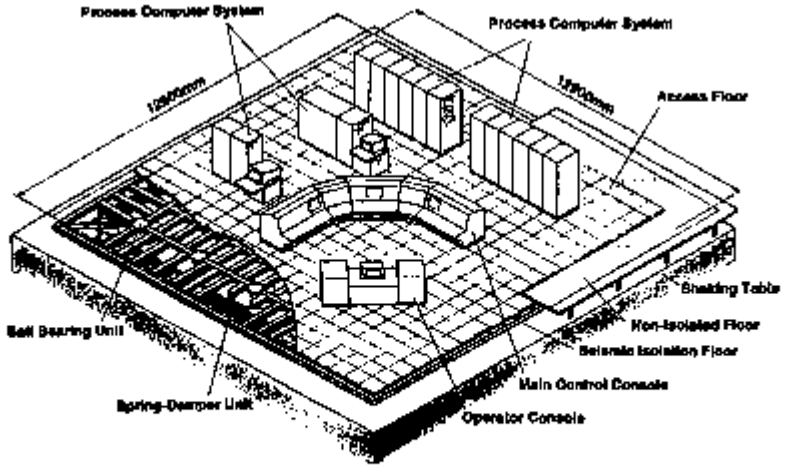

Fig. 2 Overview of the seismic isolation floor test model

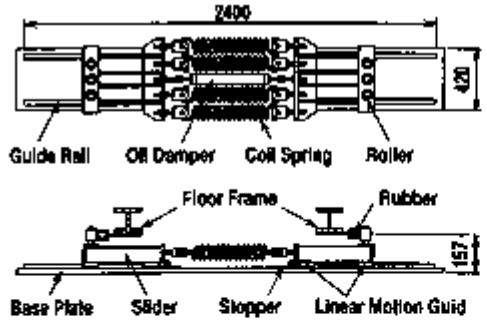

Fig. 3 Spring damper unit

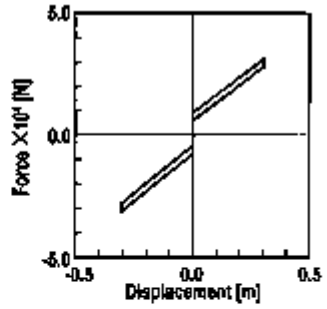

Fig. 4 Restoring force property of the seismic isolation floor

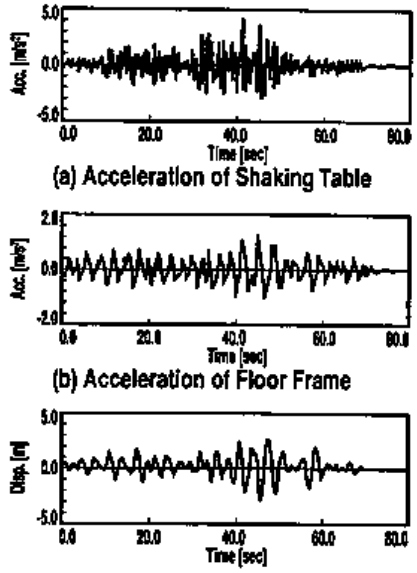

Fig. 5 Response time histories of the seismic isolation floor for S1(L) wave input

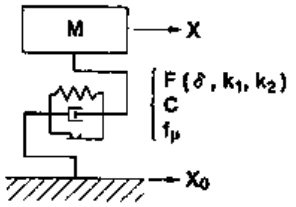

Fig. 6 Analytical model A in the horizontal direction

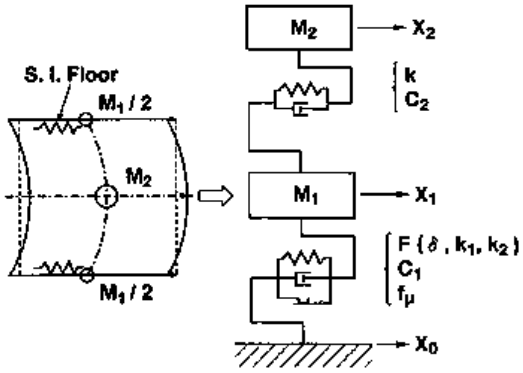

Fig. 7 Analytical model B in the horizontal direction

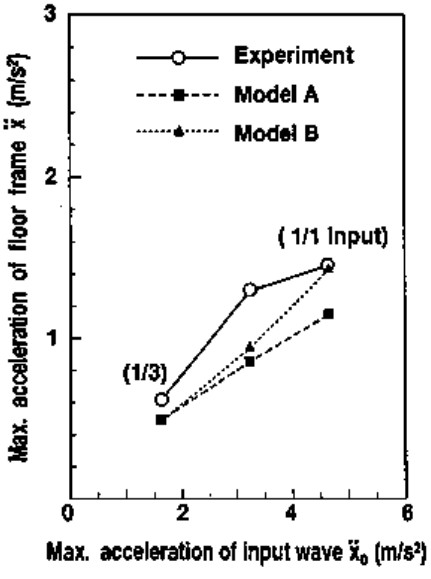

Fig. 8 Maximum response acceleration of the floor frame for S1(L) waves

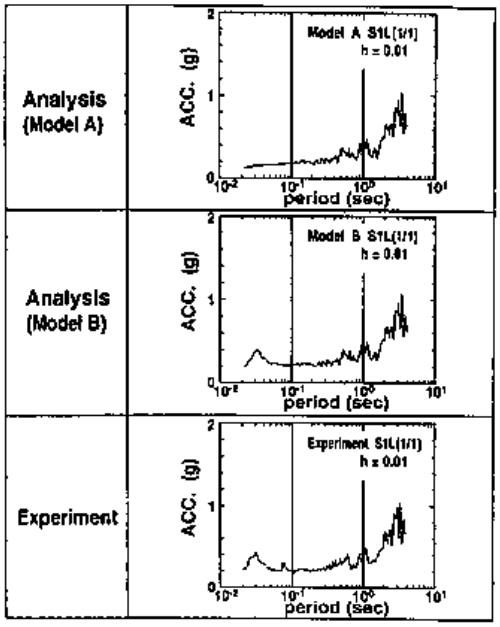

Fig. 9 Floor response acceleration spectra on the floor frame for S1(L) wave